

**Inside or Out:  
Characterizing petrobactin use by *Bacillus anthracis***

By

Ada Kendra Hagan

A dissertation submitted in partial fulfillment  
of the requirements for the degree of  
Doctor of Philosophy  
(Microbiology and Immunology)  
in the University of Michigan  
2018

Doctoral Committee:

Professor Philip C. Hanna, Chair  
Associate Professor Suzanne Dawid  
Professor Harry Mobley  
Assistant Professor Randy Stockbridge

Ada K. Hagan

akhagan@umich.edu

ORCID iD: 0000-0001-8481-1457

© Ada K Hagan, 2018

## **Dedication**

This dissertation is dedicated to me, who spent the last eighteen years dreaming of becoming a microbiologist.

And to my son—may you never stop learning.

## **Acknowledgements**

I first need to acknowledge my mentors in microbiology, without whom I wouldn't have matured to become the researcher I am today. Dr. Philip Hanna, who provided the tools, scaffold, and space for me to learn and grow through the research described in this work. Dr. Ranjan Chakraborty, who took a chance on a curious undergrad and taught me how to both seek out and tell good science stories. Dr. Christopher Pritchett, who pushed me to apply to the University of Michigan and Dr. Eric Mustain, who shared his love for immunology. Drs. Suzanne Dawid, Randy Stockbridge, Carol Fierke, and Harry Mobley who served on my dissertation committee.

The work described here wouldn't have been possible but for the current and former members of the Hanna lab whose own work served as a foundation from which to build: Drs. Paul Carlson, Shandee Dixon, Stephen Cendrowski, Karla Passalacqua, Nicholas Bergman, Tyler Nusca, Nathan Fisher, Brian Janes, and many more. Nor would it have been possible without the help of my collaborators—Dr. Ashu Tripathi, Dr. David Sherman, and Zach Mendel—or my undergraduates Ryan Dingle, Daniel Berger, and Yael Plotnik.

There are also many, many present and former research colleagues, peer mentors, and friends who have helped make this work possible by sharing their knowledge, resources, and time including: Travis Kochan, Sean Stacey, Hayley Warsinski, Leslie and David Hammond, Melanie McCurry, and Robin Grindstaff.

I also want to acknowledge those along the way who have fostered my curiosity and love of learning, especially my high school A.P. Biology teacher Mrs. Kathryn Gemmer—who gave me the tools for my first microbiology experiment—and my middle school teachers, Mrs. Karen Corpening and Mrs. Gayle Hughes.

Lastly, I lovingly and gratefully acknowledge my family—who loved, supported, and never questioned, my quest for knowledge—but especially my husband, whose constant questions always kept me learning.

## Preface

This dissertation contains four chapters comprising much of my research into how *Bacillus anthracis* uses the siderophore petrobactin for its growth.

Chapter one is an introduction to *Bacillus anthracis* and the current body of literature regarding petrobactin. A portion of this chapter was published in a review article during my graduate studies. (**Hagan, A.K.**, Carlson, P.E. Jr., and P.C. Hanna. Flying under the radar: The biochemistry and molecular biology of petrobactin in *Bacillus anthracis*. *Mol Microbiol*. 2016 Oct; 102(2):196-206. doi: 10.1111/mmi.13465 *EPub 9 Aug 2016*).

Chapter two details my work identifying the petrobactin exporter, ApeX, and characterizing the petrobactin components exported in its absence. The work described in this chapter was previously published. (**Hagan, A.K.**, Tripathi, A., Berger, D., Sherman, D., and P.C. Hanna. Petrobactin is exported from *Bacillus anthracis* by the RND-type exporter ApeX. *mBio*. 2017 Sept; 8:e01238-17).

Chapter three explores the role of petrobactin in *B. anthracis* spore biology. A manuscript encompassing portions of this chapter was submitted to biorxiv.org and prepared for submission to *mSphere* for peer review.

Finally, I discuss potential future directions for these research projects in Chapter 4.

## Table of Contents

<b>Dedication .....</b>	<b>ii</b>
<b>Acknowledgements .....</b>	<b>iii</b>
<b>Preface.....</b>	<b>v</b>
<b>List of Tables .....</b>	<b>viii</b>
<b>List of Figures.....</b>	<b>ix</b>
<b>Abstract.....</b>	<b>xi</b>
<b>Chapter 1 Flying under the radar: The non-canonical biochemistry and molecular biology of petrobactin from <i>Bacillus anthracis</i> .....</b>	<b>1</b>
Abstract.....	1
Introduction .....	2
Petrobactin Structure .....	3
Petrobactin Biosynthesis.....	4
Regulation of Petrobactin Biosynthesis.....	11
Petrobactin Transport Across Membranes.....	13
Iron Release from Petrobactin .....	15
Petrobactin and Pathogenesis .....	17
A Target for Antibiotics?.....	18
Summary and Future Directions.....	19
<b>Chapter 2 Petrobactin is exported from <i>Bacillus anthracis</i> by the RND-type exporter ApeX .....</b>	<b>20</b>
Abstract.....	20
Introduction .....	21
Materials and Methods .....	25
Bacterial growth conditions and sporulation.....	25
Cell viability.....	26
Gallium supplementation .....	26
Culture medium supplementation .....	26
Dipyridyl and precursor supplementation .....	27
LAESI-MS .....	27
LC-HRESIMS .....	28
Murine infections .....	28
Results .....	34
Selection of candidate petrobactin exporters.....	34
Screening candidate petrobactin exporters.....	36

LAESI-MS detects intact petrobactin in culture media and cell pellets.....	37
GBAA_2407 encodes a resistance-nodulation-cell division (RND)-type transporter that exports intact petrobactin.....	40
The 2407 mutant strain exports petrobactin components that maintain growth in vitro.....	42
Components could originate from truncated biosynthesis of petrobactin.....	48
Petrobactin components use an alternate receptor and maintain <i>B. anthracis</i> Sterne virulence.....	51
Discussion.....	52
<b>Chapter 3 Rapid sporulation in <i>Bacillus anthracis</i> requires petrobactin.....</b>	<b>59</b>
Abstract.....	59
Introduction.....	60
Materials and Methods.....	63
Bacterial growth conditions and sporulation.....	63
Spore germination and outgrowth.....	64
Supplementation of <i>asb</i> mutant sporulation with petrobactin and outgrowth.....	64
Reporter growth, measurement, and analysis.....	64
Microscopy.....	65
LAESI-MS.....	65
Sporulation efficiency.....	66
ICP-MS.....	66
Results.....	68
Petrobactin is not required for spore germination.....	68
Petrobactin, but not bacillibactin, is required for sporulation in ModG medium.....	71
The <i>asb</i> operon is transcribed and translated during late stage growth and early sporulation.....	72
Petrobactin is associated with the spore with indeterminate effects on iron storage.....	76
Petrobactin, but not hemin, is required for rapid growth and sporulation in bovine blood.....	77
Discussion.....	79
<b>Chapter 4 Discussion and future directions.....</b>	<b>85</b>
Dissertation summary.....	85
Export of petrobactin components.....	87
Removal of iron from the ferric-petrobactin complex.....	89
Petrobactin regulation suggests alternate functions.....	92
Optimization and adaptation of LAESI-MS.....	94
Conclusion.....	96
<b>Appendix.....</b>	<b>98</b>
<b>References.....</b>	<b>101</b>



## List of Tables

Table 2.1 Strains of <i>Bacillus anthracis</i> Sterne 34F2 used in this work.....	30
Table 2.2 Primers used to generate mutant strains used in this work.....	31
Table 2.3 Candidate petrobactin exporters .....	35
Table 2.4 Candidate petrobactin exporter phenotypes at six hours post-inoculation in IDM .....	37
Table 2.5 The structures and molecular weights of predicted petrobactin components present in <i>asbA-F</i> mutants .....	47
Table 2.6 Growth of individual <i>asbA-F</i> disruption mutants in IDM .....	49
Table 3.1 Strains of <i>B. anthracis</i> Sterne 34F2 used in this work.....	67
Table 3.2 Primers used to generate mutant strains used in this work. ....	67
Table A.1 Candidate petrobactin iron-removal proteins.....	98
Table A.2 Primers used to generate the strains used in this work .....	99
Table A.3 Candidate petrobactin iron-removal enzyme phenotypes at six hours post-inoculation in IDM.....	100

## List of Figures

Figure 1.1 Structure and biosynthesis of petrobactin by <i>Bacillus anthracis</i> .....	6
Figure 1.2 AsbF structure and active site.....	8
Figure 1.3 AsbB structure and active site .....	10
Figure 1.4 Proposed schematic of petrobactin import, export and iron removal in <i>B. anthracis</i> .	15
Figure 2.1 GBAA_2407 encodes a petrobactin exporter.....	39
Figure 2.2 <i>In trans</i> complementation of the 2407 mutant strain restores petrobactin export, reduces cellular accumulation, and is confirmed by HRESIMS.....	41
Figure 2.3 The 2407 mutant strain resembles wild-type in cell viability and dose-dependent response to dipyriddy.....	42
Figure 2.4 The 2407 mutant strain exports petrobactin components that import iron but are less efficient than intact petrobactin .....	46
Figure 2.5 Petrobactin components from truncated biosynthesis are exported and supplement growth of the <i>asb</i> mutant strain .....	50
Figure 2.6 Petrobactin components use a different receptor from petrobactin and maintain <i>B. anthracis</i> Sterne virulence .....	51
Figure 2.7 Predicted structure of ApeX. ....	54
Figure 2.8 Model of petrobactin use in <i>B. anthracis</i> .....	56
Figure 3.1 Schematic of sporulation and the spore architecture.....	61
Figure 3.2 <i>asb</i> mutant spores do not have a germination defect but fail to outgrow in iron-depleted medium.....	70
Figure 3.3 Petrobactin supplementation of the <i>asb</i> mutant strain during sporulation does not rescue outgrowth in iron-depleted medium .....	71
Figure 3.4 Petrobactin, but not bacillibactin, is required for sporulation in ModG medium.....	72
Figure 3.5 Schematic of putative transcriptional regulator binding sites upstream of <i>asbA</i> .....	73

Figure 3.6 *asb* transcriptional and translational fluorescent reporters illuminate expression during late stage growth ..... 75

Figure 3.7 Petrobactin is associated with the *B. anthracis* spore and has indeterminate effects on iron storage..... 77

Figure 3.8 Petrobactin, but not hemin, is required for growth and sporulation in bovine blood.. 79

Figure 3.9 Proposed model of petrobactin use by *B. anthracis* during late stage growth and early sporulation..... 84

Figure 4.1 Proposed model of *B. anthracis* petrobactin use throughout the cycle of infection and transmission ..... 97

## Abstract

*Bacillus anthracis* is a Gram-positive, spore-forming bacillus and causes the disease anthrax. Anthrax is a deadly infection that begins with phagocytosis of a *B. anthracis* spore by an antigen presenting cell and ends when bacilli-laden blood from the carcass is exposed to oxygen, which initiates sporulation. Each step in the infection process requires access to nutrients, including iron. Iron is required as a protein co-factor for many different cellular processes but is also tightly regulated within organisms, including both the mammalian host and the bacterium. To gather iron during infection, *B. anthracis* employs a heme acquisition system as well as two siderophores, petrobactin and bacillibactin. Of these three systems, only petrobactin is required for growth in iron-deplete medium, macrophages, and to cause disease in mouse models of infection. Chapter one describes what is understood about petrobactin including biosynthesis by the *asb* operon, regulation of biosynthesis, how the ferric-petrobactin complex is imported, and relevance to disease. I also highlight remaining questions such as how petrobactin is exported from the cell and its role in spore biology.

In chapter two, I describe my work identifying the petrobactin exporter ApeX. Using a bioinformatics-based protocol to identify putative targets for petrobactin export, I generated single deletion mutants. Laser ablation electrospray ionization mass spectroscopy (LAESI-MS) was adapted to screen for deletion mutants that failed to export petrobactin, enabling identification of ApeX as a petrobactin exporter. An *apeX* deletion mutant unable to export

petrobactin, instead accumulated the molecule within the cell pellet and exported components. These petrobactin components are still able to transport iron and cause disease in a mouse model of inhalational anthrax. I also used LAESI-MS in chapter three to detect petrobactin within *B. anthracis* spores and explore the role of petrobactin in spore biology. Petrobactin is not required for germination from the spore, but is required for rapid sporulation in the iron-rich ModG sporulation medium. Fluorescent reporters show induction of the *asb* operon during late stage growth and early sporulation. This phenotype is likely relevant to disease transmission since experiments in defibrinated bovine blood demonstrate that petrobactin is the preferred iron acquisition system during growth in blood and is required for sporulation in aerated blood. Chapter four offers hypotheses and suggestions for how to answer remaining questions not addressed by the research done in this work. I also make hypotheses regarding alternative, non-iron-scavenging functions for petrobactin and discuss the future potential for LAESI-MS as a research tool.

## Chapter 1

# **Flying under the radar: The non-canonical biochemistry and molecular biology of petrobactin from *Bacillus anthracis***

### Abstract

The dramatic, rapid growth of *Bacillus anthracis* that occurs during systemic anthrax implies a crucial requirement for the efficient acquisition of iron. While recent advances in our understanding of *B. anthracis* iron acquisition systems indicate the use of strategies similar to other pathogens, this review focuses on unique features of the major siderophore system, petrobactin. Ways that petrobactin differs from other siderophores include: A. unique ferric iron binding moieties that allow petrobactin to evade host immune proteins; B. a biosynthetic operon that encodes enzymes from both major siderophore biosynthesis classes; C. redundancy in membrane transport systems for acquisition of Fe-petrobactin holo-complexes; and, D. regulation that appears to be controlled predominately by sensing the host-like environmental signals of temperature, CO<sub>2</sub> levels and oxidative stress, as opposed to canonical sensing of intracellular iron levels. I argue that these differences contribute in meaningful ways to *B. anthracis* pathogenesis. This chapter will also outline current major gaps in our understanding of the petrobactin iron acquisition system, some projected means for exploiting current knowledge, and potential future research directions.

## Introduction

Iron is the fourth most abundant element on earth and almost all living organisms require iron's redox properties for life. However, these same properties can be toxic for cells, necessitating biological solutions to balance acquisition with stringent regulation (1, 2). The roles of iron as an enzyme cofactor and in electron transfer are a double-edged sword. High, unregulated quantities of iron in the cell are toxic due to the Fenton reaction in which oxidation of ferrous iron generates superoxide radicals resulting in DNA damage (1, 2). Accordingly, iron is tightly regulated at both the cellular and organismal level (3). Within humans, several proteins are dedicated to iron storage, transfer, and collection: *e.g.*, ferritin, transferrin and lactoferrin, respectively (3, 4). Maintaining free ferric iron at concentrations less than  $10^{-18}$  M prevents iron toxicity and easy acquisition by invading bacterial or parasitic pathogens that require iron for growth (2, 4, 5).

*Bacillus anthracis* is one pathogen that requires iron for growth within a host. The causative agent of anthrax, *B. anthracis* is a Gram-positive, spore-forming bacillus. The metabolically inactive spore is the infectious particle, initiating disease after exposure to an open wound, the respiratory tract, the gastrointestinal tract, or by subcutaneous injection (6–8). Preceding systemic anthrax, the spores are engulfed by phagocytes, which migrate to nearby lymph nodes. Simultaneous to this migration, spores germinate within the macrophage or dendritic cell leading to outgrowth of vegetative cells (6, 9, 10). The vegetative bacilli replicate and produce toxins, resulting in phagocyte destruction and direct release of bacilli into the lymph or blood (6, 7, 11). There, they quickly replicate to titers in excess of  $10^8$  CFU/mL, preceding death of the host (7, 12, 13). This rapid replication requires access to many important nutrients, including iron.

*B. anthracis* possesses two known mechanisms for acquisition of ferric iron in addition to others for acquisition of ferrous iron (*e.g.*, heme) (14). The ferric iron acquisition systems employ iron scavengers known as siderophores. During low iron stress, these small molecules are synthesized and transported into the extracellular host milieu to bind ferric iron with a high affinity (15). The iron-bound (holo) siderophores are then reacquired by the bacterium via a specific receptor thus allowing iron acquisition and sustained growth (15). *B. anthracis* encodes the biosynthetic machinery for two distinct siderophores, bacillibactin and petrobactin (16).

Of the ferric iron acquisition methods, only the siderophore petrobactin is necessary for virulence in murine models of anthrax (16, 17). Cendrowski, *et al.*, first observed the importance of petrobactin for *B. anthracis* growth when deletion of the anthrax siderophore biosynthetic operon, *asbABCDEF*, led to defects in growth within macrophages *in vitro* and attenuation in spore-challenged mice (16). In contrast, strains deficient in bacillibactin biosynthesis fail to demonstrate similar growth or virulence defects in either *in vitro* or *in vivo* experiments (16, 17). It is interesting that while bacillibactin is a common siderophore among many *Bacillus* spp., petrobactin biosynthesis has only been identified in the *B. cereus sensu lato* group (*B. cereus*, *B. thuringiensis* and *B. anthracis*) and the unrelated Gram-negatives *Marinobacter hydrocarbinoclasticus* and *M. aquaeoli* (18–20). Since the discovery of petrobactin relevance to *B. anthracis* pathogenesis, research has been ongoing.

### Petrobactin Structure

Siderophores are generally classified into four groups according to the major iron binding moieties: hydroxamate, catechol,  $\alpha$ -hydroxycarboxylate and mixed (*i.e.*, either two or more differing moieties or the use of less common iron binding moieties) (2). These coordinating



ligands determine the affinity of a siderophore (pM) for its ferric ligand based on their charge densities and deprotonation values and is calculated based on the concentration of free  $\text{Fe}^{3+}$  remaining at equilibrium (2, 21). Petrobactin is composed of a citrate backbone with two spermidine arms, each capped by a 3,4-dihydroxybenzoate (3,4-DHB) moiety (Figure 1.1C) (18, 22). A single ferric iron atom is coordinated between the catechol groups of 3,4-dihydroxybenzoate and the  $\alpha$ -hydroxycarboxylate of the citrate backbone, indicating classification as a mixed-type siderophore (18, 23). Interestingly, petrobactin is the sole siderophore known to use 3,4-dihydroxybenzoate instead of the canonical 2,3 configuration. The coordination of ferric iron with these alternate catechol moieties and  $\alpha$ -hydroxycarboxylate results in a ferric affinity of 23pM for petrobactin (21). In contrast, siderophores with three 2,3-dihydroxybenzoate moieties (*e.g.*, bacillibactin) have higher ferric affinities of about 35pM, a 12 log difference (21, 23). Additionally, the citrate backbone lends holo-petrobactin to being photolabile. Barbeau *et al.* demonstrated that sunlight acted to decarboxylate and oxidize the citrate backbone via a charge transfer directly to the iron atom. The resultant product is 3-ketoglutarate with the enol group hypothesized to maintain the ability of the photoproduct to bind ferric iron (18). The impact of this on either *Marinobacter* or *B. anthracis* iron acquisition has not been investigated though this photolysis does increase the affinity of the compound for ferric iron (24).

### Petrobactin Biosynthesis

Siderophores are synthesized by enzymes belonging to either of two families found within operons, the non-ribosomal peptide synthetases (NRPS) or the independent of NRPS synthetases (NIS) (2, 25). Petrobactin biosynthesis is unique, however, in that both NRPS and

NIS enzymes are required. NRPS enzymes are large, multi-enzyme complexes acting in an assembly line fashion to condense a target amino acid into a polypeptide chain (25, 26). This machinery has three main domains: the adenylation domain, which activates and recognizes the amino acid, the peptidyl carrier protein (PCP) domain containing a thiolation site, and the condensation domain that incorporates the amino acid into the chain (26–32). After the appropriate number of condensation reactions, the peptide is cyclized by a C-terminal thioesterase domain (26, 33, 34).

NIS systems, however, are characterized by the presence of ATP-dependent synthetases divided into three functional types, with one split further based on phylogenetics (35). Type A synthetases condense citric acid with either amines or alcohols (36). Type B uses  $\alpha$ -ketoglutarate as a substrate for condensation with amines, the subgroup type A' acts on citric acid (36). Lastly, type C synthetases condense citric acid or succinic acid derivatives with an amine or alcohol (36–38). These can also oligomerize or macrocyclize  $\sigma$ -amino-carboxylic acids containing a hydroxamate group (36, 37). NIS synthetases can be either “modular”, participating in a single condensation reaction or “iterative” participating in two or more condensations with similar substrates (36). This difference cannot be distinguished by sequence comparison analysis (36).

The *asbABCDEF* operon encodes for six enzymes: two belonging to the NIS family (*asbAB*), three NRPS enzymes (*asbCDE*) and one dehydroshikimate dehydratase (*asbF*) (16, 39–42). Briefly, the biosynthetic pathway of petrobactin (Figure 1.1) begins when AsbF generates 3,4-dihydroxybenzoate, which is transferred by AsbC to AsbD. AsbE condenses the 3,4-dihydroxybenzoate moiety from AsbD to a molecule of spermidine (41, 42). Spermidine and citric acid condensation is mediated by AsbA and AsbB to generate multiple intermediates, with the potential for the second 3,4-dihydroxybenzoate condensation to occur at multiple points.

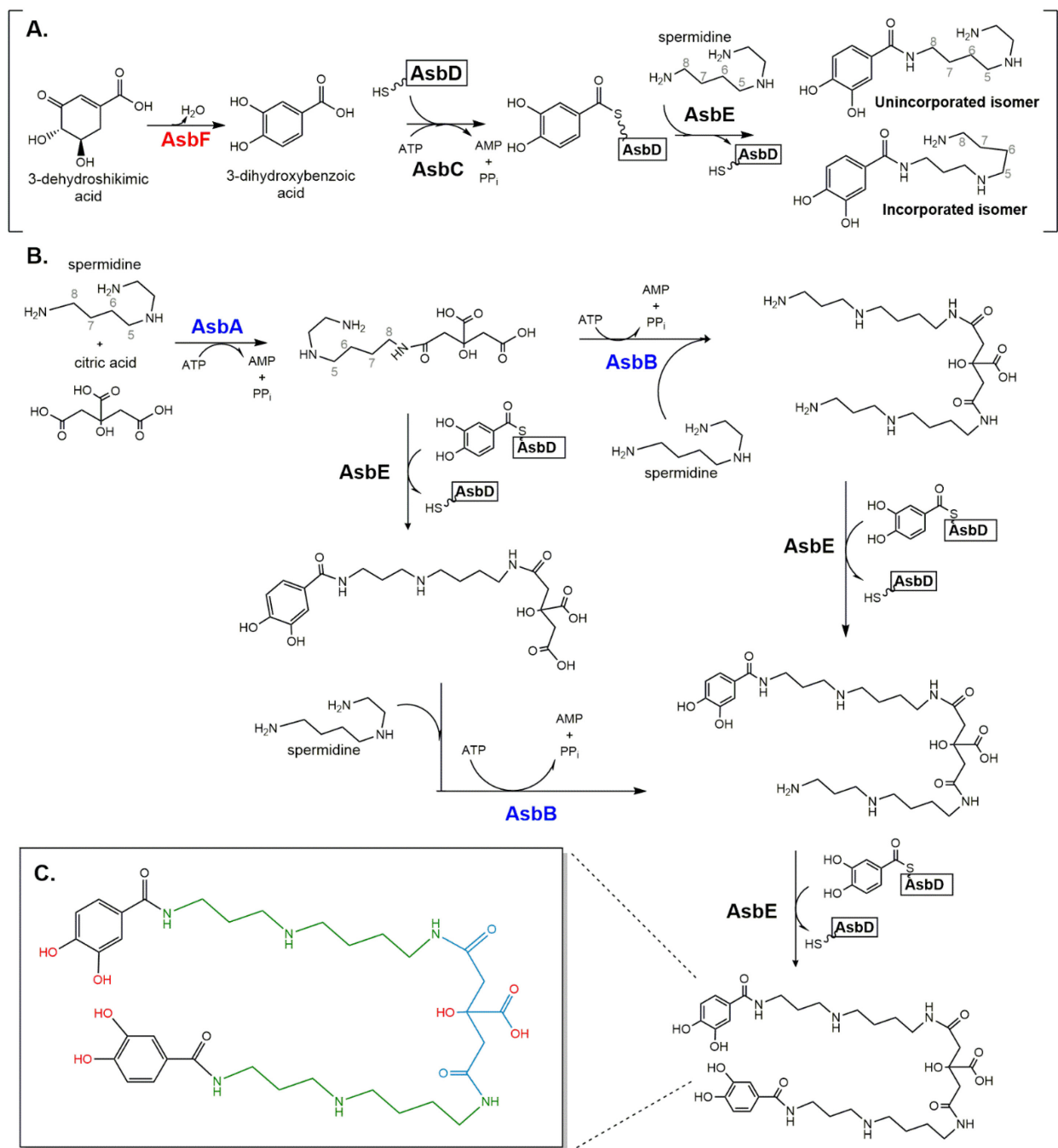


**Figure 1.1 Structure and biosynthesis of petrobactin by *Bacillus anthracis*.** A) Following generation of 3,4-DHB by AsbF (red), it is incorporated into petrobactin by three NRPS enzymes, AsbCDE (black text). First it is loaded on to the aryl-carrier protein AsbD by the transferase AsbC. Condensation of 3,4-DHB to a spermidine arm is performed by AsbE. Two isomers are formed, though only the isomer containing 3,4-DHB at the N1-terminus is incorporated into the final product. B) NIS enzymes AsbAB (blue text) condense the citrate backbone to spermidine arms. AsbA efficiently catalyzes the initial reaction of a single spermidine and citrate while AsbB condenses spermidine to a molecule of citryl-spermidine or 3,4-DHB-citryl-spermidine. AsbE

and AsbD cap the backbone with 3,4-DHB moieties. C) Structure of petrobactin. A citrate backbone (blue) with two spermidine arms (green) each capped with a 3,4-DHB moiety (black). A single molecule of ferric iron is coordinated between each of the 3,4-DHB catechol moieties and the  $\alpha$ -hydroxycarboxylate of the citrate backbone (red) (43).

The discovery that 3,4-dihydroxybenzoate is generated from 3-dehydroshikimate (DHS) by AsbF was published by two groups, Fox *et al.* and Pflieger *et al.* (Figure 1.1A) (41, 42). This is the first dehydroshikimate dehydratase (DHSase) to be identified as participating in a non-catabolic pathway (41, 42). As predicted by an observed TIM barrel-like fold, AsbF requires divalent cation cofactors with a preference for  $Mn^{2+}$ , though greater than 80% activity is reported with  $Mg^{2+}$ ,  $Co^{2+}$  (41, 42).  $Ca^{2+}$  and Ni also restore activity, ranging from 20 to 50% relative to  $Mg^{2+}$  (42). Notably, Fox *et al.* reported that  $Zn^{2+}$  was capable of restoring some activity to AsbF while Pflieger *et al.* reported that addition of zinc abrogated AsbF activity in a manner similar to that seen with sugar isomerases (41, 42). Structural analysis of AsbF (originally with both cofactor and the product) shows the N-terminus (Figure 1.2, blue) partially buried at the bottom of the eight stranded TIM-like barrel (Figure 1.2, green) (41). The C-terminus (Figure 1.2, salmon) is partially solvent exposed. The  $Mn^{2+}$  is coordinated by three carboxylic acid side chains (Figure 1.2B, black), a deprotonated imine (Figure 1.2B, black) and the 3-hydroxy group of 3,4-dihydroxybenzoate (not shown) (41). In addition to coordinating with  $Mn^{2+}$ , 3,4-dihydroxybenzoate was bound in the active site by aromatic residues (Figure 1.2B, red) found under a helical loop (Figure 1.2, yellow) between the  $\beta 7$  strand and  $\alpha 7$  helix (41). Conditions conferring optimum activity and kinetics of activity for AsbF are unclear, however. Fox *et al.* reported maximum activity in a pH range of 8.4-8.8 with only 15% activity remaining at pH 7.4 and a  $K_M$  five-fold lower than any other reported DHSase (42). Conversely, kinetics performed at pH 7.5 by Pflieger *et al.* resulted in a  $K_M$  similar to that reported for fungal DHSases

(41). The mechanism of 3,4-dihydroxybenzoate generation is predicted to occur in two steps, the generation of an enolate intermediate from 3-DHS, followed by a dehydration step resulting in aromatization and 3,4-DHB product (41).

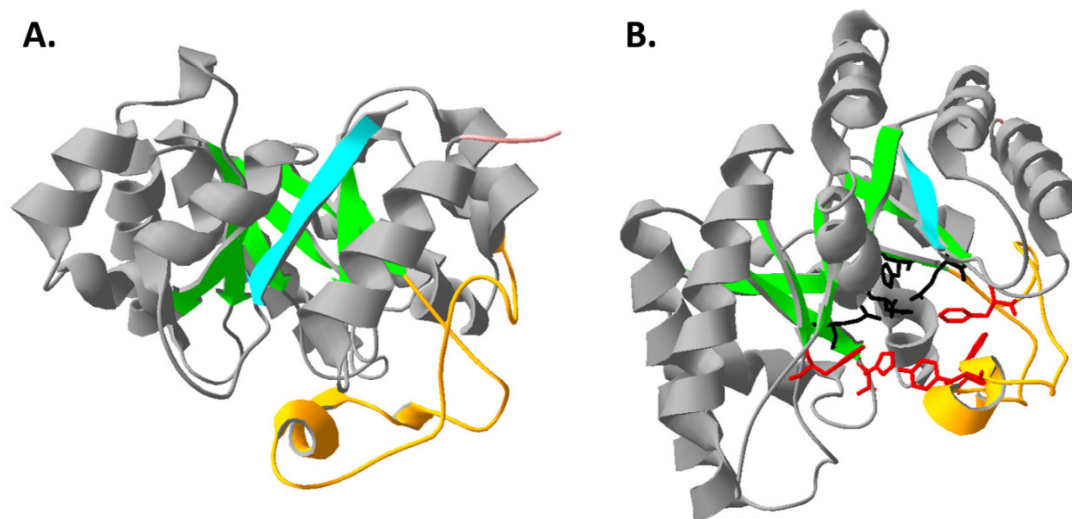


**Figure 1.2 AsbF structure and active site.** A) Crystal structure of AsbF. The eight  $\beta$ -sheet TIM-barrel (green) occludes the N-terminus (blue) while the C-terminus (salmon) is exposed. A helical loop (yellow) caps the barrel, closing the active site. B) AsbF structure rotated to demonstrate the active site. The  $Mn^{2+}$  is coordinated between residues found within the barrel (black) and 3,4-DHB. In turn, the 3,4-DHB is coordinated by the aromatic residues (red) contributed by helical loops (41, 44).

Similar to biosynthesis of NRPS siderophores, the aryl product (3,4-dihydroxybenzoate) is transferred to a carrier protein (AsbD) by an aryl transferase (AsbC) (Figure 1.1A-B) (40, 45). *In vitro*, AsbC adenylates 3,4-dihydroxybenzoate and subsequently loads the substrate, 3,4-DHB-AMP, onto holo-AsbD, the PCP. Interestingly, AsbC is highly specific to 3,4-dihydroxybenzoate. *In vitro* substitution with 2,3-dihydroxybenzoate or 2-hydroxybenzoate, two common aryl acids in siderophores, did not result in substrate adenylation or loading of AsbD (45). Carrier proteins, such as AsbD, are activated post-translationally by the addition of phosphopantetheine from coenzyme A to a conserved serine (S40 for AsbD) (45). This reaction is typically catalyzed by a cognate phosphopantetheinyl transferase (PPTase) encoded within the

same gene cluster as the carrier protein. There is no PPTase encoded by the *asb* operon, but Pflieger *et al.* predicted AsbD activation *in vivo* by a *B. subtilis sfp* homologue (45). *E. coli* PPTases were sufficient for AsbD activation *in vitro*, indicating a dedicated PPTase may not be necessary (45). After generation of 3,4-dihydroxybenzoate -loaded AsbD, AsbE catalyzes the condensation of 3,4-dihydroxybenzoate to spermidine (45). Two isomers are generated both *in vitro* and *in vivo* though only the isomer from condensation of 3,4-dihydroxybenzoate to the N1 site appears to be incorporated (Figure 1.1A) (40, 45).

AsbA and AsbB are both members of the NIS synthetase family involved in condensation of the citrate backbone to spermidine (Figure 1.1B) (39, 43, 46). AsbA is a type A synthetase responsible for the ATP-dependent condensation of citric acid to the N8 site of spermidine (39). Biochemical studies indicate AsbA can catalyze condensation reactions with citrate or spermidine analogs through a potentially novel process (47). (39, 47) Conversely, AsbB is a type C synthetase, catalyzing the condensation of a citrate derivative (in this case N8-citryl-spermidine or 3,4-DHB-citryl-spermidine) with the N8 of a second spermidine molecule (43, 46). Condensation of the citrate derivative with 3,4-DHB-spermidine is possible, though not preferred, according to AMP formation rates, suggesting it is unlikely to be a “significant intermediate” in petrobactin biosynthesis (46). Both AsbA and AsbB have similar catalytic activity with similar substrate preferences in regards to petrobactin but are not entirely redundant. In-frame deletion of *asbA* does not completely abrogate petrobactin biosynthesis as AsbB functionally compensates for the citrate spermidine condensation *in vitro*. AsbA, however, does not compensate for the loss of AsbB as mutants for AsbB fail to produce petrobactin and exhibit reduced growth in iron-deficient medium (40, 43, 46).

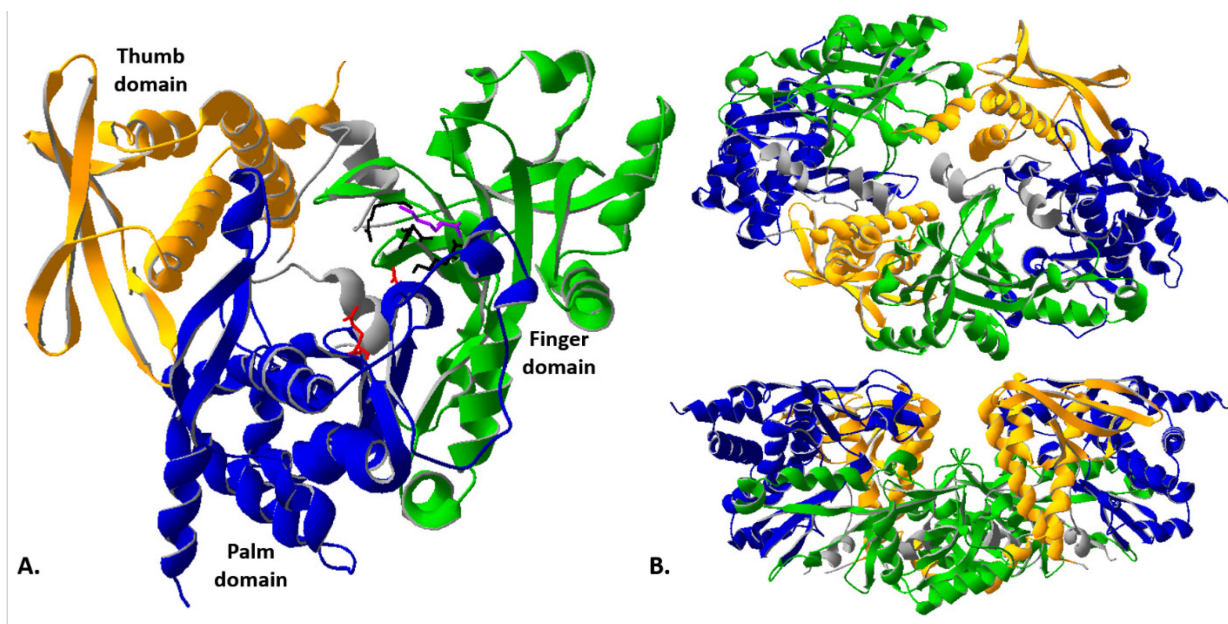


**Figure 1.3 AsbB structure and active site.** A) Structure and active site of monomeric AsbB. It is composed of three domains; the thumb (yellow), the palm (blue) and the finger (green). The active site is positioned between the palm and finger domains. Basic residues in the palm (red) are predicted to bind ATP/ADP while acidic residues in the finger domain (black, purple) stabilize and selectively recruit spermidine to the active site. B) AsbB dimerization is coordinated by the thumb domain (yellow) of one protein with the finger domain (green) of the second (top; view from bottom). This creates a solvent exposed channel (bottom; side view) (43, 44).

The structure of AsbB resembles a “cupped hand” with three domains: the thumb, palm and fingers (Figure 1.3 yellow, blue and green, respectively) (38, 43). The active site is composed of basic residues in the finger domain (Figure 1.3A, red) for the predicted binding of ATP/ADP and acidic residues (Figure 1.3A, black) responsible for recruitment and stabilization of spermidine in the palm domain (43). Both AsbA and AsbB regioselectively condense citrate to the N8 terminus of spermidine (43). Nusca, *et al.* used site-directed mutagenesis to determine that the charged residues K311 (Figure 1.3, purple) and E459 of AsbB (K315/Q468 of AsbA) play roles in determining selectivity for isomer and polyamine incorporation (43). Crystal structure and size exclusion chromatography analyses suggest dimerization of AsbB *in vivo*

(Figure 1.3B) with the pockets containing the active sites connected by a solvent exposed channel. The dimer interaction is facilitated by the helices T $\alpha$ 1, T $\alpha$ 2, and T $\alpha$ 4 in the thumb domain of one protein with a helix spanning F $\alpha$ 3 and F $\alpha$ 4 of the finger domain of the second (43).

Some questions remain regarding petrobactin biosynthesis. For example, it has not been determined whether the unique biosynthetic process involving both NRPS and NIS synthetases, plus a DHSase occurs in the context of a multi-enzyme or otherwise. There is data to suggest dimerization of AsbB (and other type C synthetases) *in vivo*, as well as the formation of a complex by AsbCDE, but nothing to determine if AsbA and/or AsbB interact *in vivo* with the AsbCDE complex or AsbF (38, 43).

### Regulation of Petrobactin Biosynthesis

For many ferric iron acquisition systems, the ferric uptake regulator (Fur), or a Fur-like protein, is responsible for negative transcriptional regulation of all aspects of the system, including biosynthesis, transport and iron removal (1). Fur is a negative regulator activated by binding two iron atoms (48–50). This allows Fur to interact with, and bind, consensus Fur-box sequences upstream of negatively regulated genes (51, 52). Under iron-limiting conditions, the intracellular concentration of iron is reduced such that iron is no longer available to bind Fur. Instead, it is used in cellular functions, blocking Fur activation and relieving its transcriptional repression (1).

In *B. anthracis*, Fur inhibits bacillibactin biosynthesis (16, 53). This is less clear with regards to petrobactin regulation. A review by Hotta, *et al.* indicates that the petrobactin biosynthesis operon does not have a conserved upstream Fur-box. Our analysis of the upstream



sequences, however, reveals predicted Fur-boxes upstream of both the *asbA* start codon and *fpuAB* (petrobactin receptor and permease, respectively) (53, 54). The *fatDCE* operon encoding petrobactin import proteins (Figure 1.4) also maintains the Fur-box consensus sequence (53). This is contrary to observed microarray data of *B. anthracis* Sterne grown in iron limiting medium where *asbABCDEF* and *fpuAB* transcript levels were not significantly altered, but *fatDCE* was significantly induced (17, 55). Investigation of bacillibactin and petrobactin regulation by Lee *et al.* found that increasing iron concentration decreased supernatant levels of petrobactin, corresponding with changes in transcript levels as measured by qRT-PCR (56). However, *asbABCDEF* transcripts were detected during growth in all tested media while bacillibactin biosynthesis transcripts (*dhb* operon) were completely abrogated in high iron conditions and rich media (56). It is possible that the predicted Fur binding sites for *fpuAB* and *asbABCDEF* are weak allowing for partial, but not complete, regulation of biosynthesis by iron.

In addition to cytoplasmic levels of iron, oxidative stress appears to play a role in petrobactin regulation and biosynthesis. Increases in oxidative stress, due to high aeration or the addition of paraquat, stimulate a dose-dependent accumulation of petrobactin in the supernatant (56). Accordingly, *asb* transcripts are upregulated during exposure to high aeration, paraquat, or hydrogen peroxide, regardless of iron levels (56, 57). This pattern differs from that of Fur and Fur-regulated operons, such as bacillibactin biosynthesis, which are upregulated only in response to paraquat (56, 57). Iron import may aid in the oxidative stress response, as paraquat doubles the amount of iron associated with the cell in only sixty minutes (58). In the context of a deficient oxidative response (*i.e.*, *sodA1* mutant strain), however, *B. anthracis* shows a decrease in supernatant petrobactin levels with paraquat addition (56, 59). Lee *et al.* predicted this was due to the sensitivity of petrobactin biosynthetic machinery to oxidative stress (56).

Siderophore biosynthesis in *B. anthracis* is also linked to temperature. Petrobactin is detected in the supernatant under all conditions tested, with amounts increasing at 30°C and at 37°C while bacillibactin production is decreased above 30°C and completely abrogated at 37°C (60, 61). Lastly, Wilson *et al.* observed that petrobactin production is increased (and bacillibactin decreased) when *B. anthracis* is cultured in the presence of 5% CO<sub>2</sub>, an atmosphere encountered during growth in the host (62). We note that the environmental conditions resulting in maximal petrobactin biosynthesis (oxidative stress, 37°C and 5% CO<sub>2</sub>) correspond with those expected to be present in the context of a mammalian host.

While many factors (iron concentration, oxidative stress, temperature, and atmosphere) affect petrobactin production, the full mechanism remains undefined. Transcript levels between high and low iron conditions do not appear to vary greatly, but supernatant levels of petrobactin do (17, 56). This indicates one or more complex mechanisms of post-transcriptional or post-translational regulation of petrobactin biosynthesis. Since petrobactin-deficient mutant spores germinate but are unable to outgrow in iron-deplete medium (IDM) or macrophages, it is possible the constitutive expression of low levels of petrobactin allow for inclusion into the spore body (16, 63). Thus, rapid germination can occur inside the iron-limiting host environment.

### Petrobactin Transport Across Membranes

Siderophore import requires a dedicated receptor, triggering uptake by specific import machinery (2). An ATP-binding cassette (ABC) transporter mediates petrobactin import (64). This importer consists of the surface receptor, FpuA (Figure 1.4, orange) that associates with multiple, specific permeases and ATPases to form three distinct ABC transporters (63, 64). These are composed of combinations of the two permeases, FpuB and FatCD (Figure 1.4, blue),

and three ATPases: FpuC, FpuD and FatE (Figure 1.4, green) (64). Interestingly, either the FpuC or FpuD ATPase can provide energy for the FpuB permease based transporter, while the FatCD permease can only function with the FatE ATPase (64). Inability to import petrobactin leads to a severe growth defect in iron-depleted medium, similar to petrobactin biosynthetic mutants, and accumulation of petrobactin in the supernatant (63, 64). These mutants are also severely attenuated in a mouse model of inhalational anthrax, the LD<sub>50</sub> of the *fpuA* mutant strain is three logs greater than wild-type *B. anthracis* (63). While the proteins involved in petrobactin import are identified, questions remain about how those proteins interact *in vivo* and the molecular mechanisms of petrobactin import.

While petrobactin import has been characterized, the mechanism of apo-petrobactin export following biosynthesis (or iron removal by reduction, if it occurs) in *B. anthracis* is unknown (Figure 1.4, red). Similar to import, siderophore export occurs via dedicated transporters, the type of transporter family employed varies by siderophore and pathogen, however (2). We hypothesize from sequence data that petrobactin export from *Marinobacter* spp. occurs from multidrug and toxic compound extrusion (MATE) family transporters located adjacent to the biosynthesis operon. In addition to the MATE family, other types of inner membrane transport proteins, including the resistance nodulation and cell division (RND), major facilitator superfamily (MFS) and ABC transport families, are responsible for export of siderophores in other organisms (2). Hydroxamate siderophores, such as achromobactin and vibrioferrin, are exported via MFS exporters (2). In contrast, pyoverdine, a hydroxamate/catechol mixed siderophore, is exported to the periplasm by an ABC-type transporter (65). It is difficult to hypothesize which transporter family a petrobactin exporter would belong to due to the unique structure and charge properties of different siderophores.

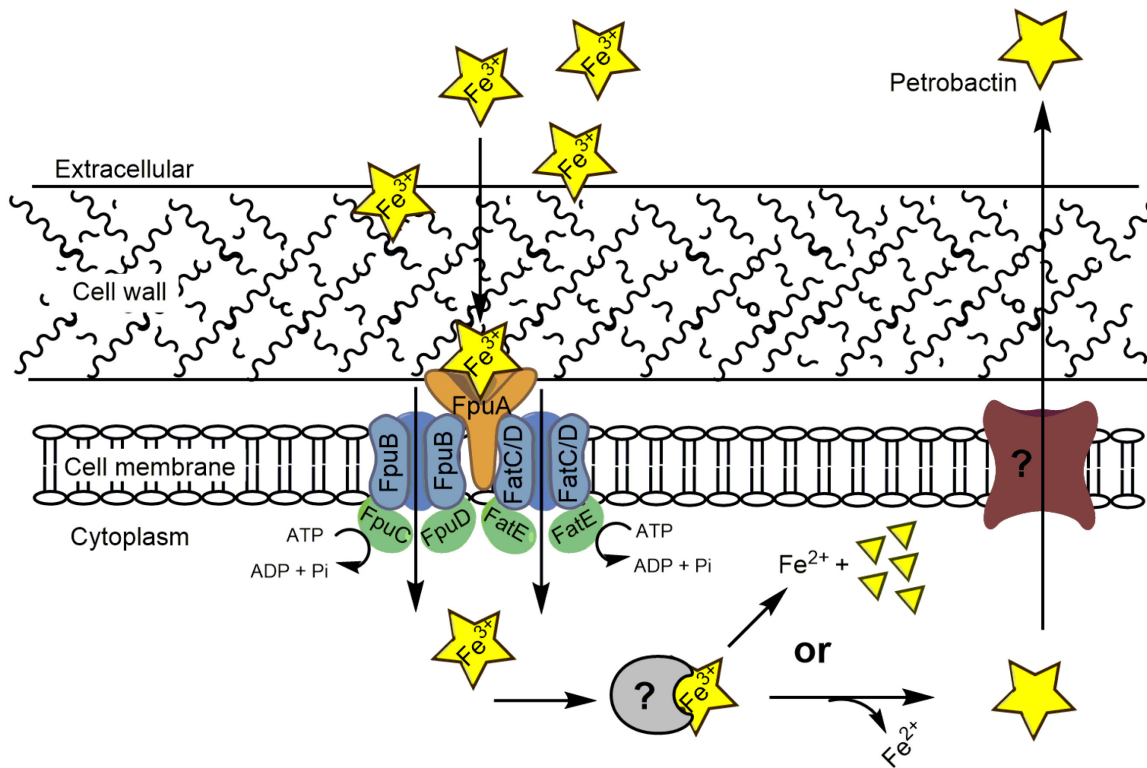


**Figure 1.4 Proposed schematic of petrobactin import, export and iron removal in *B. anthracis*.** Petrobactin (yellow star) is exported via an unknown mechanism. In the supernatant, petrobactin chelates ferric iron and is bound for import by the cell surface recognition protein FpuA (orange). The Fe-petrobactin is then transported by either of two permeases (blue) FpuB or FatCD complexed with an ATPase (green). Energy for transport via FpuB is provided by either FpuC or FpuD while FatCD complexes with the ATPase FatE. The iron is removed from petrobactin by an unknown mechanism (gray) resulting in reduction of iron from intact or hydrolyzed petrobactin (63, 64).

### Iron Release from Petrobactin

There are two possible fates for enzymatic removal of iron from the siderophore, metal reduction or siderophore hydrolysis. The mechanism for iron removal from petrobactin is unclear, but probably occurs by one of these two mechanisms (Figure 1.4, gray). Enzymatic hydrolysis of the siderophore backbone in the cytoplasm precedes enzymatic reduction of the iron for incorporation into cellular components. This method is required for siderophores with very high affinities for ferric iron and has been demonstrated in siderophores containing a

triacetate backbone such as enterobactin and salmochelin. In these cases, cleavage occurs at ester sites located on the backbone, requiring specific action by esterases including Fes, IroD and IroE (2, 66). Although petrobactin lacks an ester site, cleavage could occur by amide hydrolysis at the citrate/spermidine junctions.

Enzymatic reduction of the iron to its ferrous state lessens the affinity of the siderophore for the substrate. This allows the siderophore to remain intact during iron removal and be recycled extracellularly (2). This has been demonstrated in siderophores with ferric stability constants less than 30pM, *e.g.* reduction of ferric-ferrioxamine B by FhuF in *E. coli* (67). As the stability constant of petrobactin is 23pM and hydrolysis of amides is more difficult (thus costlier) than ester hydrolysis, I hypothesize iron removal from petrobactin occurs via reduction, not hydrolysis. Central to addressing the question is understanding whether petrobactin is fully imported into the cell for iron removal. In the case of *Pseudomonas aeruginosa*, pyoverdine is only imported as far as the periplasm where it undergoes reduction for removal of the iron and is re-exported from the cell (68). It is possible ferric-petrobactin is reduced by an unknown enzyme after capture by FpuA then released back to the extracellular milieu for re-use. The identified ABC transporters would be responsible for importing the iron. That seems unlikely, however, for a few reasons. First, it would be more efficient to use the ferrous iron transporter, FeoB, than dedicated permeases. Second, growth of *B. anthracis* in the presence of non-reducible gallium negatively impacts growth. This requires transport of gallium into the cell by petrobactin, thus implying full import of petrobactin-Fe. Third, there is no evidence for this mechanism in Gram-positives (63, 64).

## Petrobactin and Pathogenesis

Petrobactin is the only method of iron acquisition required for full virulence in a murine model of inhalational anthrax (16). Indeed, petrobactin null strains, whether driven by lack of biosynthesis (*asbABCDEF* mutant strain) or import (*fpuA* mutant strain), exhibit a two to three log decrease in LD<sub>50</sub> (16, 63). Mutants defective in bacillibactin or heme utilization demonstrate little to no effect on virulence (16, 17, 69). What makes petrobactin more relevant to *B. anthracis* pathogenesis? We attribute it to regulation and structural features that enable avoidance of the innate immune response and increased iron acquisition.

Studies of petrobactin regulation indicate that conditions relevant to host physiology (5% CO<sub>2</sub> and 37°C) increase petrobactin production but decrease bacillibactin production (60–62). The differences in petrobactin and bacillibactin regulation reflect what is known about the contribution of petrobactin to iron acquisition in the mammalian host over bacillibactin. In addition to iron sequestration, neutrophils produce a protein known as siderocalin or lipocalin (70). Siderocalin directly interferes with pathogen iron acquisition by binding siderophores (70). It is capable of binding to ferric-enterobactin and ferric-bacillibactin but not glycosylated enterobactin (salmochelin), as glycosylation makes the siderophore too large for the binding pocket (71). Ferric-petrobactin is the correct size and charge to be bound by siderocalin (71). However, siderocalin did not recognize petrobactin in *in vitro* studies leading to its designation as the anthrax “stealth siderophore” (71). Abergel, *et. al.* predicted that the orientation of the 3,4-DHB moieties creates a steric hindrance, thus preventing interaction with the rigid binding pocket of siderocalin (71). Another interesting feature of the 3,4-DHB moieties is that they appear to improve sequestration of ferric iron away from transferrin (24). While enterobactin has a higher overall affinity for ferric iron, petrobactin removes Fe<sup>3+</sup> from transferrin up to six times

more rapidly than enterobactin and 100 times more quickly than the hydroxamate/ $\alpha$ -hydroxycarboxylate aerobactin (24). The authors hypothesized the 3,4-DHB moieties were responsible for this phenomenon. The catechol moieties improve affinity for iron over hydroxamate moieties, hence the increased rate compared to aerobactin (24). Since the overall affinity of petrobactin is still lower than enterobactin, perhaps the unique orientation of the hydroxyl groups provide an increased rate of transfer (24). Avoiding sequestration by siderocalin, and thus detection of the innate immune response, together with an increased ability to retrieve ferric iron from transferrin help account for petrobactin's relevance in *B. anthracis* pathogenesis.

### A Target for Antibiotics?

The unique structure of petrobactin confers multiple advantages within the mammalian host environment, and this along with the patterns of regulation, support extrapolation of murine data to the human host. As is the case with other siderophore-producing pathogens, such as *Mycobacterium tuberculosis*, this implies petrobactin use (inclusive of biosynthesis, transport and iron removal) is a viable target for rational anti-*anthracis* drug design (72). To date, two studies have reported the generation or identification of small molecules targeting petrobactin biosynthetic machinery. First, a rationally-designed acylsulfate analogue of 3,4-DHB-AMP can compete for 3,4-DHB binding to AsbC with submicro-molar affinities (45). More recently, two small molecules termed baulamycin A and baulamycin B, were found to be potent inhibitors of AsbA activity *in vitro* and of *B. anthracis* growth in both IDM and IDM supplemented with 20 $\mu$ M iron, or iron-replete medium (IRM) (73). These compounds have yet to be tested in animal models. Regardless, the requirement of petrobactin for virulence in *B. anthracis*, and for

siderophores in other pathogens, warrants further exploration of small molecules that can inhibit siderophore production and/or use. In addition, the possibility of exploiting this necessity through the generation of petrobactin-drug conjugates is an intriguing prospect in the quest for new antibiotics.

### Summary and Future Directions

This review summarized the current knowledge about petrobactin in the context of the pathogen, *Bacillus anthracis*. Interestingly, recent studies have revealed many features of petrobactin regulation, biosynthesis, structure and transport that are unusual, or even unique, in the field of bacterial siderophores. Together, these features enable *B. anthracis* to produce a siderophore under relevant host conditions, that not only gathers the requisite iron for growth, but does so efficiently while “flying under the radar” of host innate immunity. However, many gaps remain in the current body of knowledge about petrobactin. These include identification of the mechanisms responsible for apo-petrobactin export, iron-removal from holo-petrobactin and regulation of petrobactin biosynthesis. Future research into petrobactin use by *B. anthracis* should focus on addressing these issues and may reveal other non-canonical methods for siderophore acquisition systems. In addition to broadening the field of siderophore research, understanding the “life cycle” of petrobactin use by *B. anthracis* is key for the continued development of targeted antimicrobial therapies.



## Chapter 2

### Petrobactin is exported from *Bacillus anthracis* by the RND-type exporter

#### ApeX

#### Abstract

*Bacillus anthracis*—a Gram-positive, spore-forming bacterium—causes anthrax, a highly lethal disease with high bacteremia titers. Such rapid growth requires ample access to nutrients, including iron. However, access to this critical metal is heavily restricted in mammals, which requires *B. anthracis* to employ petrobactin, an iron-scavenging small molecule known as a siderophore. Petrobactin biosynthesis is mediated by *asb* gene products, and import of the iron-bound (holo)-siderophore into the bacterium has been well studied. In contrast, little is known about the mechanism of petrobactin export following its production in *B. anthracis* cells. Using a combination of bioinformatics data, gene deletions, and laser ablation electrospray ionization mass spectrometry (LAESI-MS), I identified a resistance-nodulation-cell-division-type transporter, termed Apex, as a putative petrobactin exporter. Deleting *apeX* abrogated export of intact petrobactin, which accumulated inside the cell. However, growth of the *apeX* mutant strain in iron-depleted medium was not affected and virulence in mice was not attenuated. Instead, petrobactin components were determined to be exported through a different protein, which enables iron transport sufficient for growth, albeit with a slightly lower affinity for iron. This is the first report to identify of a functional siderophore exporter in *B. anthracis* and the *in vivo* functionality of siderophore components. Moreover, this is the first application of LAESI-MS to sample a

virulence factor/metabolite directly from bacterial culture media and cell pellets of a human pathogen.

## Introduction

Nearly all cellular life requires iron for growth. The redox potential of iron enables efficient electron transfer, making it a useful cofactor for proteins functioning in processes such as ATP generation, DNA replication, and electron transfer. Harnessing iron for cellular growth, however, comes at a cost since free iron can undergo Fenton-type chemistry whereby the reductive properties create damaging superoxide radicals (74). To prevent cellular damage, mammals tightly sequester iron with iron-binding proteins such as transferrin, ferritin and lactoferrin. This reduces the pool of free ferric iron to less than  $10^{-18}$ M and prevents iron from being readily accessed by invading bacterial pathogens (4). Iron acquisition is a growth-limiting step for nearly all bacterial pathogens and is frequently overcome by the production of siderophores (2). Siderophores are small molecules biosynthesized by bacteria during low iron stress, and are exported from the cell to scavenge ferric iron from the environment. In addition to siderophore biosynthesis operons, such pathogens must also encode dedicated proteins for unbound, or apo, siderophore export, iron-bound siderophore import, and iron release (2).

*Bacillus anthracis*, is a Gram-positive, spore-forming bacillus with three operons encoding active iron acquisition systems: one for heme acquisition plus two siderophores, bacillibactin and petrobactin (16, 61, 75). Exposure to *B. anthracis* spores can result in either inhalational, gastrointestinal, injectional or subcutaneous anthrax, varying by the route of infection (6, 76). Using antigen presenting cells as Trojan Horses, *B. anthracis* can quickly reach the blood or lymph. Once in the blood, *B. anthracis* grows quickly, reaching septicemic loads as

high as  $10^8$  CFUs per mL (6, 7, 9). Such rapid growth requires an ample supply of nutrients, including trace elements like iron.

Of the three systems encoded for by *B. anthracis*, only the siderophore petrobactin has been shown to be required for virulence in murine models of inhalational anthrax (16). Since its description, the *B. anthracis* petrobactin biosynthesis operon, *asbABCDEF* (anthrochelin biosynthesis (16)) and petrobactin have been well studied (77) and explored as a drug target (73). Extracellular  $\text{Fe}^{3+}$ -petrobactin is recognized by its surface receptor FpuA and imported by the action of redundant, ATP binding cassette (ABC) transporters (permeases—FpuB, FatC/D; ATPases—FpuC, FpuD, FatE) (63, 64).

In general, and relative to siderophore import systems, export systems of siderophores remain under described. Currently, the mechanism of iron-free petrobactin export has not been identified. In described systems from other pathogens, siderophore export across the cell membrane can occur through dedicated proteins from transporter families including: ABC, multi-facilitator superfamily (MFS), and resistance-nodulation-cell division (RND) (2).

ABC-type transporters consist of a permease and ATPase, which powers transport of the ligand via ATP. While import ABCs typically encode separate polypeptides for each domain, exporter ABC transporters often have a single polypeptide encoding both permease and ATPase domains (78). ABC-type siderophore exporters include: the *Mycobacterium smegmatis* exochelin exporter ExiT, the *Salmonella enterica* salmochelin exporter IroC, and the *Pseudomonas aeruginosa* pyoverdine exporter PvdE (65, 79, 80).

MFS-type transporters are characterized by the MFS fold, 12 transmembrane helices split into the N and C domains. Transport is catalyzed by antiport or symport, whereby two or more ligands are transported in either opposing or parallel directions, frequently by the proton motive

force (81). MFS siderophore exporters include: *Staphylococcus aureus* NorA, *Azotobacter vinelandii* protochelin exporter CsbX, and the *Escherichia coli* enterobactin exporter EntS (82–84).

RND-type exporters resemble MFS transporters in structure but are often found in Gram-negative bacteria where they form an export complex with a periplasmic protein and an outer membrane transporter (85). This is the case in *E. coli* where following enterobactin export into the cytoplasm by EntS, extracellular export is facilitated by three RND-type efflux systems, each complexed with the outer membrane channel TolC (86). The cell membrane mycobactin and carboxymycobactin exporters in *Mycobacterium tuberculosis*, MmpL4/L5, were the first reported RND-type siderophore transporters (87). While the outer membrane efflux channel is unknown, MmpL4 and MmpL5 require the action of cognate periplasmic accessory proteins, MmpS4/S5, to facilitate biosynthesis and recycling of its siderophores (87, 88).

The *B. anthracis* genome does not contain evident siderophore accessory genes near the *asb* operon (the receptor, permease, and ATPases are located elsewhere on the genome). Thus, I developed a bioinformatics-based protocol to identify petrobactin exporter candidates. From this list, marker-less deletions were made and screened for their ability to grow in iron-limiting medium and to export petrobactin. To screen my mutants, Ashu Tripathi and I adapted laser ablation electrospray ionization mass spectrometry (LAESI-MS) for detection of bacterial metabolites, specifically petrobactin. Previous studies have used complex sample extraction techniques coupled with analytical methods, including thin layer chromatography or mass spectroscopy, to screen for the presence or absence of petrobactin in a sample (16, 18, 60, 61, 63, 64, 89). But such extensive sample preparation presented a bottleneck to high-throughput

analysis and introduced experimental error, reducing our ability to quantify petrobactin and related molecules in a large sample set.

LAESI is an ambient ionization technique for mass spectrometry that uses an infrared laser and relies on the water present in the sample as a makeshift matrix to promote ion formation (90). The energy from the irradiated sample generates a fine plume of mostly neutral droplets. The analytes in the plume are subjected to charge transfer by a mist of electrosprayed buffer, which ionizes and propels them to the mass spectrometer for mass-to-charge ( $m/z$ ) analysis. The majority of LAESI applications to-date have focused on mass spectrometry imaging of plant and animal tissues, though recent studies have used LAESI to sample and identify bacterial metabolites from roadkill and soybean microbiomes (91–96). Thus, the application of LAESI-MS for the identification of the import/export gene partners for bacterial metabolites has not been explored.

Using LAESI-MS as a high-throughput, high accuracy analysis for petrobactin detection, I directly demonstrate petrobactin in the cells and supernatant of predicted exporter mutants. These results were confirmed using liquid chromatography high resolution electrospray ionization mass spectrometry (LC-HRESIMS). Through this novel application of LAESI-MS I identified the apo-petrobactin exporter (ApeX), a member of the RND-type transporter family, and observed the export of petrobactin components in its absence. I also show that these siderophore components can bind and transport sufficient iron for growth and are therefore, relevant to disease in a murine model of inhalational anthrax.

## Materials and Methods

*Bacterial growth conditions and sporulation* – Strains used are described in Table 2.1. All mutants were derived from *Bacillus anthracis* Sterne 34F2 (pXO1<sup>+</sup>, pXO2<sup>-</sup>) and generated by allelic exchange, as described by Janes and Stibitz (97). Complementation of GBAA\_2407 was generated by PCR amplification and Gibson cloning (New England Biolabs) of the gene into pMJ01 under control of the native promoter (98). All necessary primers are listed in Table 2.2. Modified G medium was used for the generation of *B. anthracis* spores at 37°C for 72 hours (99). Spores were collected at 2,800rpm then washed and stored in sterile water at room temperature following heat activation at 65°C. Bacterial strains were plated on BHI (Difco) and grown in BHI at 30°C overnight. Overnight cultures were back diluted 1:50 into fresh BHI and incubated at 37°C for one hour. To remove contaminating iron and prepare the cells for growth in iron-depleted medium (IDM), the cells were pelleted at 2,800rpm for 10 minutes (Centrifuge 5810 R, Eppendorf) and washed in 1mL of fresh IDM five times (16). 25mL of IDM was inoculated at a starting optical density of 600nm (OD<sub>600</sub>) of 0.05 and grown at 37°C with hourly measurements for five to six hours. Strains containing the complementation plasmid were grown in the presence of 10µg/mL chloramphenicol. Media and chemicals were purchased from Fisher Scientific or Sigma Aldrich.

*Catechol measurement* – The Arnow's catechol assay was used to measure catechol rings in IDM culture media (100). Beginning at three hours post-inoculation, 300µL of each culture was pelleted at 13,000rpm (Centrifuge 5415 R, Eppendorf) for one minute and pipetted into three, 40µL aliquots in a clear 96-well plate. To each well, 40µL of 0.5M HCl, 40µL of nitrate-molybdate reagent (10% sodium nitrate and 10% sodium molybdate) and 40µL 1N NaOH were

added sequentially. The absorbance was measured at 515nm in a SpectraMAX M2 spectrophotometer and subtracted from a medium blank. Data are presented as per cent wild-type after being normalized according to cell density as measured by OD<sub>600</sub>.

*Cell viability* — Cell viability was measured using the LIVE/DEAD BacLight kit (Invitrogen). Briefly, 300µL aliquots were taken from *B. anthracis* Sterne cultures grown in IDM for four hours. The cells were pelleted for one minute at 13,000rpm, washed once and re-suspended in an equal volume of sterile phosphate-buffered saline. 100µL aliquots were distributed into three wells of a 96-well black, clear-bottomed microtiter plate. An equal volume of 2x Cyto9/propidium iodide was added to each well, then incubated in the dark for 15 minutes. Florescence was measured at 530nm and 630nm (Excitation 485) in a SpectraMAX M2 spectrophotometer. Data are presented as a live/dead ratio (530/630).

*Gallium supplementation* — In IDM, each strain was used to inoculate two flasks. One was supplemented with 20µM GaSO<sub>4</sub> in 0.1% nitric acid at both zero and two hours post-incubation, the second was left untreated. They were grown at 37°C for four hours. Data are presented as per cent growth of the untreated control at four hours  $\left( \frac{Treated\ 4hr\ OD600}{Untreated\ 4hr\ OD600} \times 100 \right)$ .

*Culture medium supplementation* — For each strain, the appropriate number of flasks containing 15mL IDM plus 10mL filter-sterilized spent IDM were inoculated at identical starting optical densities no less than OD<sub>600</sub> of 0.01. Spent culture media were obtained from IDM cultures grown as indicated above but which had their culture media collected at five hours, filter-sterilized with a 0.22µm filter and stored at -80°C. The culture-medium-supplemented cultures

were grown at 37°C for five hours. Data are presented as per cent increased growth relative to the fresh IDM-only control at five hours  $\left(\frac{Treated\ 4hr\ OD600 - Untreated\ 4hr\ OD600}{Untreated\ 4hr\ OD600} \times 100\right)$ .

*Dipyridyl and precursor supplementation* — 3mL of IDM was inoculated with the appropriate strain for a starting OD<sub>600</sub> of 0.05 (WPA biowave CO9000 Cell Density Meter) and supplemented with the indicated concentrations of either 2,2'-dipyridyl, citrate, spermidine, or 3,4-dihydroxybenzoate. Stock solutions were suspended in water and filter-sterilized. Cultures were grown at 37°C with shaking for five hours. Data are presented as per cent increased growth relative to the IDM-only control at five hours  $\left(\frac{Treated\ 4hr\ OD600 - Untreated\ 4hr\ OD600}{Untreated\ 4hr\ OD600} \times 100\right)$ .

*LAESI-MS* – For analysis, culture media and pellets were collected from cultures grown in IDM for four and five hours. Culture media were separated from the cells by centrifugation then frozen at -80°C until analysis. Pellets were washed in an equal volume of fresh IDM and frozen at -80°C. After thawing at room temperature, the pellets were re-suspended in 30µL of water for analysis. 20µL of each sample were plated in triplicate wells of shallow 96-well plates and subjected to laser-based ablation. Here, the sample is heated by irradiation from a 2940nm infrared laser, leading to vaporization of molecules from the surface. The process initiates a dynamic equilibrium between energy deposition and consumption of the vaporization process. Any shift towards larger deposition of energy (such as re-entry of the vaporized droplets) results in expulsion of a second plume, which is primarily responsible for ablation efficiency. During method development, the data obtained from the first well positions of a 96-well plate varied greatly compared to other columns. A possible cause for this phenomenon are air currents created by movement of the LAESI stage, which might disrupt the ion sampling. To offset this



observed stage effect, the initial wells in each column were left either blank or filled with water. The ESI mass spectrograph was obtained using a ThermoFisher LTQ XL mass spectrometer, containing an atmospheric pressure ionization stack with a tube lens and skimmer, three multipoles, a single linear trap configuration and a set of two electron multipliers with conversion dynodes. The mass spectrometer was connected to a Protea LAESI DP-1000 instrument with an ESI electrospray emitter for ambient ionization. The collected data points were exported to Gubbs™ Mass Spec Utilities (101) and processed using Generic Chromatographic Viewer for individual  $m/z$  (ThermoFisher Scientific).

*LC-HRESIMS* – For final confirmation of our findings from LAESI-MS, HRESIMS spectra was acquired using an Agilent 6520 Q-TOF mass spectrometer equipped with an Agilent 1290 HPLC system at the Life Sciences Institute core facility. For this analysis, cultures were grown in IDM for five to six hours and 20mL of culture medium was collected by filter sterilization through a 0.22 $\mu$ m filter then stored at -80°C. Culture media were dried down (Labconco Freeze Dry System) and the pellet re-suspended in 1mL of ACS grade methanol. Undissolved particulates were removed by centrifugation at 5000xg for one minute and the supernatant used for analysis. Reverse-phase HPLC was performed using Luna® 5 $\mu$ m C18(2) 100 Å, 100x2mm HPLC column and a solvent gradient from 30% water (plus 0.1% formic acid) to 90% methanol (plus 0.1% formic acid) over 16 minutes.

*Murine infections* – Five, six to eight-week-old, female DBA/J2 mice (Jackson Laboratories) were infected intra-tracheally with  $1.5 \times 10^5$  spores as described in Heffernan et. al, 2007 (102). Prior to infection, spores were passed through a 3.1 micron glass microfiber filter (National

Scientific Company) to increase purity and reduce clumping, then counted by hemocytometer. Mice were monitored for morbidity for 14 days post-infection and euthanized when moribund. All mouse experiments were performed using protocols (PRO00007362) approved by the University of Michigan Committee on the Use and Care of Animals.

Table 2.1 Strains of *Bacillus anthracis* Sterne 34F2 used in this work

Strain	Relevant characteristics	Reference
<i>Bacillus anthracis</i> Sterne 34F2 Wild type (pXO1 <sup>+</sup> , pXO2 <sup>-</sup> )		Sterne, 1939
34F2, $\Delta$ asbABCDEF	Petrobactin biosynthesis mutant	Lee et al., 2007
34F2, $\Delta$ asbA		Pfleger et al., 2008
34F2, $\Delta$ asbB		Pfleger et al., 2008
34F2, $\Delta$ asbC		Pfleger et al., 2008
34F2, $\Delta$ asbD		Pfleger et al., 2008
34F2, $\Delta$ asbE		Pfleger et al., 2008
34F2, $\Delta$ asbF		Pfleger et al., 2008
34F2, $\Delta$ fpuA	Petrobactin receptor mutant	Carlson, et al., 2010
34F2, $\Delta$ GBAA_3296		This work
34F2, $\Delta$ GBAA_1642		This work
34F2, $\Delta$ 1642 $\Delta$ 3296		This work
34F2, $\Delta$ GBAA_2407		This work
34F2, $\Delta$ GBAA_1302		This work
34F2, $\Delta$ 2407 $\Delta$ 1302		This work
34F2, $\Delta$ 2407 pAH001	$\Delta$ GBAA2407 + pAH001	This work
34F2, $\Delta$ 2407 p2407	$\Delta$ GBAA2407 + 2407pAH001	This work
34F2, $\Delta$ GBAA_0181		This work
34F2, $\Delta$ GBAA_0787		This work
34F2, $\Delta$ GBAA_4961		This work
34F2, $\Delta$ GBAA_5668		This work
34F2, $\Delta$ GBAA_0835		This work
34F2, $\Delta$ GBAA_1858		This work
34F2, $\Delta$ GBAA_2004		This work
34F2, $\Delta$ GBAA_3157		This work
34F2, $\Delta$ 0835 $\Delta$ 1858		This work
34F2, $\Delta$ 4961 $\Delta$ 5668		This work
34F2, $\Delta$ GBAA_0852		This work
34F2, $\Delta$ GBAA_0528		This work
34F2, $\Delta$ GBAA_1652		This work
34F2, $\Delta$ GBAA_5411		This work
34F2, $\Delta$ GBAA_2346		This work
34F2, $\Delta$ GBAA_4504		This work
34F2, $\Delta$ GBAA_4595-96		This work
34F2, $\Delta$ 0528 $\Delta$ 0852 $\Delta$ 5411		This work

**Table 2.2 Primers used to generate mutant strains used in this work**

<b>Primer</b>	<b>Sequence (5'→3')</b>
GBAA_1302-GibsP1	AAGTTGATAAGTGGGGGAAGGTAACCTGGTGCCTTTACTG
GBAA_1302-GibsP2	AAAGCAAACGCACCAGTTACCTTCCCCACTTATCAACTTTATGTACA
GBAA_1302-GibsP3	GAACAAAAGCTGGAGCTCCACCGCGGTGGCCGGTGCCTGTTATAAGTTTACTTGTTTTTTG
GBAA_1302-GibsP4	GATATCAGATCTGACGTCTCTAGAGCGGCCCGGATCACTTCTTGTATTTTGTAACTCATC
GBAA_1302-P5	GGCGTTACAGTGATGG
GBAA_1302-P6	GTCATTTTCGCACCATT
GBAA_2407-P1	CATCCGTTACATATGTTAGGGGAAGTACAAAAGGTGGATGC
GBAA_2407-P2	GCATCCACCTTTTGTACTTCCCCTAACATATGTAACGGATG
GBAA_2407-GibsP3	GAACAAAAGCTGGAGCTCCACCGCGGTGGCCTTTAATTGTTCTTCAGATAAAGATAGTTTTGC
GBAA_2407-GibsP4	GATATCAGATCTGACGTCTCTAGAGCGGCCGTAATATCAACATTTACTGTCATACTAAACG
GBAA_2407-P5	CCAATAAAAAGAAACGATTT
GBAA_2407-P6	CTCGGGATCATTTCCT
2407 MJcomp F	CAATAAATGTCCTGTTAAAGGAGGTGTTTTCTAGAATGAAAAAGCATCCGTTACATATG
2407 MJcomp R	GAAGCTCGGCGGATTTGTCCTACTCAAGCTCTATGCATCCACCTTTTGTACTTCTTC
GBAA-1642 P1	ATAGTAATGTAATGAAGAAAATCCCCTTGAGCAAGTA
GBAA-1642 P2	TCTTCATTACACTACTATTTTGCTCCTTTTTTCAACG
GBAA-1642 P3	CGCGCGCCGCTACTACATTCATTCGTTGCAAAAAA
GBAA-1642 P4	CGCGCGCCGCGTTATTACATGTTTGCATTTAATCC
GBAA_1642-GibsP1	AAAAGTTTATTTATCCATTAAACATGGCAGGAGAGAAG
GBAA_1642-GibsP2	GCCATGTTTAAATGGGATAAATAAACTTTTTAATTGGTTTTTCTCTTAATT
GBAA_1642-GibsP3	GGAACAAAAGCTGGAGCTCCACCGCGGTGGCCTTATTTTCTGGAGATATCGGTGTAACCTG
GBAA_1642-GibsP4	GGATATCAGATCTGACGTCTCTAGAGCGGCCCTATTCAACAAAATAAATCGTTTTATTCTCG
GBAA_1642 P5	GAGGCAAATGGATGATAG
GBAA_1642 P6	CATTTAATCCTTACAAAATTAAGC
GBAA_3296 P1	GAAATCAAATATGTAGAATAGAAGATGAAAAATGATAT
GBAA_3296 P2	CATCTTCTATTCTACATATTTGATTTCCCCTTTTATTG
GBAA_3296 P3	CGCGCGCCGCGCAGCAGTTAGCAAAAAGCTAACTACTC
GBAA_3296 P4	CGCGCGCCGCTTTTCAAGAAAAGGTATAGGTAAA
GBAA_3296 P5	CATCATTTTGGAACATACTTAATAA
GBAA_3296 P6	AATTATTGGATTTATAGACTTATGA
GBAA_0181-GibsP1	CGGGTGCATCTCTAGCACAGGAGGTTTAAATGTATAAAGAAGAGCTGATTCA
GBAA_0181-GibsP2	CTTCTTTATACATTAACCTCCTGTGCTAGAGATGCACCCGTTT
GBAA_0181-GibsP3	GAACAAAAGCTGGAGCTCCACCGCGGTGGCGACCAACTTCAAGTAGTAAAGAGGCAC
GBAA_0181-GibsP4	GATATCAGATCTGACGTCTCTAGAGCGGCCGATCAATATCTTCTAACATGCTCGTCCG
GBAA_0181 P5	GCCCATACTGTTATCTATGC
GBAA_0181 P6	CGTTTATAGTATGTCGATGCTG
GBAA_0787-GibsP1	GCAATAAGTAGTAGAGAGGGGCCAATGTAACAGTCAAGGAAGG
GBAA_0787-GibsP2	CCTTGACTGTTACATTGGCCCTCTCTACTACTTATTGCTTTCTGTT
GBAA_0787-GibsP3	GAACAAAAGCTGGAGCTCCACCGCGGTGGCCGATCTAGAATATCGCGAAGACGATC
GBAA_0787-GibsP4	GATATCAGATCTGACGTCTCTAGAGCGGCCGAAAAACGATAAATCGTTATATGAAATACC

GBAA_0787 P5	CGTACCGATGTTTCGC
GBAA_0787 P6	CAATTTTAAAGCCATACGG
GBAA_4961 P1	GCGATTCTGTAATTTTATCGCACGTTATTTATATGAGCACTTTC
GBAA_4961 P2	GAAAGTGCTCATATAAATAACGTGCGATAAAAATTACAGAATCGC
GBAA_4961 P3	GCGGCCGCGCGCCAAGCTGGACAAGTTTCTC
GBAA_4961 P4	GCGGCCGCGCGCAAGGCTAAGTGTCCATC
GBAA_4961 P5	GAACAACCTATTCCAGCGC
GBAA_4961 P6	CGGCTGGAACATCC
GBAA_4504-GibsP1	GTAACCTTTTATATGCAGGGGGTGCATTTTTATGGAAGAAGAAAAAAC
GBAA_4504-GibsP2	CTTCTTCCATAAAATCGCACCCCCTGCATATAAAGAGTTACGTAAAAAGTC
GBAA_4504-GibsP3	GAACAAAAGCTGGAGCTCCACCGCGGTGGCCCGGCAACTGTGTTGAAGTTG
GBAA_4504-GibsP4	GATATCAGATCTGACGTCTCTAGAGCGGCCGTTGCCACAATATTTGTGAGCAAC
GBAA_4504 P5	CGGCAACTGTGTTTG
GBAA_4504 P6	GTTGCCCAATATTTGTG
GBAA_2346 GibsP1	GACTTTAGGCTAAAACATGCGTCTTTTTATCATTGCATATGGAGGC
GBAA_2346 GibsP2	CATATGCAAATGATAAAAAGACGCATGTTTTAGCCTAAAGTCCTATC
GBAA_2346 GibsP3	GAACAAAAGCTGGAGCTCCACCGCGGTGGCGTAATGCAGGAGAGGCCCTG
GBAA_2346 GibsP4	GATATCAGATCTGACGTCTCTAGAGCGGCCCTTTTTGCCTAATTGCTGTTTACAAAAAAC
GBAA_2346 P5	CACACAACCGGAGACTG
GBAA_2346 P6	GCCTTTACAATATTGTGAAACTAC
GBAA_0835 P1	GAACAAAAGATGTAATAAAACCCCTTACAACGGTAAG
GBAA_0835 P2	GGGGTTTTATTACATCTTTTGTCTTTTATCGGTTTC
GBAA_0835 P3	CGCGCGGCCGCATAGAGGAATATCGTGAAATACAAG
GBAA_0835 P4	CGCGCGGCCGCCCTTTGTATTTCATATTGCTATTG
GBAA_0835 P5	ACGCAAGTAATAGATGCGGTATTTTC
GBAA_0835 P6	TTACCCCATGAAAATCACCTCCCC
GBAA_1858 P1	GTGAAAAATGTAACCTAAGTGAATGAAAAAAGGATG
GBAA_1858 P2	CACTTAGTTACATTTTTACACCTTCTTTCTTTAG
GBAA_1858 P3	CGCGCGGCCGCTGAGAAATTAGTAAGTTTTGTTAGT
GBAA_1858 P4	CGCGCGGCCGCTCCATCATAATATGACGAGAGGTTT
GBAA_1858 P5	TCATGTTAGAAAGGCTAACTCTTCT
GBAA_1858 P6	GTTAGAAACAAAGTTTAAAAACAAA
GBAA_2004 P1	GATTTAAAATGTAAAGTCTTTACAAATAAAAAAGAG
GBAA_2004 P2	GTAAAGACTTTACATTTTAAATCTTCTCCTTTTATAT
GBAA_2004 P3	CGCGCGGCCGCCTTTGGGATATTAGGTGGTAAATA
GBAA_2004 P4	CGCGCGGCCGCCAAATTATTGCGACGTTAGTCTATA
GBAA_2004 P5	GTATTTCAATTTATCCCTTACGGGCC
GBAA_2004 P6	ATCGGGAAAGCTGATGAGAAGATTC
GBAA_3157-GibsP1	CAAAATAAAAAAAGACTACTTATGCAGTACTTTATCTTTAAATTTCTAAAGATTTTTTAAAG
GBAA_3157-GibsP2	GAAATTTAAAGATAAAGTACTGCATAAGTAGTCTTTTTTTATTTTGAACGAATACTATTTTC
GBAA_3157-GibsP3	GAACAAAAGCTGGAGCTCCACCGCGGTGGCCTCTTTTAGAACTTCATATAAAGGATTTGAAATC
GBAA_3157-GibsP4	GATATCAGATCTGACGTCTCTAGAGCGGCCGACATTTTTATCCAGCTTTAGAACCTTTTATG

GBAA_3157 P5	CTCTTTTAGAACTTCATATAAAGG
GBAA_3157 P6	GACATTTTATCCAGCTTTAG
GBAA_0852-GibsP1	GTATTACTAAAGTTAAAGTGGCGAGCTGTTATTCAAATCCAGAAATTTAAT
GBAA_0852-GibsP2	GGATTTTGAATAACAGCTCGCCACTTTAACTTTAGTAATACTGAAAACAATGTAATC
GBAA_0852-GibsP3	GAACAAAAGCTGGAGCTCCACCGCGGTGGCCGATTTCTTATGAAGTTTTATTTGTATGC
GBAA_0852-GibsP4	GATATCAGATCTGACGTCTCTAGAGCGGCCATCACGCGTACTTCTTTTCCTTTTTTC
GBAA_0852 P5	GATTCTTATGAAGTTTTATTTTG
GBAA_0852 P6	CAAAGTAATATTGAAAACCGAC
GBAA_0528-GibsP1	GTAAACCATATCGATGGCATATAACAGAAACAGCTCCTTTAGCG
GBAA_0528-GibsP2	CTGTTTCTGTTATATGCCATCGATATGGTTTAAACAATTGC
GBAA_0528-GibsP3	GAACAAAAGCTGGAGCTCCACCGCGGTGGCAGTCTTGTAATCGGAGCGAATGATC
GBAA_0528-GibsP4	GATATCAGATCTGACGTCTCTAGAGCGGCCAAGTACAGTTCGCAAAAATTCGTAAGC
GBAA_0528 P5	CAATTTTAAAAGGGACACAG
GBAA_0528 P6	GAAGAAAGAAGTTACACGAAAA
GBAA_1652-GibsP1	CTTCTTAAAACAAATAAAAACGGGAACTTAGTGAAGAATCTACCATTACTTAATAG
GBAA_1652-GibsP2	GATTCTTCACTAAGTTTCCCGTTTTTATTTGTTTTAAGAAAGTGCGBAATAAG
GBAA_1652-GibsP3	GAACAAAAGCTGGAGCTCCACCGCGGTGGCGCATTTTTACTTAGGAGGATTACAATGATTAAAG
GBAA_1652-GibsP4	GATATCAGATCTGACGTCTCTAGAGCGGCCCTGTGTAACCTCCCATGTAAGCTGTTGTAAT
GBAA_1652 P5	GCATTTTTACTTAGGAGGATTAC
GBAA_1652 P6	CTTGTGTAACCTCCCATG
GBAA_5411-GibsP1	CTTACTATAAACCGGGATACAGCAGGTTATACGAAGCG
GBAA_5411-GibsP2	GTATAACCTGCTGTATCCCGGTTTATAGTAAGAAAAAATTTACGTAGC
GBAA_5411-GibsP3	GAACAAAAGCTGGAGCTCCACCGCGGTGGCGAATTTTATGATGCGCTTCAAACG
GBAA_5411-GibsP4	GATATCAGATCTGACGTCTCTAGAGCGGCCCTATATATCGACGGGACCTTCCG
GBAA_5411 P5	CCAAGAAGCGCTGAG
GBAA_5411 P6	GTAAAGAAGCACTCTAATGTCTTC
GBAA_4595/96-GibsP1	GTGAAGTAGTAAGGGAAGAGGAACAGAAGAACGTGTTACCACTGAGTTAG
GBAA_4595/96-GibsP2	GGTAACACGTTCTTCTGTTCCCTTCCCTTACTACTTCACTACTTTCCATAC
GBAA_4595/96-GibsP3	GAACAAAAGCTGGAGCTCCACCGCGGTGGCGAGCTATATGGAACGATAATGAAGAAAAGAAG
GBAA_4595/96-GibsP4	GATATCAGATCTGACGTCTCTAGAGCGGCCCTAGCATAAAGAAAACACTACAATTGAGGGG
GBAA_4595/96 P5	GAGCTATATGGAACGATAATG
GBAA_4595/96 P6	CTAGCATAAAGAAAACACTACAATTG
GBAA_5668-GibsP1	GGTGAAAGAAATTTGGAAGGAAACGAAACAACGAGAATTAGTATAAGATG
GBAA_5668-GibsP2	CTAATTCTCGTTGTTTCGTTTCCTTCGAAATTTCTTTCACCTTGCC
GBAA_5668-GibsP3	GAACAAAAGCTGGAGCTCCACCGCGGTGGCCGAGACAAGAGAATTCATCCAAACG
GBAA_5668-GibsP4	GATATCAGATCTGACGTCTCTAGAGCGGCCCTGAAAACGAAATGCCGTAATGG
GBAA_5668 P5	CGAGACAAGAGAACTTCATC
GBAA_5668 P6	GCTTGAAAACGAAATGC

## Results

*Selection of candidate petrobactin exporters.* To select candidate petrobactin exporters, I took advantage of two types of bioinformatics data sets. First, most components of siderophore iron acquisition systems are expressed only during iron-starved growth. Multiple microarrays of *B. anthracis* Sterne growth in iron-limiting conditions exist, including growth in mammalian blood, within macrophages and in IDM (17, 55, 103). Next, the *B. anthracis* genome was queried for homologues of known siderophore exporters (65, 79, 82, 83, 87) using their amino acid sequences in a position-specific iterative (PSI) BLAST search (104). The returned siderophore exporter homologues were then cross-referenced against iron-limiting growth microarray data, searching for those upregulated in one or more conditions. Through this protocol, I identified the candidate petrobactin exporters described in Table 2.3, including some transporters identified by their up-regulation in iron-limiting growth, some siderophore exporter homologues with no regulation changes, and two genes (GBAA\_1642 and GBAA\_3296) encoding multi-drug and toxic compound extrusion (MATE) family transporters (Table 1). The MATE transporters were hypothesized to be petrobactin exporters due to their proximity to the petrobactin operon in *Marinobacter* spp (77). We focused on single gene targets, and constructed unmarked, in-frame deletion mutants in *B. anthracis* Sterne 34F2 for the candidate exporters in Table 2.4 using allelic exchange protocols established by Janes and Stibitz (97).

**Table 2.3 Candidate petrobactin exporters**

Family	Exporter Homologue	Gene <sup>a</sup>	PSI-Blast (%)		IDM <sup>c</sup>			Blood <sup>d</sup>	MΦ <sup>e</sup>		
			Cov	Id	2	3	4	2	0	1-2	3+
MATE	-	1642	-	-	0.99	0.97	0.99	1.13	-	-	-
	-	3296	-	-	1.01	1.10	1.02	0.90	-	-	-
RND	Mmp14/5, <i>Mycobacterium tuberculosis</i>	1302	69	25	0.97	0.89	0.94	1.15	-	-	-
		2407	62	27	0.99	0.89	1.86	0.68	-	-	-
MFS	NorA, <i>Staphylococcus aureus</i>	0181 <sup>b</sup>	44	26	1.01	0.95	0.91	0.69	-	-	-
		0787 <sup>b</sup>	99	23	0.95	0.89	1.43	0.43	-	-	-
		2346	80	22	1.07	1.08	1.06	0.94	-	-	-
		4961 <sup>b</sup>	37	33	0.96	0.75	0.91	1.02	-	-	-
		5668	46	24	0.96	0.96	0.94	3.94	-	2.80	23.93
		0835	96	40	0.85	0.65	0.50	0.63	-	-	-
		1858 <sup>b</sup>	89	20	0.98	0.99	1.50	1.03	-	2.44	7.01
		2004 <sup>b</sup>	89	24	0.99	0.94	0.84	0.76	-	-2.10	-2.10
-	3157	-	-	-	-	1.58	4.12	-	-	-	
ABC	IroC, <i>Escherichia</i>	0852 <sup>b</sup>	81	28	1.00	0.80	0.61	1.26	-	3.22	-
		0528 <sup>b</sup>	84	31	0.97	0.90	0.86	1.21	-	-	2.08
	EntS, <i>E. coli</i>	1652	87	22	1.09	0.60	0.62	1.44	-	-	2.49
	PvdE, <i>Psuedomonas aeruginosa</i>	5411 <sup>b</sup>	97	21	1.57	3.77	3.77	2.40	-	-	4.72
	-	0349-51	-	-	1.84	5.06	2.83	5.63	-	-	3.22
	-	3190-91	-	-	0.97	1.09	1.48	1.27	5.16	2.12	21.06
	-	3531-34	-	-	2.32	6.92	6.09	6.43	-	-	2.24
	-	4504	-	-	1.10	-	-	-	-	3.83	-
-	4595-96	-	-	3.01	28.07	19.38	11.82	-	-	6.60	
-	5221-22	-	-	1.12	-	-	-	-	2.23	2.34	

<sup>a</sup> GBAA\_, *Bacillus anthracis* str. 'Ames Ancestor' (taxid:261594) <sup>c</sup> Carlson et al. 2009

<sup>b</sup> Identified by multiple blast searches

<sup>d</sup> Carlson et al. 2015

<sup>e</sup> Bergman et al. 2007



*Screening candidate petrobactin exporters.* We reasoned that a *B. anthracis* Sterne mutant unable to export petrobactin would exhibit both reduced growth in iron-limiting conditions and reduced levels of petrobactin in culture medium. Accordingly, each of the mutants were screened for their ability to grow in IDM and for the presence of the petrobactin catechol component 3,4-dihydroxybenzoate (3,4-DHB). During growth of wild-type *B. anthracis*, 3,4-DHB can be measured in IDM culture medium beginning at three hours post-inoculation using the Arnow's assay, which detects catechols (100). When tested, all candidate export mutants both grew to wildtype-levels in IDM and secreted wildtype-levels of catechols (Table 2.4).

To explore a parallel redundancy in petrobactin export machinery as exists for petrobactin import (64), one triple and several double deletion mutants of the exporter candidates were generated—grouping them by transporter family. All double and triple deletions similarly grew to wildtype-levels in IDM and contained wildtype-levels of catechol rings in the culture medium (Table 2.4). I surmised that the lack of a predicted phenotype could be due to either of two reasons: either the candidate identification strategy was flawed or the detection of 3,4-DHB in the culture medium was not a valid proxy for export of intact petrobactin in the search for an exporter mutant.

**Table 2.4 Candidate petrobactin exporter phenotypes at six hours post-inoculation in IDM**

Family	Deletion Strain	Growth (OD <sub>600</sub> )		Catechols (% WT) <sup>a</sup>		Petrobactin (% WT) <sup>a</sup>	
		Avg	SD	Avg	SD	Avg	SD
MATE	Δ1642	0.52	0.05	85.58	9.29	-	-
	Δ3296	0.51	0.02	99.30	11.23	-	-
	Δ1642Δ3296	0.49	0.00	91.56	3.93	72.13	15.63
RND	Δ1302	0.53	0.05	94.56	13.61	99.67	37.31
	<b>Δ2407</b>	<b>0.53</b>	<b>0.05</b>	<b>93.32</b>	<b>17.09</b>	<b>30.79</b>	<b>99.01</b>
	<b>Δ2407 + pAH001<sup>b</sup></b>	<b>0.46</b>	<b>0.01</b>	<b>108.22</b>	<b>33.73</b>	<b>10.48</b>	<b>2.47</b>
	<b>Δ2407 + 2407 pAH001<sup>l</sup></b>	<b>0.54</b>	<b>0.11</b>	<b>95.79</b>	<b>16.79</b>	<b>42.73</b>	<b>3.17</b>
	Δ1302Δ2407	0.51	0.01	90.43	8.68	0.00	0.00
MFS	Δ0181	0.51	0.04	94.08	9.33	23.00	4.04
	Δ0787	0.50	0.04	94.84	3.89	13.19	4.25
	Δ4961	0.52	0.04	114.93	27.71	-	-
	Δ5668	0.62	0.04	113.87	15.68	-	-
	Δ0835	0.64	0.02	100.47	11.71	-	-
	Δ1858	0.63	0.02	94.74	13.37	-	-
	Δ2004	0.45	0.10	102.33	34.11	-	-
	Δ3157	0.51	0.01	89.59	5.98	13.56	65.05
	Δ0835Δ1858	0.48	0.06	96.25	12.00	22.38	14.72
	Δ4961Δ5668	0.48	0.01	96.68	5.59	30.44	3.49
ABC	Δ0852	0.64	0.03	95.85	21.66	-	-
	Δ0528	0.52	0.07	94.66	8.55	-	-
	Δ1652	0.52	0.03	109.82	14.57	-	-
	Δ5411	0.61	0.06	-	-	-	-
	Δ4595-96	0.57	0.03	109.11	22.99	-	-
	Δ0528Δ0852Δ5411	0.50	0.04	113.35	30.07	14.70	19.27

<sup>a</sup> normalized to cell density (OD<sub>600</sub>) and presented as relative to wildtype set as 100%

<sup>b</sup> data compiled from two biological replicates

*LAESI-MS detects intact petrobactin in culture media and cell pellets.* To address whether the mutant strains were exporting intact petrobactin and/or petrobactin components (e.g., 3,4-DHB and other biosynthetic precursors (43, 61)), culture medium from growth in IDM at four or five hours post-inoculation were queried using LAESI-MS. Previously, the Hanna

laboratory has employed high performance liquid chromatograph (HPLC) for the detection of petrobactin in sample supernatants (63, 64). This method is effective, but not amenable to a high-throughput analysis of candidate exporter mutants. LAESI-MS provided the opportunity to conduct a sampling campaign of aqueous solutions (*e.g.*, culture medium), while bypassing sample preparation steps required by other MS techniques (105). During optimization of LAESI-MS for petrobactin analysis, the sensitivity of the instrument was determined using a sample of pure petrobactin added to IDM at different concentrations (ranging from 0.004 – 1mM). We observed a high mass accuracy of + 0.2ppm with a mass plus hydrogen ion ( $[M+H]^+$ ) peak at  $m/z$  719.21. We further improved the LAESI peak shape to provide increased resolution and allowed more laser pulses to be averaged per MS scan by increasing the maximum injection time to 100ms, which synchronized the LAESI pulse and the MS scan rate. By keeping the number of pulses per well at 20 with a frequency of 10 Hz, least four data points per well were obtained. Each mutant is therefore, represented by two timepoints from three independent growth curves, with technical replicates performed in triplicate.

The processed data were normalized to the sample cell density ( $OD_{600}$ ) and presented as per cent wild-type. We began by screening a selection of eight mutants, primarily consisting of double and triple deletions (Table 2.4). Petrobactin was absent from the culture medium of both the negative control *asb* mutant strain (no petrobactin biosynthesis) and the *1302/2407* double mutant strain, (RND-type transporters) (Figure 2.1A). As an example of a candidate exporter mutant with wildtype-levels of petrobactin in the culture medium, and to disprove the hypothesis regarding their involvement in petrobactin export (77), I include the data from the *1642/3296* double mutant strain (MATE-type transporters) in Figure 2.1.

We next hypothesized that an inability to export petrobactin would result in accumulation of the molecule within the bacterial cell. Cell pellets from cultures grown in IDM were obtained at four and five hours post-inoculation, washed twice with fresh IDM, re-suspended in 30 $\mu$ L water and subjected to sampling by LAESI-MS. The data were normalized to cell density ( $OD_{600}$ ) and presented as per cent of wild-type petrobactin levels. As with the culture medium,

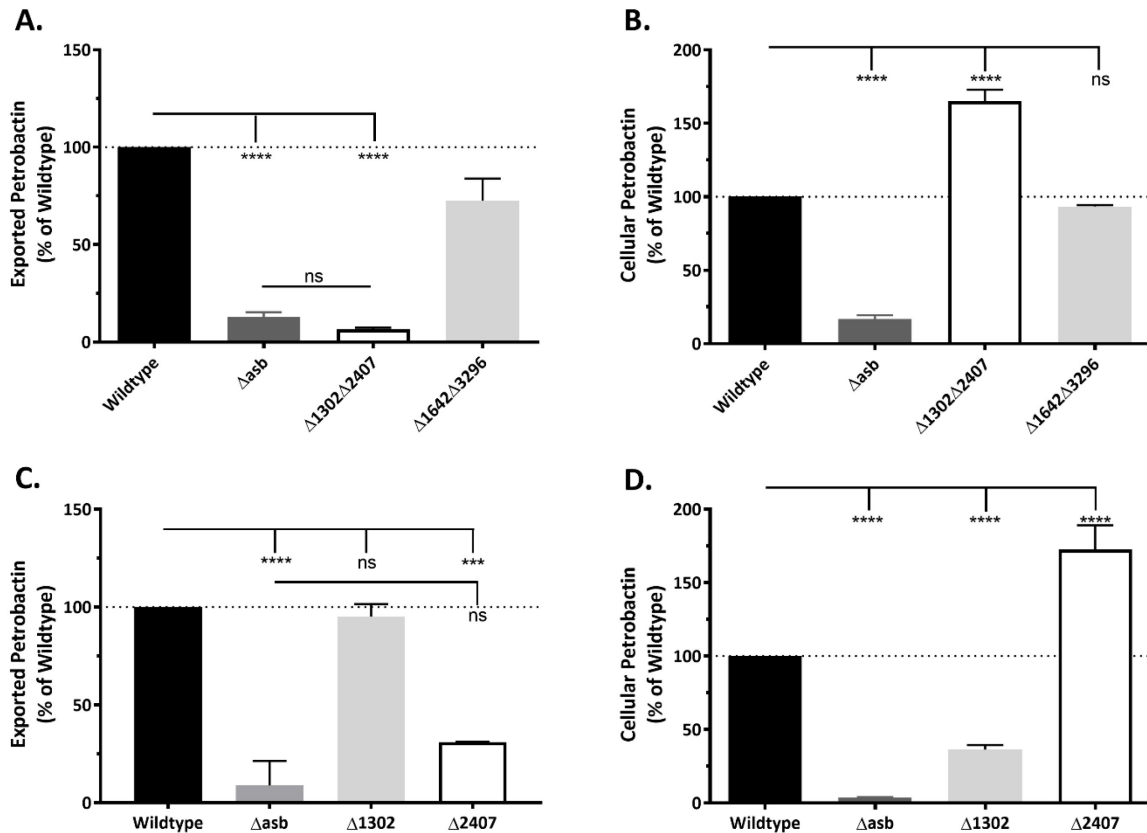


**Figure 2.1 GBAA\_2407 encodes a petrobactin exporter.** LAESI-MS was used to detect petrobactin in spent media (A,C) and cell pellets (B,D) from cultures grown in IDM for four and five hours. A, B) MATE double deletion (*1642/3296*) and RND double deletion (*1302/2407*). C ,D) RND single deletion mutant strains *1302* and *2407*. Wild-type and the *asb* mutant strain are present in all panels as positive and negative controls, respectively. Data were normalized to cell density at the time of sample collection and are presented relative to wild-type. Error bars represent standard deviation, results are from two timepoints taken from three independent experiments, measured in triplicate. Statistical significance determined by two-way ANOVA with a Tukey's multiple comparison posttest. \*\*\*\* $p \leq 0.0001$ , \*\*\* $p = 0.0005$ , ns = no significance

*1642/3296* mutant strain cell pellet petrobactin levels were similar to wild-type, and the *asb* mutant strain contained no petrobactin in the cell pellet. However, *1302/2407* mutant strain cell pellets accumulated nearly twice the amount of petrobactin than wild-type (Figure 2.1B).

*GBAA\_2407* encodes a resistance-nodulation-cell division (RND)-type transporter that exports intact petrobactin. Since the initial LAESI-MS experiments were conducted on double deletion mutants, I returned to the single RND-type transporter deletion mutants, *1302* and *2407*, to determine which transporter(s) was responsible for petrobactin export. As with the double mutant, culture medium and cell pellets were analyzed by LAESI-MS for the presence of intact petrobactin molecules. Culture medium and cell pellets of the *1302* mutant strain contained wild-type-like levels of petrobactin (Figure 2.1C,D). The siderophore was not detected in the *2407* mutant strain culture medium, but was instead detected within the cell pellet as I predicted for a mutant defective in petrobactin export (Figure 2.1C,D). Conducting *in trans* complementation of *GBAA\_2407* under the native promoter ( $\Delta 2407$  p2407) rescued export of petrobactin into the culture medium (albeit not to wildtype-like levels, Figure 2.2A) and reduced its accumulation within the cell pellet (Figure 2.2B). Analysis of the vector control ( $\Delta 2407$  pAH001) matched previous data (Figure 2.2B). Collectively, these data strongly indicate that the *GBAA\_2407* gene product exports petrobactin.

As this appears to be the first application of LAESI-MS to measure siderophores directly in culture medium, I next validated the presence or absence of petrobactin in culture medium from wild-type, the *asb*, *2407* pAH001, and *2407* p2407 mutant strains by LC-HRESIMS. Five-hour, 25mL IDM cultures were dried down, the pellets re-suspended in methanol and analyzed. These data matched the LAESI-MS data with petrobactin being detected in wild-type and the

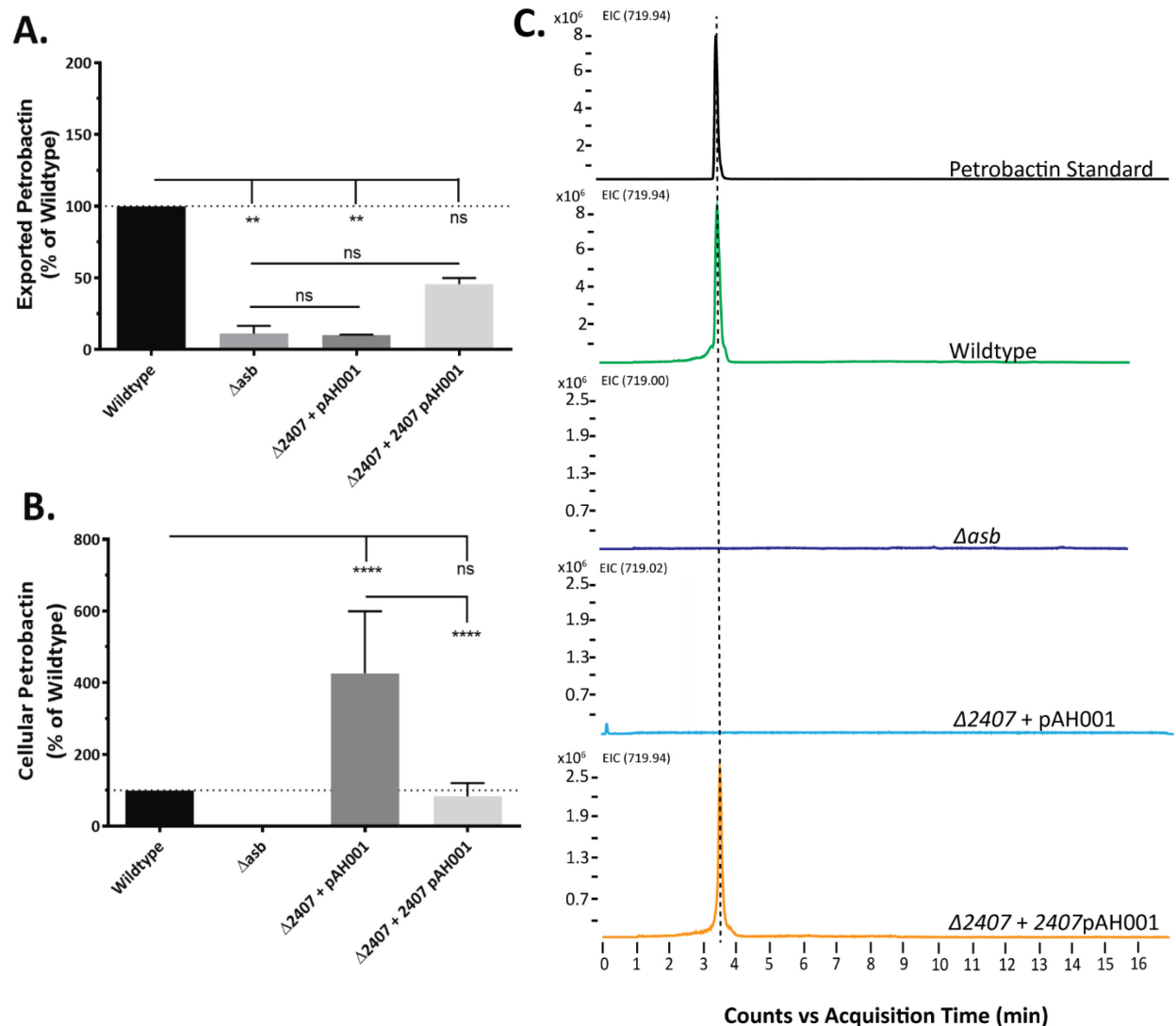


**Figure 2.2** *In trans* complementation of the 2407 mutant strain restores petrobactin export, reduces cellular accumulation, and is confirmed by HRESIMS. LAESI-MS was used to detect petrobactin in A) spent media and B) cell pellets from cultures grown in IDM for four and five hours. Both panels A and B contain the 2407 pAH001 (empty vector), and 2407 p2407 (pAH001 GBAA\_2407 with native promoter) mutant strains plus wild-type and the *asb* mutant strain, positive and negative controls, respectively. Data were normalized to cell density at the time of sample collection and are presented relative to wild-type. Results reported are from two timepoints taken from three independent experiments, measured in triplicate. Error bars indicate standard deviation and statistical significance was determined by two-way ANOVA with a Tukey's multiple comparison posttest. \*\*\*\*p  $\leq$  0.0001, \*\*p < 0.005, ns = no significance (C-G) Cultures were grown in IDM for five hours, filter-sterilized, frozen at -80C and lyophilized to dryness. Sample pellets were resuspended in methanol and subjected to HRESIMS. C)Petrobactin standard D)Wild-type E)*asb* mutant strain F)2407 pAH001 mutant strain G)2407 p2407 mutant strain

2407 p2407 mutant strain culture media, but absent from the culture media of both 2407 pAH001 and *asb* mutant strains (Figure 2.2C).

*The 2407 mutant strain exports petrobactin components that maintain growth in vitro.*

Despite the inability to export intact petrobactin (Figure 2.1C), the 2407 mutant strain maintained wildtype-like levels of growth in IDM as well as wildtype-like levels of the petrobactin component 3,4-DHB in the culture medium (Table 2.4). To explain the discrepancy between the absence of petrobactin (as measured by LAESI-MS) and the presence of 3,4-DHB in the culture medium I hypothesized that when unable to export intact petrobactin, the 2407 mutant strain degraded the molecule, exporting petrobactin components through an unidentified transporter.

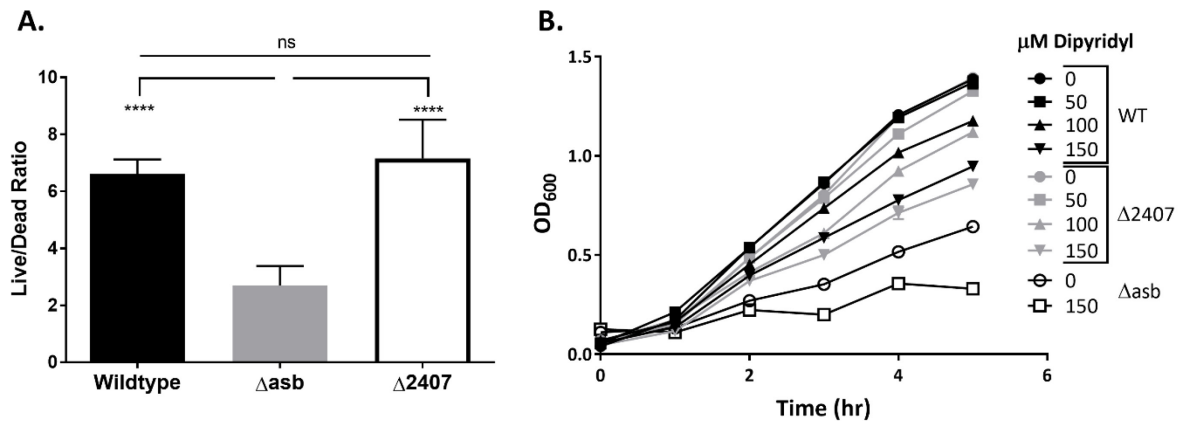


**Figure 2.3** The 2407 mutant strain resembles wild-type in cell viability and dose-dependent response to dipyrldyl. A) Wild-type, the 2407 and the *asb* mutant strain were grown in IDM for four hours and stained for cell permeability. Data are presented as a ratio of live cells to dead and are the average and standard deviation from three independent experiments, measured in triplicate. Statistical significance determined by two-way ANOVA with a Tukey’s multiple comparison posttest. \*\*\*\* $p \leq 0.0001$ , ns = no significance. B) Wild-type, the 2407 and the *asb* mutant strain in IDM were supplemented with either 0 $\mu M$ , 50 $\mu M$ , 100 $\mu M$ , or 150 $\mu M$  of the iron chelator, 2,2-dipyrldyl. Their growth was measured by OD<sub>600</sub> every hour for five hours. Data is representative of three independent experiments with triplicate measurements.

First, I ruled out an alternate hypothesis that in addition to the export of petrobactin components, sub-detectable amounts of petrobactin might be “leaking” from dead or dying 2407

mutant cells. Petrobactin accumulation within *2407* mutant cells could impact cell viability, resulting in elevated levels of cell death and leakage of petrobactin sufficient to rescue growth of the surviving cells. To test this alternate hypothesis, cultures grown in IDM for four hours were stained for cell permeability using the LIVE/DEAD Bac Light kit. Consistent with its poor growth in IDM, the *asb* mutant strain had a low ratio of live/dead cells while wild-type had a higher ratio indicating less cell death (Figure 2.3A). The *2407* mutant strain maintained wildtype-like levels of cell viability suggesting that there was not a gross increase of cell death and leakage in the absence of intact petrobactin export.

Next, I further hypothesized that petrobactin components can import sufficient iron to maintain *2407* mutant strain growth in IDM. To test this, I both supplemented growth of the petrobactin biosynthesis mutant (*asb*) in IDM with spent medium from the *2407* mutant strain and tested for the ability of the *2407* mutant strain to import iron using gallium supplementation. Thus, the *asb* mutant strain was supplemented with spent culture medium from either the *2407* mutant strain, wild-type, or the *asb* mutant strain (Figure 2.4A). Both wild-type and the *2407* mutant strain spent medium increased growth of the *asb* mutant strain, wild-type increased growth approximately 100%, and there was almost a 200% increase with supplementation from the *2407* mutant strain (Figure 2.4A). The second approach employed the gallium toxicity assay. Gallium ( $\text{Ga}^{3+}$ ) resembles iron in both charge and size and can be imported by siderophores for incorporation as an enzymatic co-factor. However, while iron improves growth in iron-limiting conditions,  $\text{Ga}^{3+}$  inhibits bacterial growth since its redox potential is more limited than iron (106). Cultures grown in IDM were supplemented with  $20\mu\text{M}$   $\text{GaSO}_4$  at zero and two hours post-inoculation and their growth at four hours compared to untreated controls. Growth of the petrobactin biosynthesis mutant the *asb* mutant strain was not affected, since it lacks a

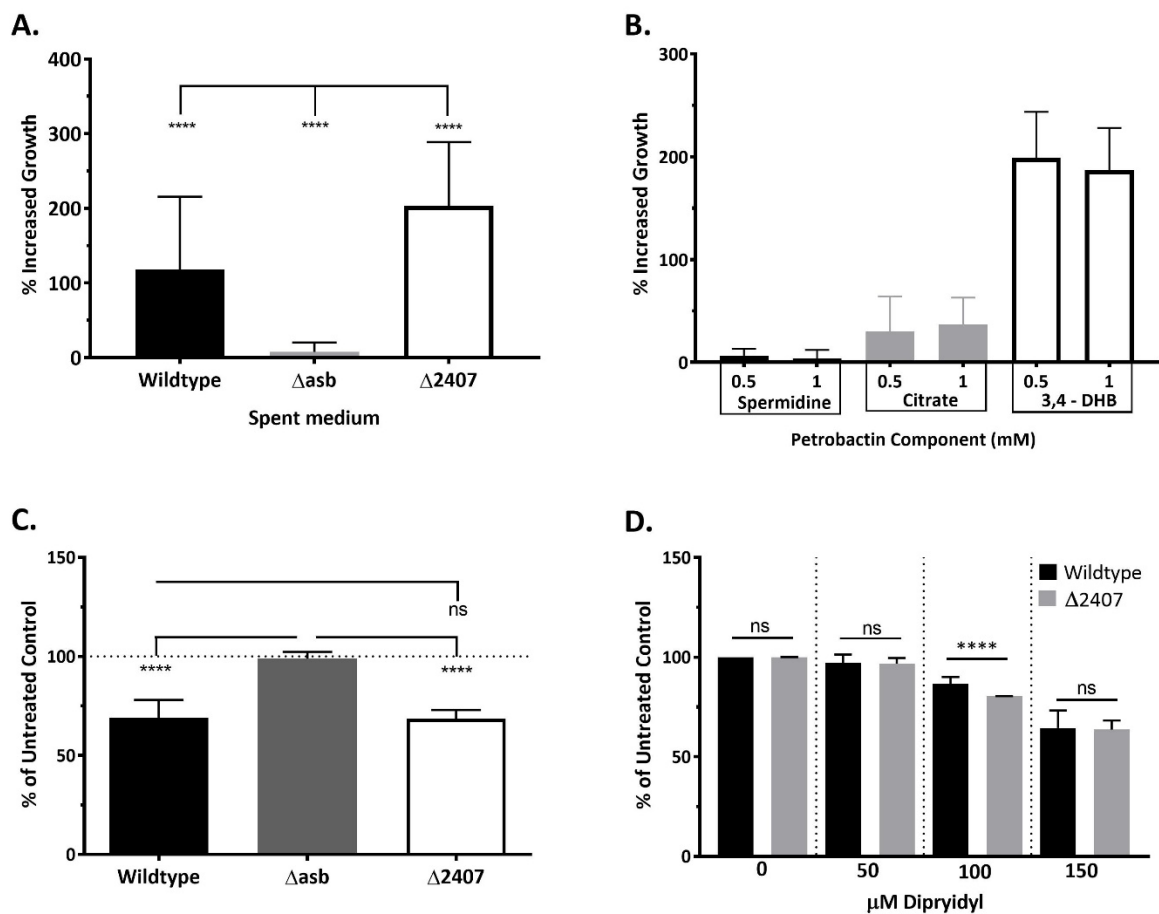


siderophore, while growth of wild-type is inhibited about 30-40%. The 2407 mutant strain growth in IDM was inhibited to similar levels compared with wild-type *B. anthracis*, indicating effective Ga<sup>3+</sup> import, and thus Fe<sup>3+</sup> (Figure 2.4C).

We reasoned that if the petrobactin components exported by the 2407 mutant strain had a lower affinity for iron, then growth of the 2407 mutant strain in IDM would be limited by a lower concentration of the iron chelator, 2,2-dipyridyl than wild-type *B. anthracis*. To determine if the 2407 mutant strain petrobactin components had the same or less affinity for iron as intact petrobactin, I cultured the 2407 mutant strain, wild-type and the *asb* mutant strain in IDM with either 0μM, 50μM, 100μM, or 150μM of dipyridyl. To quantify and compare across discrete growth curves, at five hours post-inoculation I calculated the per cent growth of each sample as compared to the untreated control. All strains demonstrated dose-dependent growth inhibition (Figure 2.3B), however, at 100μM there was a statistically significant difference between per cent growth of the 2407 mutant strain as compared to wild-type (Figure 2.4D). This confirms our hypothesis that the petrobactin components exported by the 2407 mutant strain are not as efficient at iron scavenging as the intact molecule, but still maintain some limited iron-binding abilities.

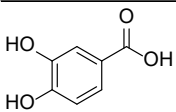
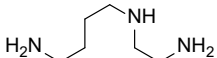
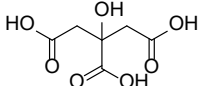
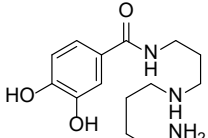
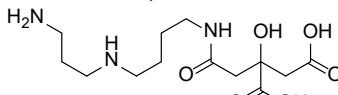
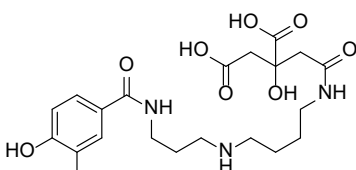
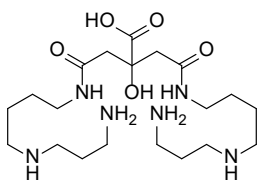
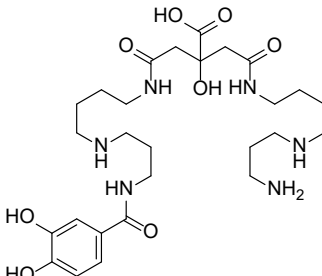
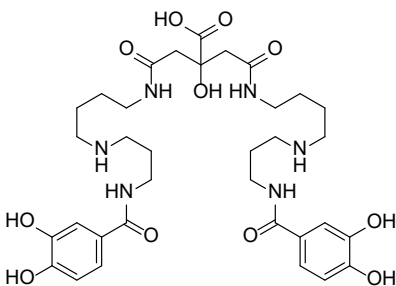
Petrobactin is composed of a central citrate moiety bearing two spermidine arms, each capped by a 3,4-DHB moiety (18). To identify which biosynthetic precursors of petrobactin maintain support of iron transport in *B. anthracis*, the *asb* mutant growth in IDM was supplemented with either 0.5mM or 1mM concentrations of citrate, spermidine, or 3,4-DHB. Spermidine did not improve the *asb* mutant growth in IDM, and citrate had marginal effects averaging 30% and 37% increased growth in 0.5mM and 1mM, respectively. 3,4-DHB, however, enhanced growth of the *asb* mutant strain by nearly 200% in both concentrations tested (Figure

2.4B). This data does not identify the exact petrobactin components produced by the *2407* mutant strain but does indicate that some (though not all) petrobactin-based components can assist in iron transport.



**Figure 2.4** The *2407* mutant strain exports petrobactin components that import iron but are less efficient than intact petrobactin. A) 10mL of spent media from either wild-type, the *2407* and the *asb* mutant strain were filter-sterilized and added to 15mL of fresh IDM inoculated with the *asb* mutant strain. B) Growth of the *asb* mutant strain in 3mL of fresh IDM was supplemented with either 0.5mM or 1mM concentrations of either citrate, spermidine, or 3,4-dihydroxybenzoate (3,4-DHB). Data from A and B are presented as per cent increased growth (as compared to the *asb* mutant strain in IDM alone) at five hours of growth and are the compiled average and standard deviation of three independent experiments. C) Wild-type, the *2407* and the *asb* mutant strain were grown in IDM supplemented with 20 $\mu M$  gallium sulfate at zero and two hours post-inoculation. D) The *2407* mutant strain and wild-type in IDM were supplemented with either 0 $\mu M$ , 50 $\mu M$ , 100 $\mu M$ , or 150 $\mu M$  of the iron chelator, 2,2-dipyridyl. Data from C and D are presented as per cent growth (versus the untreated control) at four or five hours of growth (C, D, respectively) and are the compiled average and standard deviation of three independent experiments. Error bars indicate standard deviation and statistical significance was determined by two-way ANOVA with a Tukey's multiple comparison posttest. \*\*\*\* $p \leq 0.0001$ , ns = no significance

**Table 2.5** The structures and molecular weights of predicted petrobactin components present in *asbA-F* mutants

Petrobactin Component	Description	Truncated Product (of <i>asb</i> mutants)	Size (MolWt)
	3,4-DHB	$\Delta asbC$ , $\Delta asbD$ , $\Delta asbE$ (AsbC-E facilitate 3,4-DHB and spermidine condensation)	154.12
	Spermidine	-	131.22
	Citrate	-	192.12
	3,4-DHB + spermidine	-	281.36
	spermidine + citrate	-	319.36
	3,4-DHB + spermidine + citrate	$\Delta asbB$ (AsbB condenses spermidine to citrate, required for condensation of second spermidine)	455.46
	2(spermidine) + citrate	$\Delta asbC$ , $\Delta asbD$ , $\Delta asbE$ (AsbC-E facilitate 3,4-DHB and spermidine condensation) & $\Delta asbF$ (3,4-DHB synthesis)	446.59
	3,4-DHB + 2(spermidine) + citrate	-	582.7
	Petrobactin	$\Delta asbA$ (AsbB is redundant for AsbA, which condenses citrate to spermidine)	718.81
-	Bacillibactin	-	881.25

*Components could originate from truncated biosynthesis of petrobactin.* There are two, non-exclusive hypotheses for the origin of extracellular petrobactin components (Table 2.5). First, petrobactin biosynthesis stalls and the resulting precursors are exported. Second, petrobactin is synthesized and then degraded, possibly after sequestering cellular iron. To test the possibility that pre-biosynthesized components are exported, mutants in various steps of petrobactin biosynthesis were tested for their ability to grow in IDM and for the presence of 3,4-DHB in the culture medium. All of the individual petrobactin biosynthetic gene disruption mutant strains tested (*asbA*, *asbB*, *asbC*, *asbD*, *asbE*, *asbF*) had impaired growth in IDM (40), however, not as severe as the operon deletion ( $\Delta$ *asb*, Table 2.6, Figure 2.5A). Additionally, all of the individual mutants except the *asbF* mutant strain—AsbF is responsible for 3,4-DHB synthesis (41, 42)—had wildtype-like levels of catechols in the culture medium, suggesting export of biosynthetic precursors (Table 2.6, Figure 2.5B). We note that AsbB is redundant for AsbA (43), though not *vice versa*. Thus, while the *asbA* mutant strain still has a functional AsbB enabling synthesis of intact petrobactin and increased growth, the *asbB* mutant strain lacks a redundant function (43). See Table 2.5 for predicted truncated products of each *asb* disruption mutant.

To determine whether the growth lag was due to the absence of petrobactin biosynthesis or presence of non-functional petrobactin biosynthetic precursors (*e.g.*, citrate, spermidine, etc.), I filter-sterilized culture media from each of the individual mutants at five hours post-inoculation to supplement the growth of the *asb* mutant strain in IDM. The *B. anthracis asb* mutant strain was grown in 15mL of fresh IDM supplemented with either 10mL of spent medium from each *asbA-F* mutant strain, the *asb* mutant strain, or wild-type (Figure 2.5C). To quantify and compare across discrete growth curves, at five hours post-inoculation, I calculated the per cent growth of

each sample compared to the untreated control (Table 2.6, Figure 2.5D). Supplementing the *asb* mutant strain growth with spent cultured medium increased growth over IDM alone, with exception of the negative control of IDM supplemented with culture medium of the *asb* mutant strain.

To characterize the exported petrobactin components, spent IDM culture media from wild-type, the *asb*, and the 2407 mutant strains, were filter-sterilized at five hours post-inoculation and frozen at -80°C. The supernatants were lyophilized to dryness, resuspended in methanol and assayed by LC-HRESIMS. Data obtained from LC-HRESIMS were queried for the presence of petrobactin and projected petrobactin components listed in Table 2.5. However, peaks at the predicted component sizes were not petrobactin-related, as they were also present in the *asb* mutant strain control (data not shown). The identities and source of petrobactin components exported by the 2407 mutant strain remain to be confirmed.

**Table 2.6 Growth of individual *asbA-F* disruption mutants in IDM**

Strain	Growth <sup>a</sup> (OD <sub>600</sub> )		Catechols <sup>b</sup> (% WT)		$\Delta asb$ Supplement <sup>c</sup> (% Increased)	
	Avg	SD	Avg	SD	Avg	SD
Wild-type	0.55	0.03	100.00	0.00	53.14	16.73
$\Delta asb$	0.18	0.03	40.88	7.93	0.02	3.16
$\Delta asbA$	0.45	0.05	140.40	9.92	44.77	26.27
$\Delta asbB$	0.29	0.02	135.40	5.04	30.01	14.10
$\Delta asbC$	0.20	0.09	150.80	22.00	64.35	21.95
$\Delta asbD$	0.29	0.07	151.60	28.72	39.86	17.51
$\Delta asbE$	0.33	0.07	157.90	35.55	39.47	12.93
$\Delta asbF$	0.25	0.06	37.82	18.11	24.27	16.99

<sup>a</sup> in IDM at 5 hours post-inoculation (pi)

<sup>b</sup> measurement of secreted petrobactin components at 5 hours pi

<sup>c</sup>  $\Delta asb$  in IDM supplemented with indicated 5hr pi medium, % increased growth is relative to  $\Delta asb$  in IDM at 5hr pi

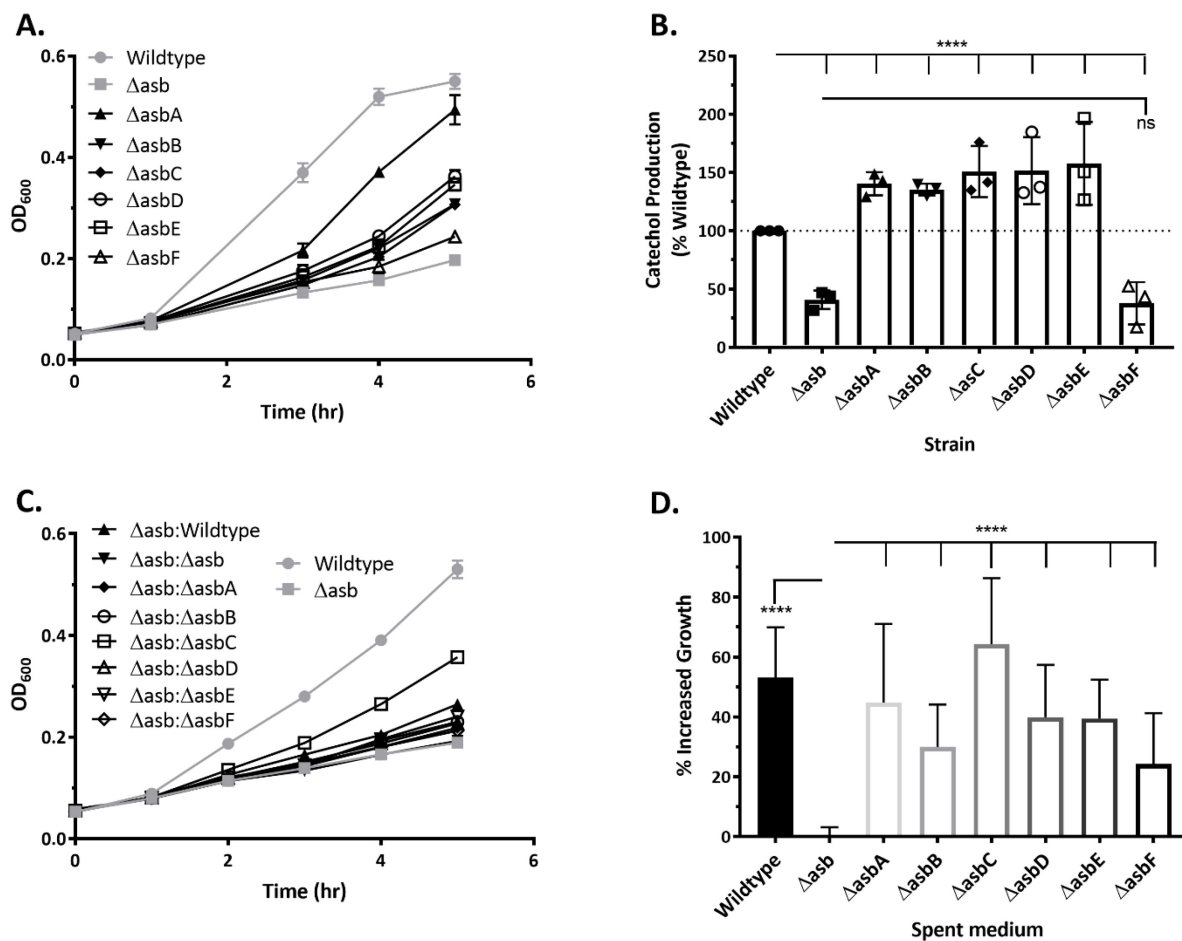


**Figure 2.5** Petrobactin components from truncated biosynthesis are exported and supplement growth of the *asb* mutant strain. A) Strains of individual mutants in petrobactin biosynthesis *asbA*, *asbB*, *asbC*, *asbD*, *asbE*, *asbF*, wild-type and the *asb* mutant strain were grown in IDM and B) assayed for the export of catechols at five hours. C) Culture media from each of the individual mutants in A was filter-sterilized at five hours post-inoculation and used to supplement the growth of the *asb* mutant strain in IDM. D) The difference in growth at five hours was calculated as per cent increased growth, relative to the *asb* mutant strain in IDM alone. Growth curves (A, C) are representative of three independent experiments and data (B, D) are compiled from three independent experiments. Error bars indicate standard deviation and statistical significance was determined by two-way ANOVA with a Dunnett's multiple comparison posttest. \*\*\*\* $p < 0.0001$ , ns = no significance

*Petrobactin components use an alternate receptor and maintain B. anthracis Sterne virulence.*

To gain insight into how petrobactin components may be transported by *B. anthracis* Sterne, I took advantage of the receptor for iron-petrobactin, FpuA. The *B. anthracis fpuA* mutant strain biosynthesizes and secretes petrobactin but grows poorly in IDM due to an inability to uptake iron-bound petrobactin (63). The 2407 mutant strain was grown in IDM for five hours and the culture medium filter-sterilized, then used to supplement the growth of the *fpuA* mutant strain. The *fpuA* mutant strain was inoculated into 25mL of IDM or 15mL of fresh IDM with 10mL of spent medium from either the 2407 or *asb* mutant strain, or wild-type. As expected supplementation with spent medium of the *asb* mutant strain, the negative control, did not improve growth of the *fpuA* mutant strain. However, supplementation with either wild-type or the 2407 mutant strain improved growth by about 75% (Figure 2.6A). These data suggest a different receptor for petrobactin components. To assess whether FpuA can recognize any petrobactin components in addition to petrobactin, growth of the *fpuA* mutant strain in IDM was supplemented with either 0.5mM or 1mM concentrations of citrate, spermidine, or 3,4-DHB. Neither 3,4-DHB nor citrate enhanced growth while spermidine inhibited growth (Figure 2.6B). The receptors and cognate uptake systems for these petrobactin components remain unknown at this point, however, our data indicate that they will be distinct from the intact petrobactin system.

Lastly, I investigated whether petrobactin components exported by the 2407 mutant strain can maintain its virulence in a mouse model of inhalational anthrax. Five, six to eight-week-old female mice were infected intratracheally with  $1 \times 10^5$  spores of either wild-type or the 2407 mutant strain (102). Mice from both groups became severely moribund, requiring euthanasia, within three to five days (Figure 2.6C). That the 2407 mutant strain, which does not export intact petrobactin, can produce wildtype-like levels of disease suggests that intact petrobactin is not



absolutely required for iron gathering within the host.

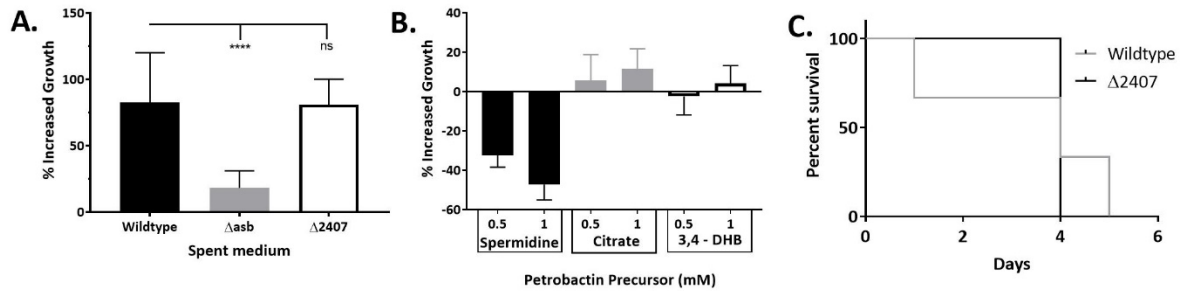


**Figure 2.6 Petrobactin components use a different receptor from petrobactin and maintain *B. anthracis* Sterne virulence.**

A) The *fpuA* mutant strain was inoculated into 25mL of IDM or 15mL of fresh IDM with 10mL of spent medium from either wild-type, the *2407*, or the *asb* mutant strain. Data are presented as per cent increased growth (as compared to the *fpuA* mutant strain in IDM alone) at five hours of growth and are the compiled average and standard deviation of three independent experiments. Statistical significance determined by two-way ANOVA with a Tukey's multiple comparison posttest. \*\*\*\* $p \leq 0.0001$ , ns = no significance B) Growth of the *fpuA* mutant strain in IDM was supplemented with either 0.5mM or 1mM of citrate, spermidine, or 3,4-DHB. The difference in growth at five hours was calculated as per cent increased growth, relative to the *fpuA* mutant strain in IDM alone. Data are compiled from three independent experiments. C) Five, six to eight-week-old, female DBA/J2 mice (Jackson Laboratories) were infected intra-tracheally with  $1.5 \times 10^5$  spores as previously described (102). Mice were monitored for morbidity for 14 days post-infection and euthanized when moribund. Data are presented as per cent survival.

## Discussion

In this work, I developed a bioinformatic-based protocol to generate a list of petrobactin export candidates (Table 1), deleted them one-by-one from the *B. anthracis* genome and screened for their ability to export petrobactin and grow in IDM (Table 2.4). To facilitate the direct high-throughput analysis of petrobactin and its components generated by select *B. anthracis* mutants, I employed a new mass spectrometry technique, LAESI-MS. Thus, a novel methodology and data processing capability for the detection of siderophores and other

metabolites from intact cells with minimal sample preparation has been developed. Applying LAESI-MS effectively identified GBAA\_2407 as a gene encoding an RND-type transporter responsible for exporting petrobactin (Figure 2.1C). I also established that in the absence of 2407, termed the apo-petrobactin exporter ApeX, petrobactin accumulates in the cell while corresponding components are exported through an unknown mechanism (Figure 2.1D, Table 2.4). I also show that petrobactin components retain the ability to retrieve iron for growth (Figure 2.4D) and employ an unknown receptor since they rescue growth in the absence of the known petrobactin receptor (Figure 2.5D, 2.6A). Lastly, these components are sufficient to enable a mutant that does not export intact petrobactin to cause disease in a murine model of inhalational anthrax (Figure 2.6C).

The *apeX* gene encodes a resistance nodulation diffusion (RND)-like transporter, which has 12 transmembrane domains and is ubiquitous across cell types. RND-type transporters frequently function as trimers and interact with other proteins to form export complexes that transport a variety of ligands. Our initial list of candidates included two RND-like transporters GBAA\_2407 and GBAA\_1302. Both were identified in a PSI-BLAST search of the *B. anthracis* genome with the *M. tuberculosis* mycobactin exporter Mmp14. In *M. tuberculosis*, Mmp14 coordinates with a periplasmic accessory protein, Mmps4, to export and recycle mycobactin in a process which also involves a last step in mycobactin biosynthesis (87, 88). ApeX is distantly related to Mmp14, with 62% identity over 27% coverage. Mmp14 and ApeX have two regions of homology with sporadic conserved residues (Figure 2.7A,B, blue), many of which lie in transmembrane helices two through seven. A PSI-BLAST search for ApeX-like proteins from the *Marinobacter* genus (data not shown), members of whom also produce petrobactin, also revealed sequence similarity to transmembrane helices two through seven (dark pink, Figure

2.7A,B). Overlays of Phyre2 protein predictions indicate some structural conservation between Mmpl4 (purple) and ApeX (grey) transmembrane domains but none in the extracellular (pore) domains (Figure 2.7C) (107, 108). As *B. anthracis* is a Gram-positive, ApeX lacks a docking domain to interact with outer membrane export complexes (Figure 2.7C).

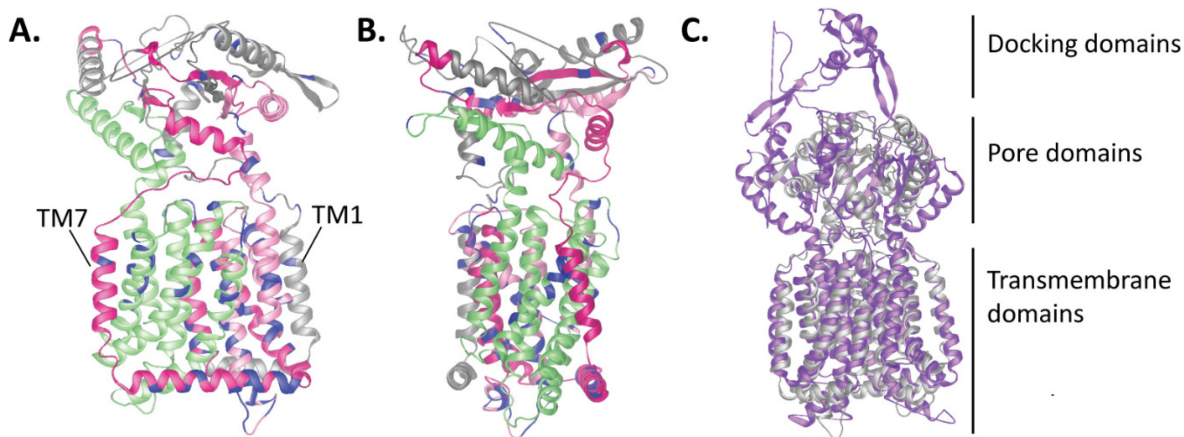


**Figure 2.7 Predicted structure of ApeX.** A, B) Phyre2 predicted structure of ApeX Homology between Mmpl4 and ApeX is strongest in two areas: transmembrane helices two through seven, extracellular beta sheets three through six, and extracellular helices four through seven (pink and dark pink); transmembrane helices eight through twelve, extracellular beta sheets seven and eight, and extracellular helices nine and ten (green). Blue indicates conserved residues and dark pink indicates regions homologous in a PSI-BLAST search of ApeX against *Marinobacter* group, members of whom also produce petrobactin (data not shown). C) Overlays of Phyre2 protein predictions indicate some structural conservation between Mmpl4 (purple) and ApeX (grey) transmembrane domains but none in the extracellular (pore) domains and ApeX is not predicted to have a docking domain.

It remains unclear whether ApeX requires additional accessory proteins to facilitate petrobactin export. However, I did not identify a candidate within an operon with *apeX* and neither did a PSI-BLAST search of Mmps4 against the *B. anthracis* genome reveal homologous proteins to Mmps4. While there is a small 60 residue hypothetical protein downstream of *apeX* (GBAA\_2408), it has an unknown function and is smaller than the 140 residue Mmps4. Given that petrobactin can be fully synthesized *in vitro* by supplying purified enzymes AsbA-E with 3,4-DHB, citrate and spermidine, I hypothesize that an accessory protein is unlikely. However,

whether petrobactin biosynthesis occurs in the cell cytoplasm by transient interactions or if the biosynthetic enzymes form a discrete complex remains unknown. It is possible that an accessory protein facilitates biosynthesis by anchoring a complex to the cytoplasmic side of the cell membrane next to the exporter.

Regardless of whether petrobactin biosynthesis or export requires an accessory protein, the absence of the exporter ApeX results in the accumulation of intracellular petrobactin and export of components, which enables *B. anthracis* to retain the ability to retrieve sufficient iron for growth. This phenomenon has been described in *E. coli* siderophore systems (83) as has the ability for 2,3-dihydroxybenzoate or citrate to supplement growth in low iron media (109, 110). Our data demonstrates that *B. anthracis* can scavenge iron similarly, using either 3,4-dihydroxybenzoate or citrate (Figure 2.4B). The ability of culture medium from the *asbF* mutant strain (which lacks 3,4-dihydroxybenzoate but produces citrate-spermidine products) to rescue growth of the *asb* mutant strain was unexpected (Table 2.6, Figure 2.5D). This, along with data indicating petrobactin-dependent enhancement of petrobactin receptor mutant growth (Figure 2.6A), suggests that *B. anthracis* can import iron bound by distinct petrobactin components including those with 3,4-dihydroxybenzoate and/or citrate iron-binding moieties. The observation that *B. anthracis* can import  $\text{Fe}^{3+}$ -citrate is worthy of further studies since rapid *B. anthracis* growth can occur in the host blood stream, which might contain ferric-citrate (111). A 2004 study observed 3,4-dihydroxybenzoate in *B. anthracis* culture medium and hypothesized that it occurred from incomplete petrobactin synthesis (61). These results (Table 2.6, Figure 2.5B) confirm its presence and role but lack sufficient data to rule out enzymatic degradation of petrobactin. In fact, the observation is described as “petrobactin components” to underscore the inability to distinguish between biosynthetic precursors and enzymatically derived fragments.

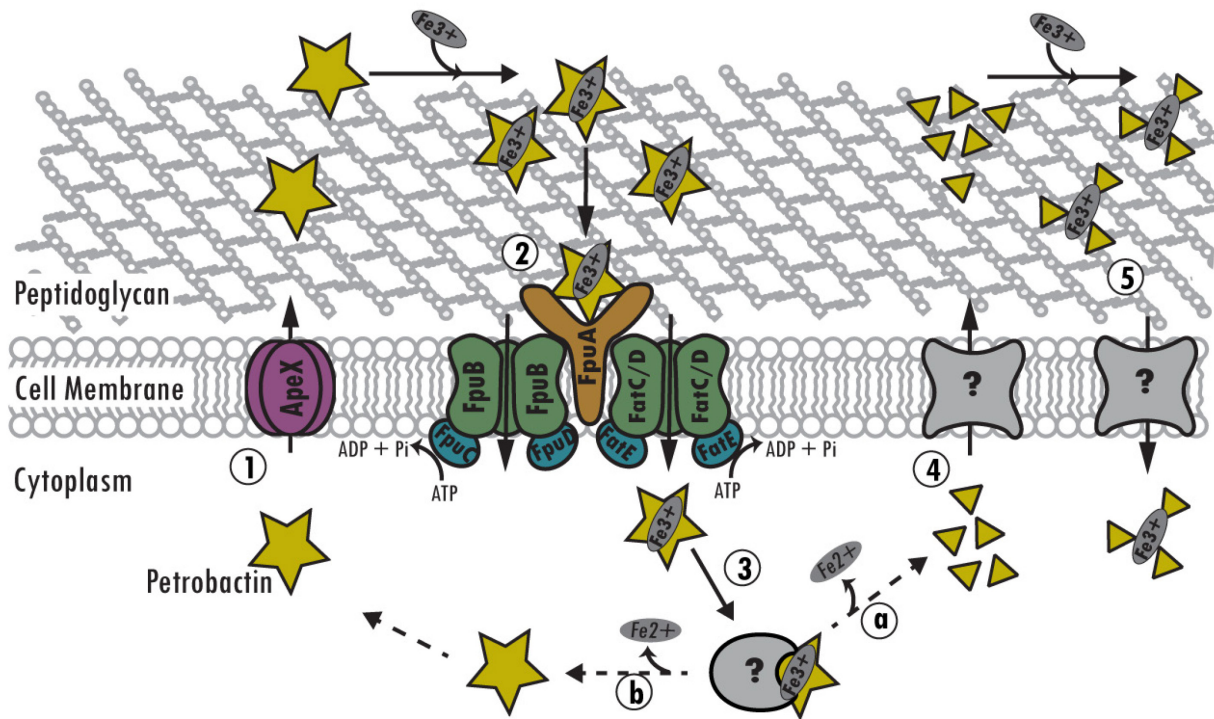


**Figure 2.8 Model of petrobactin use in *B. anthracis*.** 1) Biosynthesized petrobactin is exported into the extracellular milieu through ApeX. 2) Ferric-petrobactin is recognized by FpuA to facilitate import through cognate permeases (FpuB or FatCD) and ATPases (FpuC, FpuD, and FatE). 3) Iron is removed by either enzymatic cleavage (a) or iron reduction (b). 4) Components are exported through an unknown transporter resulting from enzymatic cleavage and/or truncated biosynthesis. 5) Petrobactin components bind iron and are re-imported by an unknown mechanism. Dashed arrows indicate unknown mechanisms.

My concept of petrobactin use by *B. anthracis* involves a model (Figure 2.8) where following biosynthesis of petrobactin, it is exported by the RND-type transporter ApeX (Figure 2.8, 1). The ferric-bound form is then recognized by FpuA for import by the ABC-type transporter permease-ATPase complexes FpuB/C, FpuB/D or FatCD/E (Figure 2.8, 2). Once in the cytoplasm, Fe<sup>3+</sup> is released from holo-petrobactin (Figure 2.8, 3) by either enzymatic cleavage or by reduction (2), which would result in recycling of the siderophore and its components. The citrate, spermidine, 3,4-dihydroxybenzoate and more complex petrobactin intermediates that originate from either truncated biosynthesis or cleavage of petrobactin are

exported through an unknown mechanism (Figure 2.8, 4), retrieve iron from the environment and are re-imported (Figure 2.8, 5). If 3,4-dihydroxybenzoate, then through the same import system or if not, then an unknown system. Iron is then released, probably by the reducing environment of the cytoplasm, and the components are probably continuously recycled. In the absence of ApeX, petrobactin accumulates in the cell where it might be degraded after sequestering iron from cellular proteins, which then target it for degradation, and/or its biosynthesis is truncated, and the components exported to retrieve iron. While *B. anthracis* encodes for a second siderophore, bacillibactin, it is not observed in the supernatant until after 10 hours of growth (62) (our experiments were performed between four and six hours), and a corresponding peak was not observed in the LC-HRESIMS data (data not shown).

Siderophore degradation and export of the resultant fragments has been observed previously (83, 110, 112, 113), but it has remained unclear whether those siderophore fragments are relevant to disease. Loss of enterobactin and/or salmochelin exporters in extraintestinal pathogenic *E. coli* (ExPEC) increased component export but reduced virulence (113). Virulence could be rescued by blocking enterobactin synthesis, which prevented the deleterious effects of synthesis and intracellular accumulation of two siderophores while the third ExPEC siderophore, aerobactin, maintained virulence (113). *B. anthracis* virulence, however, relies on a single siderophore, petrobactin (16). Here, I demonstrate for the first time that siderophore components can gather sufficient iron in the host to cause disease. This observation raises questions to address in the future. For instance, it is unclear how the difference in affinity might affect iron transfer from iron-binding proteins. And if siderophore components will suffice, what is the evolutionary value to synthesis of the entire molecule? Most importantly in our minds, knowing

if this phenomenon occurs with other pathogens is key to understanding what effect, if any, there is on treatment strategies designed to target siderophores.

If knocking out the exporter still results in export of siderophore components and no change in growth phenotype, it confounds research into identifying siderophore exporters, especially if the method used to measure the presence or absence of a siderophore does not have enough resolution to distinguish a component from the whole. This is probably the case in most research scenarios since hydroxamate and catechol colorimetric assays are the preferred method for initial screening. This is what I encountered in our early work, and why I initially turned from the low-resolution catechol assay to LAESI-MS—to measure petrobactin both in the culture medium and the cell. Adaptation of LAESI-MS for the detection and measurement of metabolites within the bacterial cell and in culture medium demonstrates it as a powerful tool. For instance, LAESI-MS could be applied to identify metabolic compounds undetected by other high-resolution detection techniques because they are either not amenable to the required extraction methods or involves low-throughput sample processing capabilities. It could also be adapted for the detection of bacterial or viral proteins or molecules directly from patient samples. This would enable a rapid diagnosis that bypasses costly sample preparations.

## Chapter 3

### **Rapid sporulation in *Bacillus anthracis* requires petrobactin**

#### Abstract

*Bacillus anthracis* is a Gram-positive bacillus. Under conditions of environmental stress such as low nutrients, *B. anthracis* can undergo sporulation, the process of converting from vegetative bacilli to highly durable spores to enable long-term survival. Sporulation is regulated by several transcription factors but requires several nutrients to complete, including excess amounts of iron. Iron is required for many cellular processes as a protein co-factor but is tightly regulated due to its reactivity with oxygen. *B. anthracis* has a heme import system and two siderophores, petrobactin and bacillibactin, for iron acquisition. Petrobactin is the only system known to be required for growth in iron-deplete conditions including within macrophages and in mouse models of disease. The extent to which petrobactin is involved in spore formation *in vitro* or *in vivo* is unknown. This work shows that rapid sporulation of *B. anthracis* *in vivo* requires petrobactin and demonstrates that the petrobactin biosynthesis operon is induced during late stage growth and early sporulation. In addition, LAESI-MS found petrobactin to be associated with the spore. Petrobactin is also required for wild-type levels of growth and sporulation in bovine blood, suggesting that it is a requirement for *B. anthracis* transmission via the spore.



## Introduction

*Bacillus anthracis* is a Gram-positive, spore-forming bacillus, which causes the disease anthrax. In humans, anthrax can manifest in four ways according to the method of exposure: cutaneous, inhalational, gastrointestinal, or injectional (6, 76). Following exposure to *B. anthracis* endospores, a metabolically dormant phase of the *B. anthracis* lifecycle, they are taken up by antigen presenting cells (APCs) such as macrophages. Within the APC endosome, small molecules and amino acids from the host initiate germination of endospores into vegetative bacilli. Following germination, bacilli rapidly initiate cellular functions and within 30 minutes begin transcription and translation of required proteins, including the toxins that enable escape from the APC (114). If the APC is in transit to the nearest lymph node, then the bacilli are released directly into the blood or lymph to replicate, reaching titers greater than  $10^8$  CFUs/mL (7, 9).

The *B. anthracis* spore is regarded as the infectious particle for its role in anthrax transmission, but broadly speaking the spore is a bacterial bunker into which a bacillus can retreat to survive harsh conditions including nutrient deprivation, extreme temperatures, radiation and desiccation (7, 115–118). As nutrients diminish and waste products accumulate, environmental sensors initiate a cascade of transcriptional regulators to construct a spore from both the inside out and the outside in (119–121). Most of the research describing sporulation has been conducted in *B. subtilis* and will be described in brief here (Figure 3.1A) (119).

The first morphological change is asymmetric division of a bacillus into the mother cell and prespore, which is initiated by phosphorylation of the transcriptional regulator Spo0A and activation of sporulation-specific  $\sigma^H$  (119, 122, 123). The next step in transcriptional regulation is the compartmentalized activation of two early sporulation sigma factors,  $\sigma^F$  and  $\sigma^E$ , in the

prespore and mother cell, respectively (119). A suite of  $\sigma^F$ - and  $\sigma^E$ -dependent proteins enable engulfment of the prespore by the mother cell (119, 124). Final maturation of the spore is regulated by the prespore-specific  $\sigma^G$  and the mother-cell-specific  $\sigma^K$  (119, 125, 126). When completed, the spore structure (Figure 3.1B) is composed of a dehydrated core, containing the genome and silent transcriptional and translational machinery, surrounded by an inner membrane; a layer of modified peptidoglycan known as the cortex; an outer membrane; a proteinaceous spore coat; and, for *B. anthracis*, the exosporium (116, 119, 121).

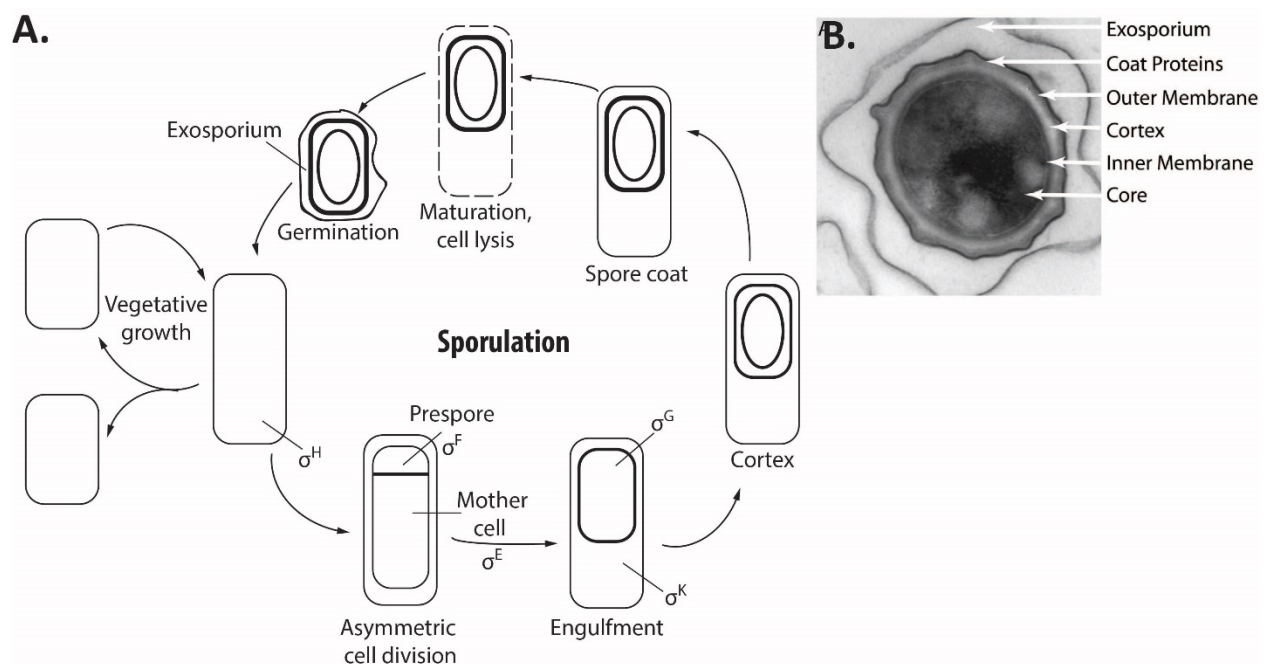


**Figure 3.1 Schematic of sporulation and the spore architecture** A) a simplified schematic showing progression of sporulation through the major stages with related sigma factor expression (adapted from Errington, 2003 (119)). B) architecture of a *B. anthracis* spore is visible by transmission electron microscopy (used with permission from Liu, et. al, 2004 (127)).

Sporulation is an energetically costly process. And while sporulation is initiated by nutrient depletion, efficient sporulation still requires access to many nutrients, including extreme amounts of iron (1.5-2mM) (128, 129). Iron is required as a cofactor for enzymes involved in environmental sensing, ATP synthesis, and even the tricarboxylic acid cycle (130). But excess

amounts of intracellular iron can participate in the Fenton reaction to generate superoxide radicals, so iron in *B. anthracis* is chaperoned by ferritins, the mini-ferritin DPS, and superoxide dismutases (58, 74). *B. anthracis* spores contain about 10 $\mu$ M iron, which is presumed to be required for outgrowth from the spore in iron-limiting conditions, such as an APC endosome, until active iron acquisition systems can be expressed one to two hours following germination (131, 127). One such system is the siderophore petrobactin, whose biosynthetic machinery is encoded by the *asb* operon, which is induced within two hours of germination (16, 131).

Siderophores are small molecules with a high affinity for iron that are synthesized by bacteria during low iron availability (15). *B. anthracis* has three active iron acquisition systems: two siderophores, petrobactin and bacillibactin, as well as a heme acquisition system. However, of these, only petrobactin is required for growth in macrophages and a mouse model (16, 75). Previous studies have elucidated much about petrobactin use in *B. anthracis* including defining: the biosynthetic pathway for petrobactin (*asb* operon), the petrobactin-iron complex receptor (FhuA), import permeases (FpuB/FatC/FatD), ATPases (FpuC/FatE), and the petrobactin exporter (ApeX) (16, 63, 64, 77, 132).

Strains lacking a functional *asb* operon exhibit a severe growth lag in iron-depleted medium (IDM) when inoculated as bacilli, but over time will reach wild-type levels of growth as measured by optical density. If the *asb* mutant strain is inoculated as spores, however, detectible levels of growth are not achieved, even after 24 hours, unless cultures are supplemented with purified petrobactin at inoculation (64). Combined with the known requirement for iron, this suggested to me a role of petrobactin in the transition between spore and vegetative bacillus or vice versa. In this work, I investigate whether petrobactin-dependent iron acquisition plays a role in the spore biology of *B. anthracis*.

In this chapter, I show that while *asb* mutant spores do not have a defect in germination, an *asb* mutant strain does have a sporulation delay in ModG medium that can be rescued by supplementation with pure petrobactin. I used fluorescent reporters to investigate regulation of the *asb* operon during sporulation. Upregulation of the *asb* operon during late stage growth in sporulation media was confirmed by microscopy, which also confirmed the presence of sporulating cells at that time point. I hypothesized that petrobactin might be packed in the spore and used laser ablation electron spray ionization mass spectrometry (LAESI-MS) to detect petrobactin packaged within *B. anthracis* spores. Lastly, I showed that the *asb* mutant strain cannot grow and sporulate in bovine blood, an essential criterium for transmission of *B. anthracis* between hosts.

## Materials and Methods

*Bacterial growth conditions and sporulation* – Strains used are described in Table 3.1. Genomic-based fluorescent reporters were generated by PCR amplification and Gibson cloning (New England Biolabs) of the genetic construct into pBKJ258 which was then inserted onto the *Bacillus anthracis* Sterne 34F2 (pXO1<sup>+</sup>, pXO2<sup>-</sup>) genome by allelic exchange, as described by Janes and Stibitz (97). All necessary primers are listed in Table 3.2. Modified G medium (ModG) was used for the generation of *B. anthracis* spores at 37°C for 72 hours (99). Spores were collected at 2,800 rpm then washed and stored in sterile water at room temperature following heat activation at 65°C. Strains containing plasmid-based reporters were grown in the presence of 10µg/mL chloramphenicol. Media and chemicals were purchased from Fisher Scientific or Sigma Aldrich.

*Spore germination and outgrowth*— Spore germination and outgrowth was measured in iron-depleted medium (IDM) supplemented with 1mM inosine, following a 20 minute heat activation at 65°C (16). To measure germination and subsequent outgrowth, spores were inoculated at a starting OD<sub>600</sub> between 0.25 and 0.5 for a final volume of 200µL. The spores were incubated for six hours at 37°C in a SpectraMAX M2 spectrophotometer with measurements of the OD<sub>600</sub> taken every five minutes for the first hour to track germination and every 30 minutes thereafter to measure growth.

*Supplementation of asb mutant sporulation with petrobactin and outgrowth*— To supplement *asb* mutant spores with petrobactin, bacilli were grown overnight at 30°C in BHI and 250µL were used to inoculate 25mL of ModG medium supplemented with 25µM of purified petrobactin. The culture was incubated for 72 hours to allow for maximal sporulation then collected by centrifugation at 2,800rpm and washed three times with 20mL of sterile, distilled, deionized water. The spores were resuspended in 1mL of fresh water following heat activation for 20 minutes at 65°C. To measure outgrowth, the OD<sub>600</sub> was measured following inoculation of the spores into either IDM or IRM supplemented with 1mM inosine and growth at 37°C for 12 hours.

*Reporter growth, measurement, and analysis* – Bacterial strains were plated on BHI (Difco) and grown in BHI at 30°C overnight. Overnight cultures were back diluted 1:50 into fresh BHI and incubated at 37°C for one hour. The cells were pelleted at 2,800 rpm for 10 minutes (Centrifuge 5810 R, Eppendorf) then either washed once in fresh BHI or in one mL of fresh iron-depleted medium (IDM) five times to remove contaminating iron (16). BHI-washed cultures were used to

inoculate 200 $\mu$ L of either BHI or ModG media while IDM washed cells were used to inoculate 200 $\mu$ L of either IDM or IDM supplemented with 20 $\mu$ M FeSO<sub>4</sub> (iron-replete medium, IRM). Each strain was inoculated into triplicate wells to a starting OD<sub>600</sub> of 0.05, covered with a gas permeable sealing membrane (Breathe-Easy, Diversified Biotech) then grown in a Synergy HTX plate reader at 37°C with continuous shaking at 237cpm for 12 hours. The OD<sub>600</sub> and fluorescence (gfp: excitation 485/20, emission 528/20) were bottom read every five minutes using a tungsten light source. Data were analyzed in R software by first subtracting a media blank from both fluorescence and OD<sub>600</sub> then normalizing fluorescence by the OD<sub>600</sub>. Background fluorescence was approximated by wild-type cells and subtracted from the reporters at corresponding timepoints.

*Microscopy* – To confirm expression of *asb* during late stage growth and early onset of sporulation, wild-type and an *asb* transcriptional reporter expressing GFP were grown in ModG medium at 37°C. From 6 to 10 hours post-inoculation, 5 $\mu$ L was spotted on a microscope slide every two hours. Phase-contrast and fluorescence microscopic images were taken using a Nikon TE300 inverted microscope equipped with a mercury arc lamp, 60 $\times$  Plan-Apochromat 1.4-numerical aperture objective, cooled digital CCD camera (Quantix Photometrics), and a temperature-controlled stage. Excitation and emission wavelengths were selected using a 69002 set (Chroma Technology). Fluorescence images of GFP were captured using an emission filter centered at 535nm and an excitation filter centered at 490nm.

*LAESI-MS* – For analysis, spores were prepared as describe above. Unless indicated otherwise, 6x10<sup>7</sup> spores from three independent spore preparations in 50% DMSO were plated in triplicate

wells of shallow 96-well plates and subjected to laser-based ablation. The ESI mass spectrograph was obtained using a ThermoFisher LTQ XL mass spectrometer, containing an atmospheric pressure ionization stack with a tube lens and skimmer, three multipoles, a single linear trap configuration and a set of 2 electron multipliers with conversion dynodes. The mass spectrometer was connected to a Protea LAESI DP-1000 instrument with an ESI electrospray emitter for ambient ionization. The collected data points were exported to Gubbs<sup>TM</sup> Mass Spec Utilities (101) and processed using Generic Chromatographic Viewer for individual *m/z* (ThermoFisher Scientific).

*Sporulation efficiency* – Wild-type, *asb*, *dhb*, and *isd* mutant strains of *B. anthracis* were grown in BHI either overnight at 30°C then inoculated at 1:1000 into 3mL of either ModG medium or defibrinated bovine blood (Hemostat laboratories). Cultures were grown at 37°C and growth and sporulation were measured at regular intervals. To enumerate total and sporulated CFUs, samples were serially diluted in PBS then plated on BHI for growth at 37°C overnight both before and after a heat treatment step (30 minutes at 65°C). Percent sporulation was calculated in R as the CFU post-heat-treatment divided by the total CFU (pre-heat-treatment) and multiplied by 100. Hemin for supplementation at 0.5µM was first suspended at 3.83mM in 1.4M NaOH, then diluted to 150µM in PBS (133).

*ICP-MS* – To measure the amount of iron present in *B. anthracis* spores, spores were harvested from either ModG medium as described above, or from 10% bovine blood plates between 48 and 72 hours of growth. The spores were washed at least three times in fresh water, heat treated at 65°C for 30 minutes passed through a 3.1-micron glass microfiber filter (National Scientific

Company) and washed twice with Nycodenz to increase purity. One milliliter of at least  $2 \times 10^9$  spores were dried at  $85^\circ\text{C}$  overnight and dissolved in 70% nitric acid overnight at  $85^\circ\text{C}$  prior to 1:10 dilution in ASTM Type 1 water. ICP-MS (PerkinElmer) was conducted with a helium KED to reduce background signal from  $\text{ArO}^+$  and using bismuth as an internal standard. Measurements were taken in triplicate from at least two independent spore harvests. Data are presented as ppb of iron per  $10^9$  spores.

**Table 3.1 Strains of *B. anthracis* Sterne 34F2 used in this work.**

Strain	Relevant characteristics	Reference
<i>Bacillus anthracis</i> Sterne 34F2	Wild-type (pXO1 <sup>+</sup> , pXO2 <sup>-</sup> )	Sterne, 1939
34F2, $\Delta$ asbABCDEF	Petrobactin biosynthesis mutant	Lee et al., 2007
34F2, $\Delta$ dhb	Bacillibactin biosynthesis mutant	Cendrowski et al., 2004
34F2, $\Delta$ isd	Heme import system mutant	This work
34F2, BA140	<i>asbA:gfp</i> transcriptional fusion	This work
34F2, BA141	<i>asbA:gfp</i> translational fusion	This work
34F2, SC140	promoterless <i>gfp</i> (pAD123)	Cendrowski Dissertation
34F2, SC136	<i>asb<sup>P</sup>:gfp</i> transcriptional fusion (pSC118)	Cendrowski Dissertation

**Table 3.2 Primers used to generate mutant strains used in this work.**

Primer	Sequence (5'→3')
Isd P1	GCTAAAATTACAAAGCATAACATACGAACGTTATAATAAAAAGCGG
Isd P2	CGITCGTATGTATGCTTTGTAAATTTAGCTGTATTGTAACAATAATC
Isd P3	GGAACAAAAGCTGGAGCTCCACCGCGGTGGCCCTCCAAGCACCTCTTTGGATTAAT
Isd P4	GGATATCAGATCTGACGCTCTAGAGCGGCCGCTTCTATAATAGAAAAGTCTCTTTTTTTGTAAAA
Isd P5	GTGATACGAGTGGACTAAAAAC
Isd P6	CTGTAGAAAAATAGAGAAAAGAG
<i>asb<sup>P</sup>:gfpmut</i> + RBS R	ACCTCCTTTAACAGGTTATGTAACGTAATCTGCTTTCATAACAGAATTAC
<i>asb<sup>P</sup>:gfpmut</i> R	TTACTAGATCTCATTGTAACGTAATCTGCTTTCATAACAGAATTA
<i>gfpmut3</i> + RBS: <i>asb<sup>P</sup></i> F	AGATTACGTTACATAACCTGTTAAAGGAGGTGTTTCTAGAATG
<i>gfpmut3</i> F	GATTACGTTACATAAATGAGATCTAGTAAAGGAGAAGAAGCTTTTCAC
<i>gfpmut3</i> R	CGATTTCTAGCCATTTTATTGTATAGTTCATCCATGCCATGT
<i>asb<sup>P</sup>:gfpmut3</i> diagnostic F	GCATCACCTTCACCCCT
<i>asb<sup>P</sup></i> _P1	GAACTATACAAAATAAAAATGGCTAGAAAATCGTAATTCTAATCAATTAG
<i>asb<sup>P</sup></i> _P2	ACAATTGTATGTACCTTAAGAAGTTACTACTCTAAATTTCTATTTGTTAGTACTTT
<i>asb<sup>P</sup></i> _P3	GGAACAAAAGCTGGAGCTCCACCGCGGTGGCCAACAAGAGAGACAAGAGTATGTGAATC
<i>asb<sup>P</sup></i> _P4	GATATCAGATCTGACGCTCTAGAGCGGCCCTCATAACAAGTGAAGTATGCAAGC
<i>asb<sup>P</sup></i> _F	GTAGTAACTTCTTAAAGGTACATAACAATTGTGAGGGAGAATTATATG
<i>asb<sup>P</sup></i> + RBS: <i>gfpmut3</i> R	TAGTGTATCAATTCATTATGTAACGTAATCTGCTTTCATAACAGAATTAC
<i>asb<sup>P</sup></i> _R	GTCAGTAACTTCCACTGTAACGTAATCTGCTTTCATAACAGAATT
<i>asb<sup>P</sup>:gfpmut3</i> diagnostic R	GGAACCATTACCATATTTCTC



## Results

*Petrobactin is not required for spore germination.* Considering the observation that spores of petrobactin-null strains fail to outgrow in iron-deplete medium, I asked whether this is due to a defect in the germination or subsequent outgrowth of the spores. To observe germination kinetics, spores of wild-type, an *asb* mutant strain, and a *dhb* (bacillibactin-null) mutant strain were incubated in IDM supplemented with 1mM inosine (IDM+I, to improve germination kinetics) for 60 minutes at 37°C. The OD<sub>600</sub> was measured every five minutes and compared to the starting OD<sub>600</sub> to calculate the percent change in optical density. The *asb* mutant did not display a defect in germination, relative to either wild-type or *dhb* mutant spores (Figure 3.2A). And at six hours (360 minutes) post-inoculation, the *asb* mutant strain had reached an optical density similar to wild-type and the *dhb* mutant (Figure 3.2B). However, when growth was monitored for 12 hours (720 minutes) following inoculation of spores into IDM+I, growth of the *asb* mutant plateaued at six hours with an OD<sub>600</sub> seemingly equivalent to one doubling (Figure 3.2C). Both wild-type and *dhb* mutant spores germinated and grew in IDM+I to stationary phase followed by cell death, possibly due to the extreme iron limitation of the medium. Wildtype-like levels of growth were restored to the *asb* mutant by supplementing its growth in IDM+I medium with 20µM ferrous sulfate, indicating an iron-dependent growth phenotype (Figure 3.2D).

To ask whether the outgrowth of the *asb* mutant was dependent on petrobactin, 25µM of pure petrobactin was added at inoculation to supplement the growth of the *asb* mutant strain in ModG sporulation medium. Spores were harvested ( $\Delta asb+sPB$ ), then inoculated in IDM+I to germinate and grow for 24 hours at 37°C. Initially, 10<sup>5</sup> spores were inoculated in 2.5mL of IDM+I with shaking, however, the culture failed to achieve detectable levels of growth after 24 hours (Figure 3.3A). (The wild-type positive control grew well, data not shown.) I reasoned that

the spore-associated petrobactin might be diluted beyond a concentration capable of supporting growth following germination, so I repeated the experiment using multiple volumes of IDM+I and numbers of spores. Inoculation of the  $\Delta asb+sPB$  spores never led to significant outgrowth in any of the IDM+I conditions tested, but were able to grow in the positive control, IDM+I supplemented with 20 $\mu$ M ferrous sulfate (IRM) (Figure 3.3B-C). For experiments in Figure 3.3 A and 3.3B, experiments were conducted in a culture tube and the lack of growth was confirmed visually. In Figure 3.3C, the cultures were grown with shaking and timepoints taken every five minutes in a plate reader. For simplicity, only the 24 hour timepoint is shown and the high initial density of the cultures required that the endpoint data be presented as fold change.

Transcriptional microarrays of *B. anthracis* Sterne spores inoculated in ModG sporulation media indicate that by 120 minutes post-inoculation (and thus 60 – 90 minutes post-germination) *asbA-F* is expressed (131). However, the observed growth defect in Figure 3.2C doesn't occur until six hours post-inoculation of spores in IDM+I, which should be sufficient time for transcription, translation, and biosynthesis of the iron-scavenging siderophore. Additionally, supplementation of the siderophore during sporulation doesn't improve growth following germination. Therefore, I attribute the observed growth defect to a lack of *de novo* petrobactin biosynthesis following germination. I next queried the role of petrobactin in sporulation.

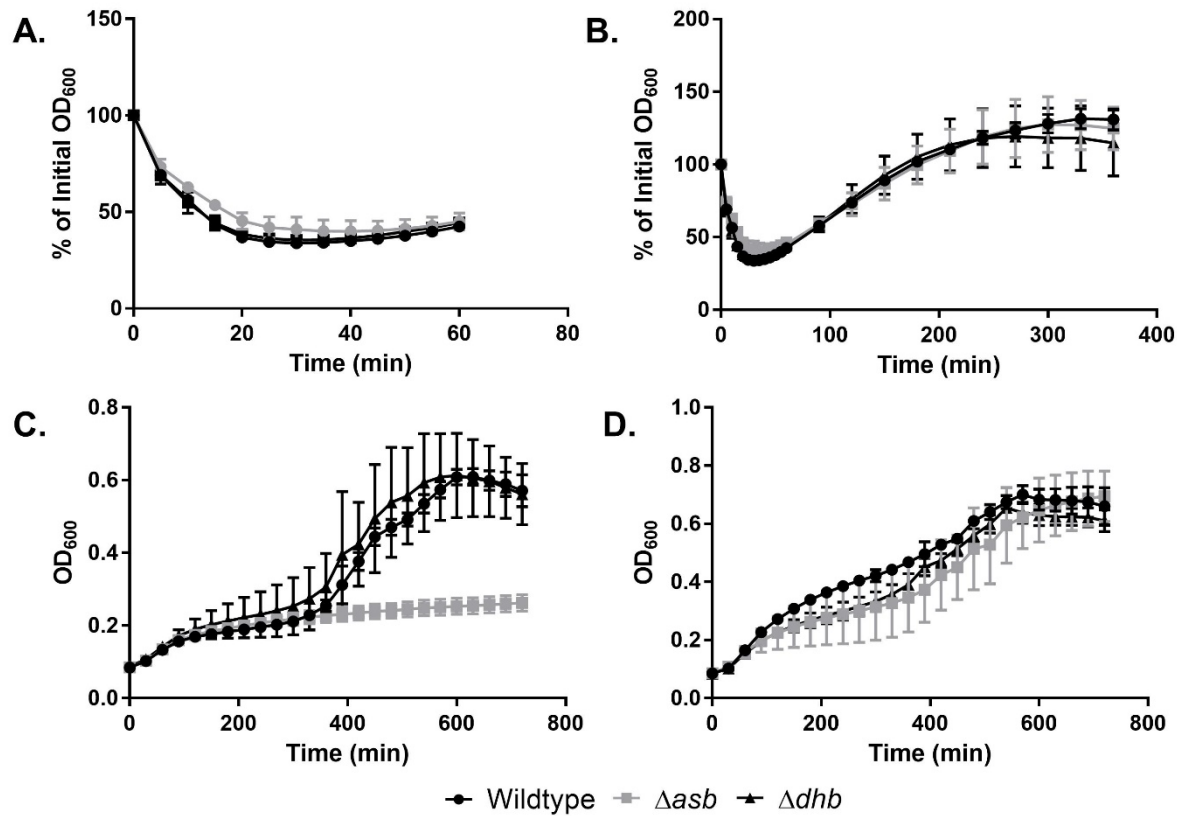


**Figure 3.2** *asb* mutant spores do not have a germination defect but fail to outgrow in iron-depleted medium Wild-type, *dhb* mutant, and *asb* mutant spores were A) inoculated in IDM + 1mM inosine (IDM+I) at a starting of  $OD_{600}$  between 0.25 and 0.5. The  $OD_{600}$  was measured every five minutes for the first hour and B) every 30 minutes for six hours thereafter. Data are presented as percent of the starting  $OD_{600}$ . C)  $10^4$  spores were inoculated in IDM+I or D) IDM+I supplemented with 20 $\mu$ M ferrous sulfate (IRM+I) and the  $OD_{600}$  measured every 30 minutes for 24 hours.

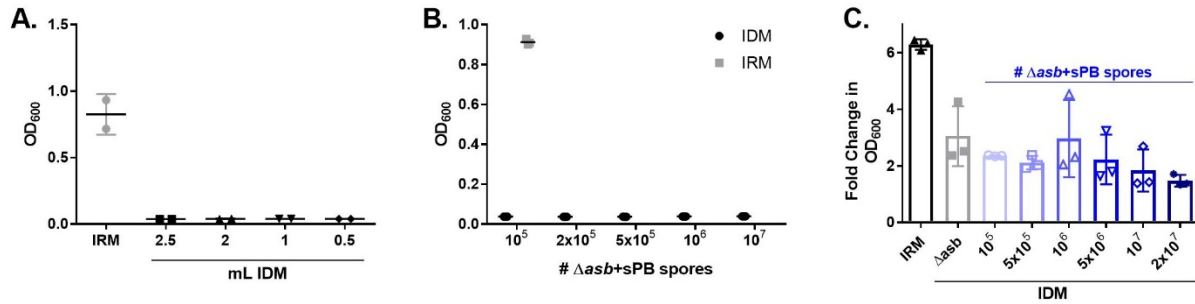


**Figure 3.3 Petrobactin supplementation of the *asb* mutant strain during sporulation does not rescue outgrowth in iron-depleted medium.** The *asb* mutant was supplemented with 25 $\mu$ M purified petrobactin during growth and sporulation in ModG medium. The resulting spores ( $\Delta asb+sPB$ ) were harvested at 72 hours post-inoculation, and washed three times with water. The spores were counted by hemocytometer prior to growth in IDM+I or IRM+I with the  $OD_{600}$  measured at 24 hours post-inoculation. A)  $10^5$  spores in decreasing volumes of IDM+I. Increasing numbers of spores in either B) 0.5 or C) 200 $\mu$ L of IDM+I. High inoculum of C) required the data to be presented as fold change in  $OD_{600}$ .

*Petrobactin, but not bacillibactin, is required for sporulation in ModG medium.* To further explore our hypothesis that petrobactin play a role in spore biology, I tested the ability of an *asb* mutant strain and a *dhb* (bacillibactin) mutant strain to sporulate relative to wild-type. Overnight cultures were inoculated 1:1000 into three mL of ModG medium and incubated with shaking at 37°C. At 12 and 36 hours, colony forming units (CFUs) were enumerated both before and after a 30-minute heat treatment at 65°C to determine total and sporulated CFUs, respectively. Despite an abundance (1.7mM) of ferrous iron in the medium and wildtype-levels of growth (Figure 3.4A), the *asb* mutant strain produced nearly two log fewer spores formed at 12 hours post-inoculation (Figure 3.4B). This translates to less than 10% sporulation compared to 50% sporulation by wild-type and the *dhb* mutant strain (Figure 3.4C). The observed defect in sporulation was not observed at 36 hours post-inoculation and could be rescued by

supplementing growth of the *asb* mutant strain in ModG with 25 $\mu$ M of purified petrobactin (Figure 3.4A-C).

The petrobactin requirement for rapid sporulation suggests the presence of petrobactin in the culture medium. However, a colorimetric catechol assay that detects the petrobactin-specific moiety 3,4-dihydroxybenzoate, failed to detect petrobactin in ModG culture medium (data not shown). This could be either due to interference with the assay by the medium, levels of petrobactin below the limit of detection, or suggest an intracellular role for petrobactin. To confirm the results of the catechol assay, spent culture medium from wild-type and *asb* mutant growth in ModG at 12 hours post-inoculation should be subjected to laser ablation electrospray ionization mass spectroscopy (LAESI-MS).

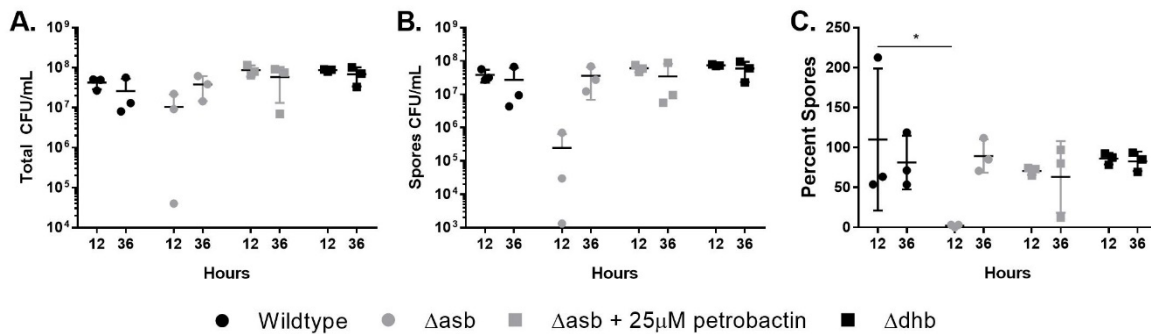


**Figure 3.4 Petrobactin, but not bacillibactin, is required for sporulation in ModG medium.** A 30°C overnight of wild-type, *asb* mutant  $\pm$  25 $\mu$ M petrobactin, and *dhb* mutant bacteria were inoculated 1:1000 into 3mL ModG medium incubated at 37°C. At 12 and 36 hours post-inoculation A) total and B) spore CFUs/mL were determined by plating and C) the percent spores was calculated. Data are compiled from three independent experiments and were analyzed using a two-way ANOVA with a Tukey's multiple comparisons test \*p-value < 0.05, \*\*p-value < 0.005.

*The asb operon is transcribed and translated during late stage growth and early sporulation.*

Using the DBTBS prediction tool and database for *Bacillus* spp. intergenic regions, I searched the 500bp upstream of *asbA* for putative sigma factor binding sites (54). Binding sites for two

sporulation specific sigma factors ( $\sigma^G$  and  $\sigma^K$ ), as well as a general stress transcription factor ( $\sigma^B$ ) were identified with at least 95% confidence (Figure 3.5). To characterize the expression of *asb* during sporulation, I generated transcription and translation reporter constructs by fusing the 500bp upstream of *asb* and the first eight codons of *asbA* either separated by a ribosomal binding site or directly to *gfpmut3*, respectively (134). I next used allelic exchange to insert the constructs on the *B. anthracis* genome, immediately downstream of the *asbA-F* transcriptional terminator to facilitate wildtype-like expression of the *asb* operon reporter. To measure expression, strains of the transcriptional and translational reporters, along with wild-type, were grown in ModG medium for 12 hours with measurements of the OD<sub>600</sub> and GFP fluorescence taken every five minutes. Despite an iron concentration of 1.7mM in ModG, both transcriptional and translational reporters of *asb* were expressed during late stage growth in three independent experiments (Figure 3.6A, black arrow).

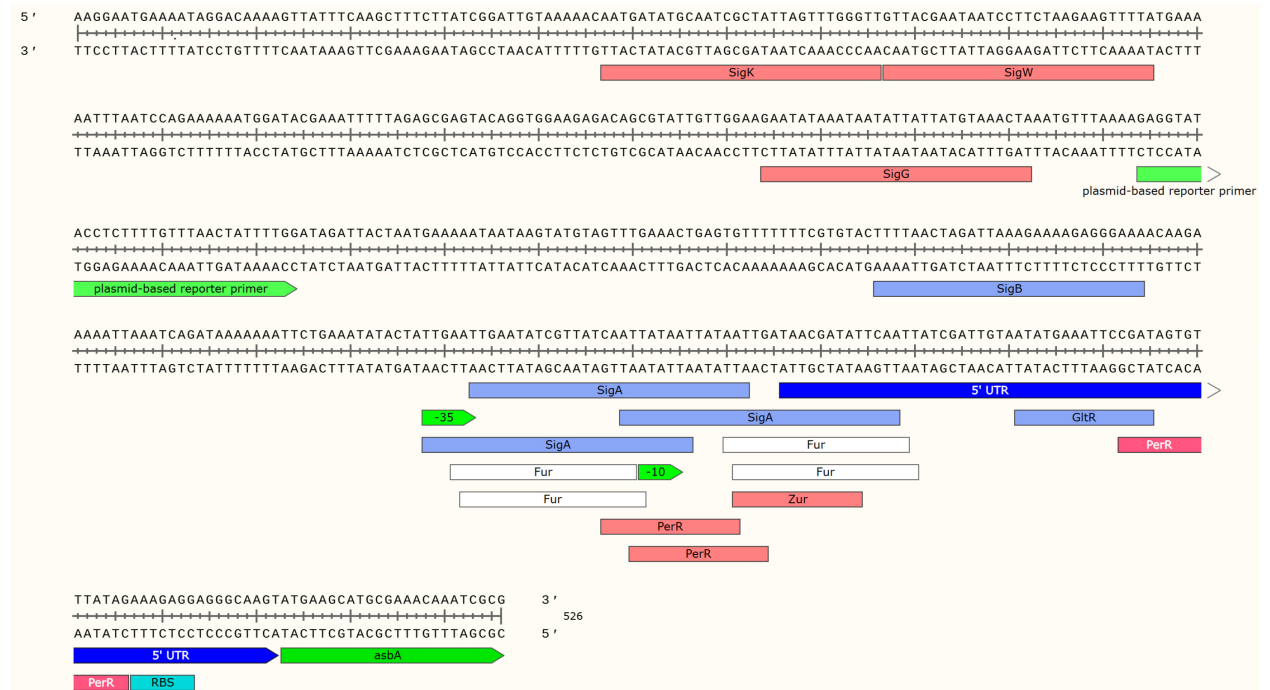
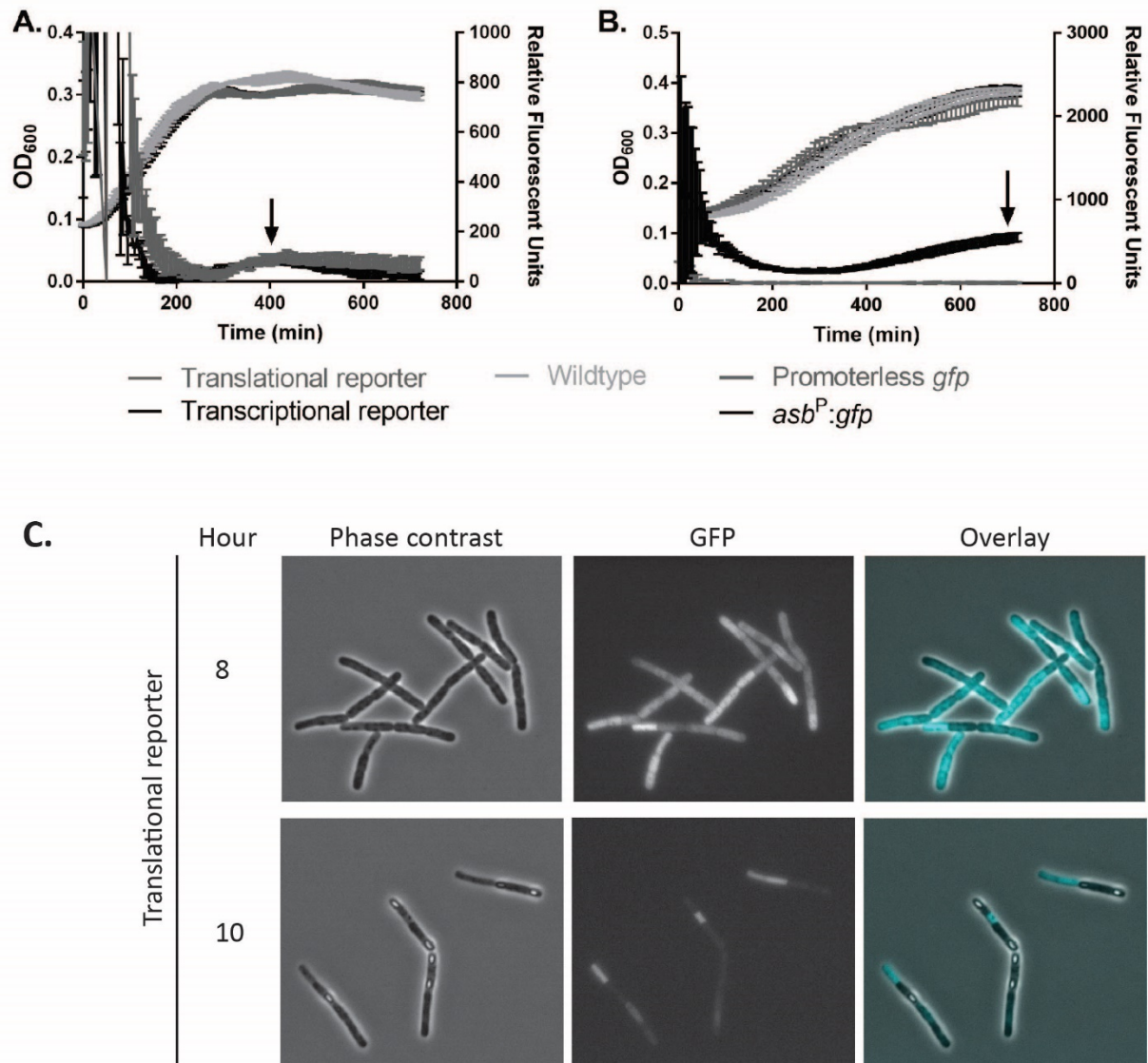


Figure 3.5 Schematic of putative transcriptional regulator binding sites upstream of *asbA*

To determine if the predicted sporulation sigma factors were responsible for the expression of *asbA-F* during late stage growth in ModG, I took advantage of plasmid-based transcriptional reporter constructs for *asb* generated previously in the lab (135). Here, the 200bp upstream of *asbA* were fused to *gfpmut3*, cloned into pAD123, and expressed in a wild-type *B. anthracis* Sterne background. Growing the transcriptional reporter and the negative control, promoter-less *gfpmut3*, strains in ModG again demonstrated late stage expression of *asb* (Figure 3.6B, black arrow). Expression of *asb* was confirmed by fluorescence microscopy of the translational reporter. Cultures grown in ModG were imaged with phase bright and fluorescence microscopy. At 8 hours post-inoculation, *gfpmut3* fluorescence was visible in all cells, indicating *asb* operon induction. By 10 hours, phase bright spores were observed in cells where *asb* was translationally dormant though sporulated cells were found adjacent to cells expressing *Gfpmut3* under translational control of the *asb* operon, suggesting that *asb* expression shuts off before maturation to phase-bright spores (Figure 3.6C).



**Figure 3.6 *asb* transcriptional and translational fluorescent reporters illuminate expression during late stage growth.**

Overnight cultures of wild-type and fluorescent reporters were washed once with BHI and inoculated into ModG (+ 10 $\mu$ g/mL chloramphenicol as needed) at a starting OD<sub>600</sub> of 0.05. Growth (Left axis, OD<sub>600</sub>) and relative fluorescence units (Right axis) were measured every five minutes for 12 hours. Black arrows indicate late stage expression of the *asb* operon A) genomic-based *asb* transcription and translation *gfp* fusion reporters B) plasmid-based promoterless *gfpmut3*, and *asb:gfpmut3* translational reporters C) 5 $\mu$ L of the translational reporter grown in ModG medium for eight and ten hours was imaged by phase bright and fluorescence microscopy.



*Petrobactin is associated with the spore with indeterminate effects on iron storage.* Given that *asb* is expressed just prior to sporulation but that petrobactin is not observed in the culture medium, I hypothesized that petrobactin may have an intracellular role and be associated with the *B. anthracis* spore. To answer this question,  $6 \times 10^7$  spores harvested from ModG were suspended in 50% DMSO and subjected to LAESI-MS. Complete ablation of the spores was confirmed by an abundance of the spore-core-component calcium dipicolinic acid in the chromatograph (data not shown). LAESI-MS detected petrobactin in wild-type, but not *asb* mutant strain, spores (Figure 3.7A). This phenotype could be restored by supplementing growth and sporulation of the *asb* mutant strain in ModG with 25  $\mu$ M of purified petrobactin.

Iron-binding proteins including ferritins and DPS store iron within the spore for growth following germination, however the role of siderophores in iron storage has not been studied. I hypothesized that petrobactin might play a role in iron storage within the *B. anthracis* spore. Spores harvested from ModG medium at 72 hours post-inoculation were washed in sterile, deionized water three times, filtered through a 3.1-micron glass filter, washed twice with nycodenz, then with water three more times. Purity was confirmed by phase contrast microscopy and spores/mL determined by haemocytometer. The spores were dried, then dissolved in 70% nitric acid at 85°C overnight and diluted 1:10 in ASTM type 1 water prior to analysis by ICP-MS (Figure 3.7B). Wild-type spores contained approximately 19 ppb of iron per  $10^9$  spores while *asb* mutant spores were measured at about 100 ppb of iron per  $10^9$  spores with substantial deviation between samples suggesting that *asb* mutant spores have an altered iron storage phenotype.

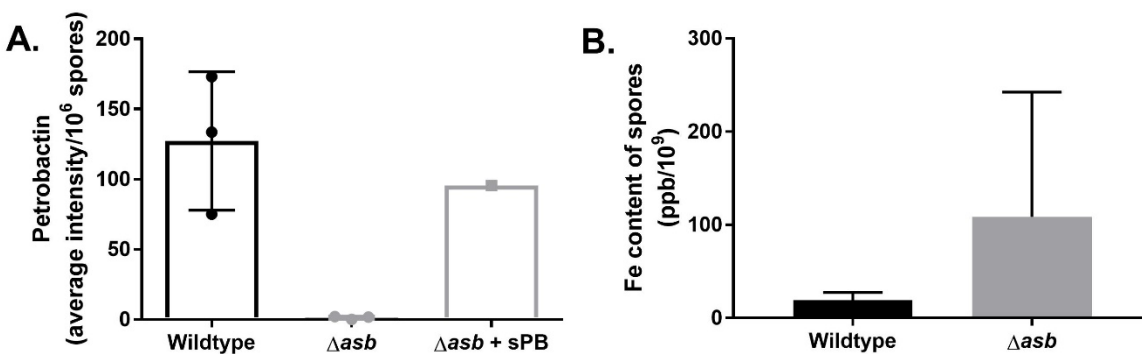


**Figure 3.7 Petrobactin is associated with the *B. anthracis* spore and has indeterminate effects on iron storage.** A)  $6 \times 10^7$  wild-type, and *asb* mutant  $\pm 25 \mu\text{M}$  petrobactin spores harvested from ModG medium were subjected to LAESI-MS. B) Spores prepared similarly were dried, then dissolved in 70% nitric acid overnight at  $85^\circ\text{C}$  for analysis by ICP-MS. Data are compiled from three technical replicates of three independent spore harvests, except the *asb* mutant +  $25 \mu\text{M}$  petrobactin ( $n=1$ ).

*Petrobactin, but not hemin, is required for rapid growth and sporulation in bovine blood.*

Following death of an infected mammal, blood laden with *B. anthracis* is exposed to the atmosphere by either hemorrhagic draining or the activity of scavengers on the carcass (118, 136, 137). This dilutes the blood-borne  $\text{CO}_2$  that suppresses sporulation, thus triggering the sporulation cascade in a race against decomposition (136). Since vegetative bacilli are not easily infectious, *B. anthracis* transmission requires sporulation in aerated blood. To determine the relevance of each iron acquisition system—petrobactin, hemin, and bacillibactin—to disease I performed the sporulation experiments described previously in bovine blood. Overnight cultures of wild-type *B. anthracis* Sterne, the *asb* mutant, the *dhb* mutant, and the *isd* mutant strain (a mutant in hemin utilization) were inoculated 1:1000 into 3mL of defibrinated bovine blood. Strains were supplemented with either petrobactin or hemin. Hemin is the oxidized form of heme, which is released into blood by the lysis of red blood cells and is bound by *B. anthracis* hemophores (138, 139). Thus, hemin was chosen as a supplement to determine if the *isd* system

could complement the *asb* mutant strain and as a negative control for the *isd* mutant strain. The blood cultures were shaken at 37°C for three days. Every 24 hours, colony forming units per mL (CFUs/mL) were enumerated both before and after a 30-minute heat treatment at 65°C to determine total and sporulated CFUs/mL, respectively.

Compared to wild-type, the *asb* mutant strain and *asb* mutant strain supplemented with hemin were reduced in growth by one log, all other strains and conditions—the *asb* mutant strain supplemented with 25µM petrobactin (n=1), the *isd* mutant strain, *isd* mutant strain supplemented with hemin and the *dhb* mutant strain (n=1)—had equivalent CFUs/mL (Figure 3.8A,B). Accordingly, percent sporulation at 48 hours and 72 hours for the *asb* mutant strain and *asb* mutant strain supplemented with hemin was about 25% compared to the wild-type strain at 80% (Figure 3.8C). Percent sporulation for the *isd* mutant strain, *isd* mutant strain supplemented with hemin and the *dhb* mutant strain were about 50%, though these were not statistically significant from wild-type. Despite the increase in both total and spore CFU/mL, supplementation of the *asb* mutant with purified petrobactin did not improve percent sporulation. More replicates are needed, but this could be due to large differences in CFU/mL that are masked by presenting the data in log scale.

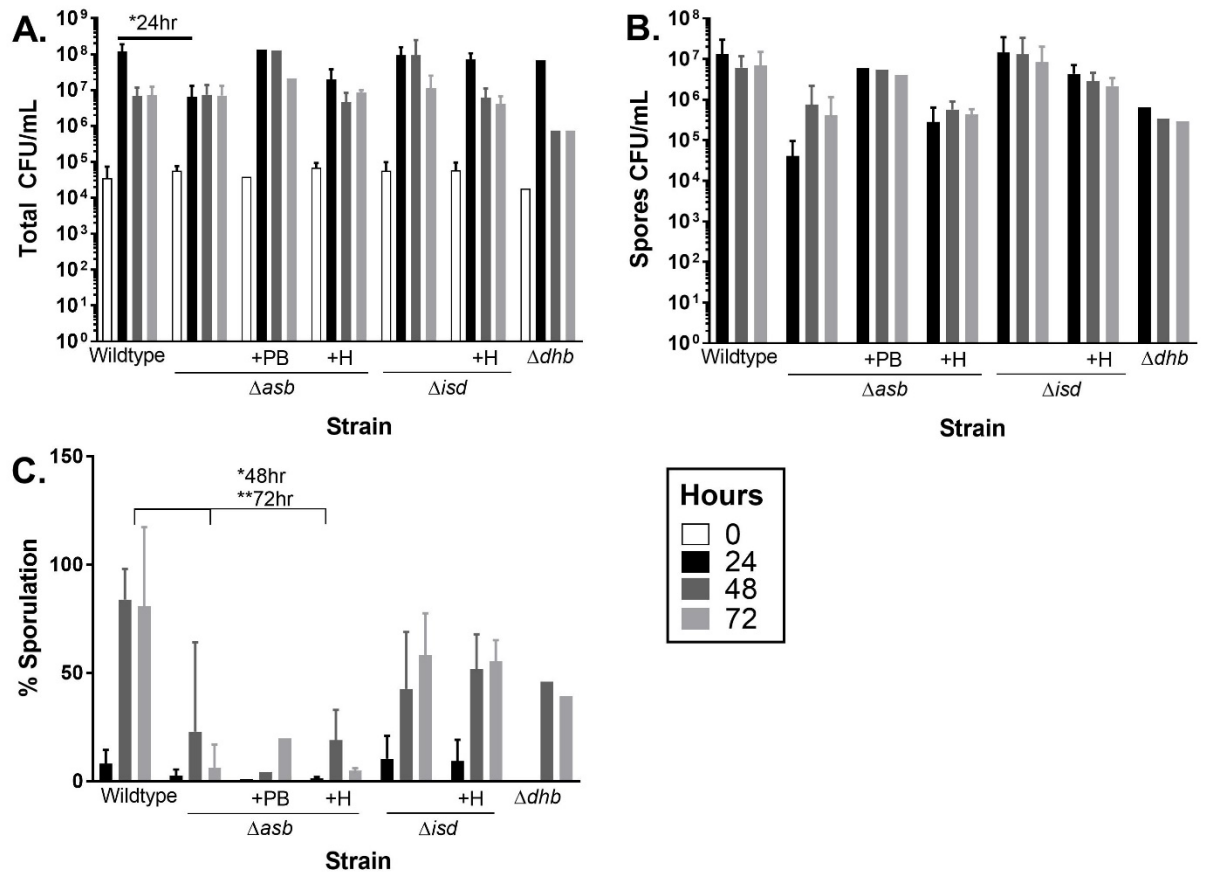


**Figure 3.8 Petrobactin, but not hemin, is required for growth and sporulation in bovine blood.** Defibrinated bovine blood was inoculated 1:1000 with either wild-type, the *asb* mutant, the *isd* mutant or the *dhb* mutant and supplemented with either 25 $\mu$ M of petrobactin (+PB) or 0.5 $\mu$ M hemin (+H) as indicated. At 24 (black), 48 (dark gray), and 72 (light gray) hours post-inoculation, CFU/mL was determined both A) before and B) after a 30-minute heat treatment at 65°C and used to calculate the C) percent sporulation. Data are compiled from three independent experiments (except for the *dhb* mutant and *asb* mutant supplemented with petrobactin, n=1) and were analyzed using a two-way ANOVA with a Tukey's multiple comparisons test \*p-value < 0.05, \*\*p-value<0.005.

## Discussion

In this chapter, I show that petrobactin is not required for *B. anthracis* germination (Figure 3.2A) but is required for rapid sporulation in ModG medium (Figure 3.4C). Using fluorescent *asbA:gfp* reporter fusions, I show that *asb* is both transcribed and translated during

late stage growth of *B. anthracis* while other cells in the population are undergoing sporulation (Figure 3.6). and that, as a result, petrobactin is associated with the *B. anthracis* spore (Figure 3.7A). Additionally, I show that these findings may have relevance to anthrax transmission since petrobactin is also required for sporulation in bovine blood (Figure 3.8C), a pre-requisite for survival and transmission of the pathogen (118, 136). This is the first demonstration that a siderophore is induced in preparation for sporulation and packaged in the complete spore.

The iron-gathering capacity of siderophores has long been appreciated for pathogenicity via survival and growth of the vegetative cell, but only recently as a function of transmission and survival by spores. In early 2017, Grandchamp et. al showed that siderophore supplementation (including with the native bacillibactin) caused the onset of sporulation in *B. subtilis* to occur earlier (140). Since the enhancement required import of the siderophore into the bacterial cell and iron removal by corresponding hydrolases, the authors hypothesized that the extra intracellular iron acted as a signal for the onset of sporulation (140). However, their study did not address bacillibactin regulation or export during sporulation. So, to my knowledge, mine is the first demonstration that a siderophore is induced in preparation for sporulation, even in high iron conditions during which siderophore expression is typically repressed.

This raises questions regarding how *asbA-F* is being regulated and how petrobactin becomes associated with the *B. anthracis* spore. Some siderophores, such as petrobactin, are biosynthesized in response to oxidative stress conditions and catecholate siderophores (*e.g.*, enterobactin and salmochelin) are protective against reactive oxygen species (56, 57, 141, 142). There are multiple non-exclusive hypotheses for siderophore upregulation under these conditions. One, that superoxide radicals oxidize iron co-factors thus inactivating key enzymes. Two, that upregulation of the enzymes to mitigate oxidative stress require metallic (*e.g.*, iron and

manganese) co-factors. Both of these would reduce the intracellular iron pool and thereby relieve iron-binding by the iron-dependent transcriptional repressor, Fur, to enable iron acquisition system expression (56, 57). Third, that a superoxide stress transcriptional regulator activates siderophore expression, in this case *asbA-F*. Sporulation has not been directly shown to be accompanied by oxidative stress, but nearly all of the stress responses that initiate sporulation also initiate oxidative stress (143). This is further supported by observations that oxidative stress protective enzymes are induced during late stage growth of *B. anthracis*, maintained during sporulation, and that two superoxide dismutases are even incorporated into the exosporium (131, 144). Additionally, the intracellular iron pool is further depleted during sporulation due to upregulation of aconitase, an iron-rich citrate isomerase and stabilizer of  $\sigma^K$ -dependent gene transcripts (145, 146).

While the demand for iron during oxidative stress and or sporulation may relieve negative regulation by Fur, it is also possible that *asbA-F* expression is induced by an unknown transcriptional regulator. This putative transcription factor may be related to oxidative stress, sporulation, or a general stress response. In *Azotobacter vinelandii*, biosynthesis of a catechol siderophore is believed to be activated by the oxidative stress response regulator, SoxS (147). The observed phenotype for *A. vinelandii* is similar to that observed by Lee et al. for petrobactin: high iron repression of the siderophore can be overcome by oxidative stress (56, 147). A similar regulation strategy for petrobactin is bolstered by a putative PerR binding site upstream of *asbA* (54). Another potential candidate for alternate regulation of petrobactin is  $\sigma^B$ , a general stress response transcription factor with a predicted binding site within 200bp upstream of the *asbA* translational start site (54). In *B. subtilis*,  $\sigma^B$  is active during early sporulation, but is not required

for sporulation, likely since most  $\sigma^B$ -regulated genes can be activated by other transcription factors (148).

Regarding association of petrobactin with the spore, it may be that small amounts biosynthesized within the cell are randomly associated with the prespore. Another possibility is that petrobactin is produced in the mother cell and transported into the forespore by ApeX or an unknown transporter, either of which might be regulated similarly to *asbA-F* during late stage growth and early sporulation. These questions might be answered by further experiments to determine where in the spore petrobactin is located (*e.g.*, spore core, spore coat, exosporium) and what genes are required to maintain association of the spore (*e.g.*, FpuA or ApeX). While I concluded that spore-packaged petrobactin is not required for outgrowth from spores, it may require petrobactin biosynthesis to occur within the prespore or mother cell. Experiments with the *asb* operon under control of an inducible promoter would be required to determine if that were the case or not.

The contribution of petrobactin toward iron storage within the spore should also be addressed. It is unknown whether the stored petrobactin is complexed with iron or not. Attempts to answer this question were inconclusive because while wild-type spores contained about 19ppb per  $10^9$  spores, the iron content of *asb* mutant spores was highly variable, reaching 130ppb per  $10^9$  spores. It is possible that *B. anthracis* must reach an iron threshold to complete sporulation, a hypothesis that fits the current understanding of iron restriction on sporulation. It is also possible that *B. anthracis* has multiple systems to reach that threshold. For instance, the *asb* mutant strain will eventually sporulate and has large amounts of iron associated with the spores. Perhaps this requirement is met by bacillibactin, soluble iron uptake systems, and the production of iron-

binding pigments such as pulcherrin—a rust-colored pigment sometimes produced during sporulation that appeared to be present in *asb* mutant spore harvests (data not shown) (149).

These data suggest that petrobactin is the preferred iron acquisition system for growth and sporulation in bovine blood, despite multiple potential iron sources. Petrobactin is required to achieve wild-type growth of  $10^8$  CFUs/mL in blood, but the *asb* mutant was still able to grow to  $10^7$  CFU/mL, suggesting that another iron acquisition source was functioning, likely either the *isd* system or bacillibactin. Greater concentrations of hemin may be needed to complement the *asb* mutant strain sporulation defect. Previous work has shown that petrobactin is required for growth in macrophages and iron-depleted medium, but had not been demonstrated for growth in blood prior to these experiments. In addition, these experiments testing the ability of each iron acquisition mutant for their ability to grow and sporulate in aerated bovine blood show a direct link between petrobactin and anthrax transmission via the spore. Growth in blood is the endpoint for an anthrax infection so not only must the bacilli grow well but also prepare for survival and transmission between hosts. Literature suggests that exposure of blood-borne bacilli to oxygen as a dying host bleeds out begins the signaling cascade for sporulation (118, 136). As a spore, it has the capability to endure in the environment, migrate, and start the cycle of infection anew.

These data contribute to the model of *B. anthracis* iron acquisition and sporulation. In this model, upon entry of the population into late stage growth, environmental stressors both deplete the intracellular iron pool and induce oxidative stress that act to upregulate the *asb* operon. Small amounts of petrobactin maybe biosynthesized for iron acquisition and/or protection against oxidative stress as the bacillus transitions into sporulation. Either direct import of petrobactin into the prespore or random association results in packaging of petrobactin into the spore.



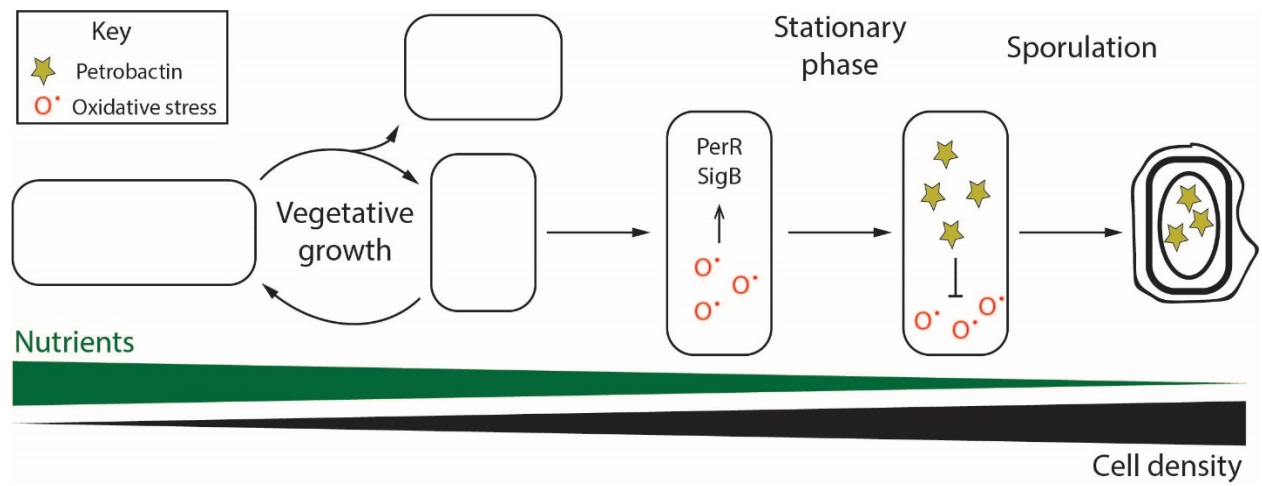


Figure 3.9 Proposed model of petrobactin use by *B. anthracis* during late stage growth and early sporulation.

## Chapter 4

### Discussion and future directions

#### Dissertation summary

*Bacillus anthracis* is a Gram-positive, spore forming bacillus that requires the siderophore petrobactin to cause infection in a mouse model of inhalational anthrax. Petrobactin and its use by *B. anthracis* have many unique characteristics relative to other siderophores. Biosynthesis is mediated by the *asb* operon, which encodes enzymes from both of the canonical siderophore synthesis pathways and an enzyme responsible for generating idiosyncratic iron-binding moieties. These moieties, 3,4-dihydroxybenzoate, cap two spermidine arms that are linked to a citrate backbone and are not employed by any other known siderophore. They protect the siderophore from capture by the siderophore-binding innate immune protein siderocalin, enabling the pathogen to gather iron while evading immune detection. Import of the iron-petrobactin complex is redundant, and facilitated by ABC-type transporters composed of a surface receptor, FpuA, two permeases, FpuB and FatCD, and three ATPases, FatE, FpuC, FpuD. (chapter one) (77).

Export of petrobactin occurs through the RND-type transporter, ApeX. In the absence of ApeX, petrobactin components, including 3,4-dihydroxybenzoate, are detected in the culture medium by a colorimetric catechol assay. Confirming the absence of petrobactin from the culture

medium of an *apeX* mutant strain required laser ablation electron spray ionization mass spectroscopy (LAESI-MS) to measure the intact molecule directly, as opposed using 3,4-dihydroxybenzoate moieties as proxies. It is unclear whether the components exported by an unknown mechanism are truncated biosynthesis products or are the result of petrobactin degradation. But supplementation of both an *asb* and a *fpuA* mutant strain with culture medium from an *apeX* mutant rescued their growth in IDM, indicating that these components gather sufficient iron to support growth and use an alternate import system. Additionally, an *apeX* mutant strain causes wild-type levels of disease in a mouse model of inhalational anthrax indicating that these components are sufficient for *in vivo* growth and immune evasion (chapter two) (132).

The endpoint of an anthrax infection is profuse bleeding and death of the mammal. As the animal bleeds out, the bacilli-filled blood is exposed to oxygen, which triggers sporulation. Petrobactin is the preferred iron acquisition system during growth and sporulation in aerated bovine blood. Despite the presence of other systems, petrobactin is required to reach the wild-type levels of growth and sporulate. Even in high iron sporulation medium, petrobactin is required for rapid sporulation. Fluorescent transcriptional and translational reporters for the *asb* operon show that the biosynthetic system is induced during late stage growth and early sporulation. This induction was confirmed by microscopy, indicating that even as some bacilli are highly expressing *asb*, those that are completing sporulation are non-fluorescent. These data suggest that petrobactin biosynthesis maybe regulated by a general or oxidative stress transcription factor. LAESI-MS analysis of *B. anthracis* spores detected petrobactin associated with the spores though it is unclear what effect petrobactin has on iron storage within the spore. Germination from the spore does not require petrobactin (chapter three).

## Export of petrobactin components

Efforts to identify the origin and structure of petrobactin components exported by an *apeX* mutant strain were unsuccessful (Chapter two). High resolution electron spray ionization mass spectroscopy was performed on the culture medium from wild-type, *asb*, *fpuA*, and *apeX* mutant strains, as well as the culture medium from *asb* mutant strain supplemented with *fpuA* mutant spent medium, to identify which molecules might be the result of petrobactin processing. I predicted that if the same component(s) were identified in the culture medium of the *apeX* mutant strain, wild-type, and *asb* supplemented with *fpuA*, but not the *asb* mutant, then it is likely to be a result of ferric-petrobactin processing within the cell. Conversely, the presence of petrobactin-dependent molecules in wild-type, *fpuA* and *apeX* mutant strains would suggest an origin point of truncated biosynthesis since an *fpuA* mutant cell cannot import ferric-petrobactin for processing. However, none of the predicted components were detected. One possibility is that petrobactin processing generates components that were not predicted. Another possibility is that the components in the samples were not concentrated enough to be detected. I predict that future experiments to identify the petrobactin components and their origin will be more fruitful if they employ a comparative metabolomics approach to detect which molecules are present or absent in each of the culture media listed above.

Which transporters are responsible for the export of petrobactin components and the import of their iron-bound complexes are other areas that will require further investigation. During my search for the petrobactin exporter, a mutant in GBAA\_0181 appeared to have lower levels of 3,4-dihydroxybenzoate in the culture medium, as determined by thin layer chromatography (TLC). Screening the transport mutants generated in chapter two for 3,4-dihydroxybenzoate export by TLC might be a good strategy for identifying the exporter of the

free 3,4-dihydroxybenzoate that has been observed in *B. anthracis* culture medium. The molecular weight of 3,4-dihydroxybenzoate is small (~154g/mol), making detection by mass spectroscopy difficult due to noise from other molecules with similar sizes. Additionally, TLC is amenable to high-throughput screening. It is very likely, however, that since there are probably a variety of petrobactin components exported there are likely to be multiple transporters involved in both component export and iron-bound import. Another possibility, which would be more difficult to demonstrate, is that the petrobactin components are small enough and carry the appropriate charge to either diffuse out of the bacterial cell, as predicted for enterobactin monomers, or use a general efflux mechanism (83). While it is possible that ferric-3(3,4-dihydroxybenzoate) could diffuse across the cell membrane, I predict that a dedicated import system would still be required for iron-bound complexes. The petrobactin receptor in *B. subtilis*, YclQ, has nanomolar affinity for these complexes and specific transporters are required for import of iron-bound enterobactin monomers in Gram-negatives (110, 150). In any case, a good first step to identifying transport would be to confirm the identity of the petrobactin components in the culture medium.

In chapter two, supplementing *asb* mutant strains with pure citrate improved growth by about 30% (Figure 2.4B). This suggests that *B. anthracis* may have an inducible ferric citrate import system. *B. subtilis* has been reported to have a ferric citrate import system while the ABC-type transport system *fecABC* is required for full virulence by *B. cereus* in an insect infection model (151, 152). *B. anthracis* doesn't have a homologue for the *B. cereus fecA* but does have ORFs designated as iron ABC transporter substrate binding proteins which belong to the FecCD family. The presence of an inducible ferric citrate import system may explain how an *asb* mutant can achieve wildtype-level cell density after 24 hours of growth in IDM. I would

predict that deletions in both a ferric citrate import system as well as the *asb* operon would abrogate the delayed growth kinetics and prevent all growth in IDM.

We hypothesize that other pathogens also export siderophore components but that the relevance of the components relies heavily on the relevance of the intact siderophore. Petrobactin components may only support *B. anthracis* growth *in vivo* because petrobactin does so. The 3,4-dihydroxybenzoate rings prevent petrobactin binding by siderocalin, an immune protein that binds iron-bound 2,3-dihydroxybenzoate siderophores such as enterobactin (71). 3,4-dihydroxybenzoate containing components may also avoid binding by siderocalin and additionally the recycling of siderophore components may enable *B. anthracis* to double-dip iron with petrobactin biosynthesis. This suggests to me that the best treatment strategies targeting iron acquisition through siderophores are those that either completely block siderophore biosynthesis or subvert siderophore recognition pathways with Trojan-horse type sideromycin treatments.

### Removal of iron from the ferric-petrobactin complex

As discussed in chapter one, there are two known mechanisms for iron removal from siderophores: enzymatic reduction or siderophore cleavage. Which mechanism is used for which siderophore appears to depend on the affinity of the siderophore for its ferric ligand. Those with a stronger affinity are generally cleaved while iron is enzymatically reduced from lower affinity siderophores. The affinity of petrobactin for ferric iron lies in the middle of these two extremes, low enough that reduction seems feasible but high enough that degradation is difficult to rule out (24). Unpublished experiments from a previous graduate student where growth of an *asb* mutant in IDM was supplemented with 6nM petrobactin were interpreted to provide evidence for petrobactin recycling. However, this interpretation was based on culture growth at 24 hours post-

inoculation when growth was not improved at six or eight hours. In my hands, the *asb* mutant strain can achieve an OD<sub>600</sub> equivalent to wild-type by 24 hours. Together, this suggests delayed activity of an alternate iron acquisition system at a slower growth rate. I argue that for concentrations of petrobactin to be interpreted as sufficient to rescue growth of the *asb* mutant strain, then they should allow for wildtype-like growth rates within the first eight hours.

Therefore, to understand petrobactin iron removal in *B. anthracis*, I used a bioinformatic selection protocol like that described in chapter two and generated a list of putative iron removal enzymes. A PSI-BLAST of known siderophore iron removal enzymes, including hydrolases and reductases (66, 67, 153–156), was conducted against the *B. anthracis* genome and combined with microarray data of *B. anthracis* grown in iron limiting conditions (17, 55, 103). This generated a list of ten candidate enzymes for removal of iron from holo-petrobactin: two hydrolases, two hypothetical hydrolases, three oxidoreductases and three hypothetical reductases (Appendix, Table A.1).

I hypothesized that if a mutant were deficient in iron removal from petrobactin, it would grow poorly in IDM and accumulate catechols in the culture medium. This was based on the prediction that since the bacterium would be unable to process ferric-petrobactin, ferric-petrobactin would accumulate within the cell, eventually blocking import of additional ferric-petrobactin thus leading to accumulation in the medium and reduced growth. Marker-less deletions of the genes encoding each of the candidate enzymes were made one-by-one in *B. anthracis* Sterne 34F2 (Table A.2), as described by Janes and Stibitz (97). Each of the deletion mutants were screened for their ability to grow in IDM and export catechols into the culture medium.

When tested, however, each of the iron removal mutants grew and produced wildtype-like levels of catechols in the culture medium (Table A.3). As redundancy is common in *B. anthracis*, I targeted the hydrolases (GBAA\_1242, GBAA\_1392, GBAA\_2694) for double and triple deletion mutants and generated a double mutant of reductases (GBAA\_0766, GBAA\_1859). Again, however, growth and catechol export phenotypes mimicked wild-type. The observation of wildtype-like phenotypes in the putative iron-removal mutants might be due to further redundancy or non-specificity of the reaction, particularly if iron reduction and petrobactin recycling is the predominant method of iron removal. Another possibility is that the initial screening protocol failed to identify the enzyme responsible.

These experiments were performed prior to the discovery discussed in chapter two, that petrobactin components are exported in the absence of the exporter ApeX (132). However, the components generated or their origin (truncated biosynthesis versus enzymatic degradation) have not been identified. So, while this suggests that petrobactin could be cleaved during processing, I cannot predict what kind of hydrolase may be responsible for any fragmentation. Accordingly, the next step in identifying processing of petrobactin by enzymatic cleavage could be identifying the components exported by *apeX* mutant strain. By purifying and identifying the components, the mechanism of action, and thus the enzyme responsible, may become clearer. One way to accomplish this might be to use purified petrobactin or culture medium from the *fpuA* mutant strain to supplement growth of the *asb* mutant strain. If Fe<sup>3+</sup>—petrobactin is enzymatically cleaved then petrobactin-derived components should be present in the culture medium following supplementation of the *asb* mutant strain, but not before. However, if Fe<sup>3+</sup>—petrobactin is recycled, then no petrobactin-derived components should be present.



Identifying the mechanism of iron-removal from petrobactin is the next major step in understanding how *Bacillus anthracis* uses the siderophore for iron scavenging. In addition, it could inform efforts to treat *B. anthracis* with sideromycins, siderophores conjugated to antibiotics, or other therapeutics. First, knowing where iron-removal occurs (*e.g.*, cell surface, cytoplasm) is key to knowing which type of antibiotic to conjugate (*e.g.*,  $\beta$ -lactamase or translation inhibitor). Second, understanding whether iron removal is performed by a single enzyme versus multiple has implications for the utility and potential development of small molecule inhibitors.

### Petrobactin regulation suggests alternate functions

Evidence for siderophore functions other than iron scavenging has accumulated since their discovery. Multiple reports have demonstrated roles of siderophores in cell signaling, sporulation initiation, protection from copper and oxidative stress, and even the generation of oxidative stress against competitors (157). As described in chapter one, siderophores are primarily regulated by the iron-dependent repressor, Fur. However, data presented in chapter three and by previous graduate students indicate that regulation of petrobactin biosynthesis is more nuanced and that this nuance may be related to alternate functions of petrobactin in *B. anthracis* (135, 158).

Enterobactin, salmochelin, and catecholate siderophores produced by *A. vinelandii* are all protective against oxidative stress (141, 147). In their study describing the protective abilities of enterobactin and salmochelin against oxidative stress, Achard et al. showed that two other siderophores, yersiniabactin and aerobactin, are not protective (141). This led the authors to conclude that siderophore-mediated protection against oxidative stress goes beyond iron

chelation and might be due to the iron-binding catechol moieties used by enterobactin and salmochelin. However, supplementation with unbound catechols (2,3-dihydroxybenzoate) did not rescue protection against hydrogen peroxide, leading the authors to further hypothesize the formation of antioxidant polyphenols. This hypothesis has since been refined by two studies demonstrating that hydrolysis of enterobactin is required for protection against oxidative stress (159, 160). Thus far, all of the siderophores directly shown to protect against oxidative stress contain catechol moieties. And for at least two of these, regulation is linked to oxidative stress. Enterobactin is positively regulated by the oxidative stress response and there is compelling evidence linking *A. vinelandii* siderophores to similar regulation (147, 159, 160).

While yersiniabactin alone does not protect against oxidative stress, its cupric complex can function as a superoxide dismutase (157, 161). Evidence also suggests that yersiniabactin signals with the host immune response to increase inflammation and spread the infection while enterobactin in the soil may cooperatively supply silicon to nearby plants (157, 162). Other siderophores are implicated in cell signaling roles. Aquatic vibrioferrin forms complexes with boron, which is hypothesized to function as either a signaling molecule for Fur or as a quorum sensing molecule (157). In other bacteria, siderophores can act as inducers for expression of cognate transporters (*e.g.*, yersiniabactin, pyoverdines), to increase biosynthesis of themselves (pyoverdines) or other siderophores, and even induce sporulation (140, 157).

As outlined in chapter one, petrobactin biosynthesis is regulated by several factors including: aeration, temperature, iron concentration, and atmosphere (*e.g.*, 5% CO<sub>2</sub>). But unpublished data from Stephen Cendrowski suggests that petrobactin biosynthesis might also be regulated by petrobactin (135). Cendrowski expressed a plasmid-based transcriptional reporter for the *asb* operon in both wild-type and *asb* mutant strains of *B. anthracis*. In addition to regulation by iron,

there was a differential regulation of the *asb* operon according to the strain background, notably *asb* was not expressed as highly in the *asb* mutant background as wild-type. Cendrowski hypothesized that petrobactin might autoregulate its own expression but did not have purified petrobactin available to test his hypothesis. Additional unpublished data using the genomic reporters described in chapter three suggest that *asbA-F* might be expressed at low cell densities then shut off during the early to mid-log phase in all media tested (BHI, IDM, IRM, ModG). This could suggest a role for petrobactin in cell signaling, or be a symptom of sweeping transcriptional changes due to changes in growth conditions. In either case, more experiments are needed to ensure that this isn't an artifact of the growth conditions used and better characterize the trend observed. The differential regulation of petrobactin suggests that it may fill multiple roles for *B. anthracis* such as protection against oxidative stress and/or as a cell signaling molecule.

### Optimization and adaptation of LAESI-MS

Key pieces of data throughout this work have been generated through collaborative work to adapt LAESI-MS to small molecule detection in unprocessed samples. Thus far, sample types that have been successfully processed for the detection of petrobactin include *B. anthracis* spores, cell pellets, and spent culture media. Previous studies using LAESI-MS have been able to detect hundreds of metabolites ranging from small secondary metabolites to lipids to proteins from plant leaves, infected root nodules, fish gills, and the agar surrounding a bacterial colony isolated from road kill (93, 95, 96, 163). The potential of LAESI-MS to address questions of spatial dynamics in microbiology and immunology is great. For instance, either clinical or basic researchers could use the technique to rapidly assay tissues taken from surgery or necropsy for

pathogen-specific metabolites. Others could better study the kinetics and patterns of dissemination of metabolites during an infection, or antibiotics into an abscess, *in vitro* interspecies interactions, and even the metabolic landscape of a biofilm. And because LAESI-MS can sample a very broad spectrum of metabolites, it could be used to develop diagnostic metabolic profiles for pathogens, which could then be used in a clinical setting.

As powerful as LAESI-MS is, there are still limitations. First, LAESI is a sampling technique whose resolution is only as sensitive as the MS used for the analysis. This could be an issue in adapting LAESI-MS for use in clinics where metabolites may only be present in very low concentrations, thus requiring highly sensitive equipment. As with other MS techniques, there's a requirement for authentic standards and those may be difficult or expensive to obtain. But an early paper on LAESI-MS identified a couple of even more crucial limitations. One is water content. LAESI-MS is a powerful technique in part because it facilitates analysis directly from aqueous samples. This bypasses time-consuming processing techniques but means that the water content of a sample affects the resolution of the analysis. When authors compared the amount of a plant metabolite in two leaves that were identical except for hydration status, they found that water content affected the analyte signal strength (163). This could present problems either when samples are less hydrated than the standard curve or when comparing tissue samples with phenotypes that may affect water content or localization. A second issue is that the LAESI technique alone doesn't employ a strategy like chromatography to separate analytes by properties other than their  $m/z$ . As a result, metabolites with identical  $m/z$  ratios cannot be distinguished from each other. Another group addressed this using ion mobility separation, whereby the ions generated by LAESI are passed through a gaseous buffer that separates ions by their shape prior to MS analysis (95).

## Conclusion

In this work, I have added to our understanding of how *B. anthracis* uses petrobactin both during growth in iron-limited medium, as well as during sporulation. This work also underscores the vital role of petrobactin in the many stages of *B. anthracis* infection, which can be summarized using the following model (Figure 4.1). A mammal is exposed to *B. anthracis* spores, for instance through inhalation, which contain petrobactin. A spore is taken up by a macrophage or other antigen presenting cell, where it germinates within the phagolysosome, scavenges iron using petrobactin, and produces toxins to escape into the cytoplasm. There, the bacillus replicates and continues toxin production, eventually killing the macrophage whose cell lysis releases vegetative bacilli into the lymph or bloodstream. Continued growth of *B. anthracis* in the bloodstream is supported by multiple iron acquisition systems including hemophores and petrobactin until the host succumbs to the infection and its associated toxins. Death of the animal results in exposure of bacilli-laden blood to air, which triggers oxidative stress, sporulation, and induction of the *asb* operon, leading to incorporation of petrobactin in spores and eventual transmission to a new host.

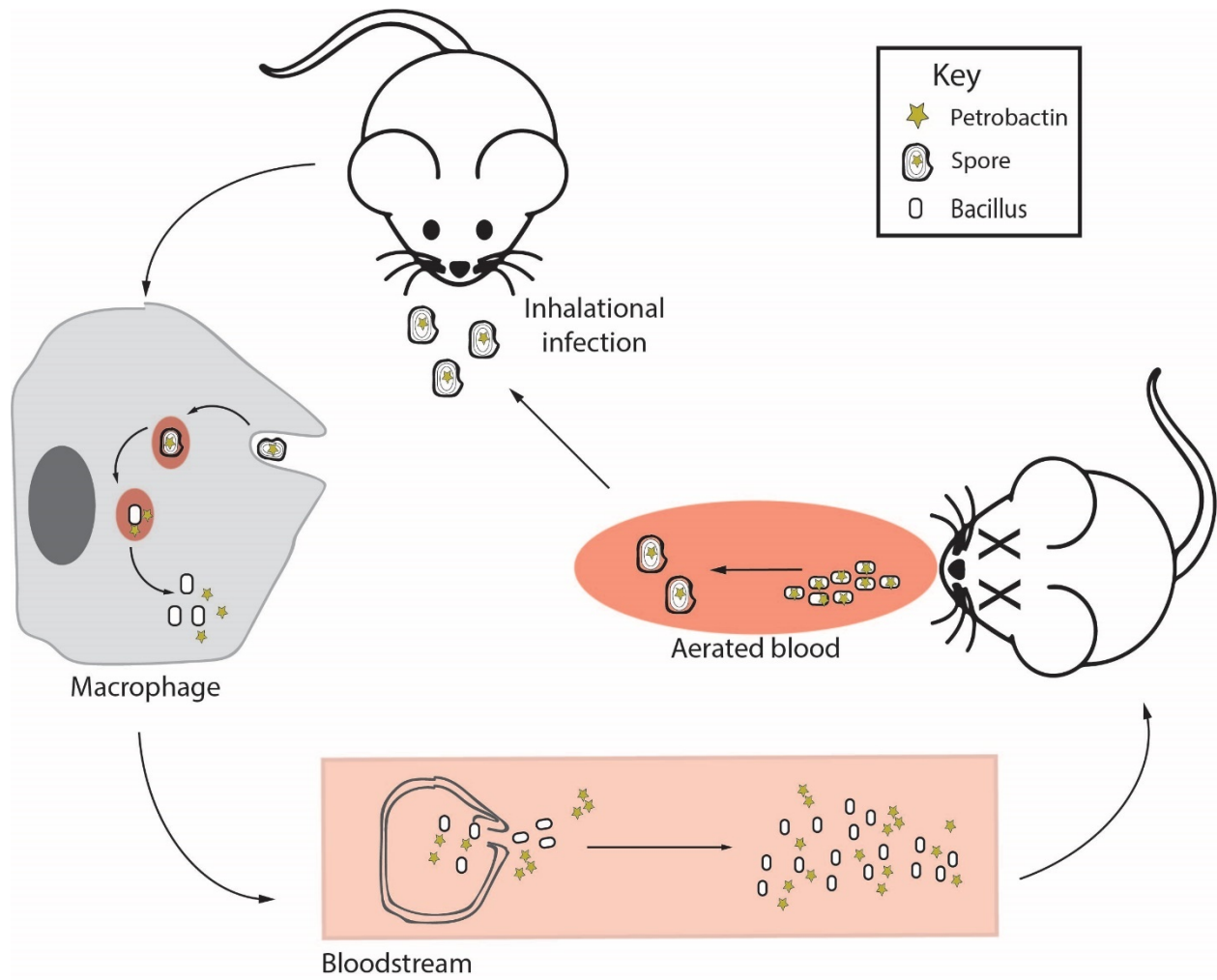


Figure 4.1 Proposed model of *B. anthracis* petrobactin use throughout the cycle of infection and transmission.

## Appendix

**Table A.1 Candidate petrobactin iron-removal proteins**

Enzyme	Gene <sup>a</sup>	Fold-change			Blood <sup>c</sup>			MΦ <sup>d</sup>	Homologue	PSI-BLAST (%)	
		IDM <sup>b</sup>	2 h	3 h	4 h	2 h	1-2 h			>3 h	Cov
Reductase	0352	1.76	4.88	2.8	4.04		4.23				
	0766	2.13	6.18	5.69							
	1859			1.6				6.92			
	1187								ViuB ( <i>V. cholera</i> ) SIP <sup>e</sup>	22	29
									YqjH ( <i>E. coli</i> ) SIP <sup>f</sup>	22	29
	3181								FhuF ( <i>B. pseudomallei</i> ) <sup>g</sup>	8	46
	4110								FhuF ( <i>B. pseudomallei</i> ) <sup>g</sup>	24	30
Hydrolase	1242	1.06	2.08	4.23		2.65			IroD ( <i>E. coli</i> ) <sup>h</sup>	27	31
									Fes ( <i>E. coli</i> ) <sup>i</sup>	14	32
	1392		1.35				2.85				
	2694	1.09	1.36	2.55					Fes ( <i>E. coli</i> ) <sup>i</sup>	86	24
									IroD ( <i>E. coli</i> ) <sup>h</sup>	92	24
									YuiI ( <i>B. subtilis</i> ) <sup>j</sup>	30	33
	3863	2.97	10.7	4.78	3.63		2.28		IroE ( <i>E. coli</i> ) <sup>h</sup>	52	33
								YuiI ( <i>B. subtilis</i> ) <sup>j</sup>	95	46	

<sup>a</sup> GBAA\_, *Bacillus anthracis* strain "Ames Ancestor" (taxid: 261594)

<sup>b</sup> Carlson et al., 2009

<sup>c</sup> Carlson et al., 2015

<sup>d</sup> Bergman et al.

<sup>e</sup> Butterson and Calderwood

<sup>f</sup> Miethke, Hou, and Marahiel

<sup>g</sup> Müller et al., NCBI AIV62096.1

<sup>h</sup> Zhu et al.

<sup>i</sup> Langman et al.

<sup>j</sup> Miethke et al.

**Table A.2 Primers used to generate the strains used in this work**

<b>Primer</b>	<b>Sequence (5'→3')</b>
GBAA_0352 P1	GAATTGTTTGATGTAACGTGTCGTGAATTGATTAAGCAGATGATGAAAT
GBAA_0352 P2	CATCTGCTTAATCAATTCACGCACAGTTACATCAAACAATTCTTCTCGATTCC
GBAA_0352 P3	GAACAAAAGCTGGAGCTCCACCGCGGTGGCGAACTTCTACTTTACCATTTTCAGATTGGTATG
GBAA_0352 P4	GATATCAGATCTGACGTCTCTAGAGCGGCCCTCATTTAACTACATCTTTATCTGATCGTATTCTTTC
GBAA_0352 P5	GCGTTTTGGATTTGC
GBAA_0352 P6	CTCATTTAACTACATCTTTATCTGATC
GBAA_0766 P1	GATTAATAGGTAATAAACTAAGGTATAATCGATTACGCTGCAACATG
GBAA_0766 P2	CATGTTGCAGCGTAATCGATTATACCTTAGTTTTTTACCTATTAATC
GBAA_0766 P3	GAACAAAAGCTGGAGCTCCACCGCGGTGGCCGATCTAGAATATCGCGAAGACGATC
GBAA_0766 P4	GATATCAGATCTGACGTCTCTAGAGCGGCCGAAAAACGATAAATCGTTATATGAAATACC
GBAA_0766 P5	CATATTTGCTAATTGTTGCGAG
GBAA_0766 P6	GTTCGTATCTAATAAAAAGGC
GBAA_1859 P1	TTTTAGCACACGGATCACCGCTTGGTACATTAAGTTATCTTTGTCTCCAATTT
GBAA_1859 P2	GATAACTTAATGTACCAAGCGGTGATCCGTGTGCTAAAAATAATG
GBAA_1859 P3	GAACAAAAGCTGGAGCTCCACCGCGGTGGCCATTTCCGAAACAAAGATCACATCAG
GBAA_1859 P4	GATATCAGATCTGACGTCTCTAGAGCGGCCGTCAGCGACAGGATTAGCGGTTATTTTG
GBAA_1859 P5	CATTTCGAAACAAAGATC
GBAA_1859 P6	GTCAGCGACAGGATTAGC
GBAA_1187 P1	GTATGGGTAAATTGGGAAATGGAAAACGAGCAAAAAGGTA
GBAA_1187 P2	CTCGTTTTCCATTTCCCAATTTACCCATACATCATGTAGATATAAC
GBAA_1187 P3	GAACAAAAGCTGGAGCTCCACCGCGGTGGCGATACGATGATTATGGAAGGATTAGCTG
GBAA_1187 P4	GATATCAGATCTGACGTCTCTAGAGCGGCCGATACGCGACTTTAAAGGCG
GBAA_1187 P5	GACGAAAGAAACAGAATATACATTAC
GBAA_1187 P6	GCAATGTACGAAGGAAAAG
GBAA_3181 P1	AAAAAGGTTTTATTGGCTAATAAAGTAGCTGAATGCATGAATTA
GBAA_3181 P2	CAGCTACTTTATTAGCCAATAAAACCTTTTTATTCTTTGCATTCA
GBAA_3181 P3	GAACAAAAGCTGGAGCTCCACCGCGGTGGCCATAATTATGATTGGAAACAGGATGAAAG
GBAA_3181 P4	GATATCAGATCTGACGTCTCTAGAGCGGCCGTAATCTGTCCGGATCATAACAAATATTC
GBAA_3181 P5	GAAGGTAGGGCTTTTCTT
GBAA_3181 P6	CATCATTTTCATTTTTTGATTAG
GBAA_4110 P1	GAAATGGATGTACAACGCTAGCAAAATTGAATATAAAGAAAACATAACA
GBAA_4110 P2	TTCAATTTTGCTAGCGTTGTACATCCATTTTCATATCTTTTCATTCC
GBAA_4110 P3	GAACAAAAGCTGGAGCTCCACCGCGGTGGCGTGGACGAGCTATCGGATTTCAGA
GBAA_4110 P4	GATATCAGATCTGACGTCTCTAGAGCGGCCGCGTTTTTTATGCTACAGGGCAT
GBAA_4110 P5	GTAATAACAGCACATTTTGAAG
GBAA_4110 P6	GAAAATCATTTAATTATAGGGG
GBAA_1242 P1	GATAGCATATGAGAGAAAGCTTTCCTATAAAAATGAAATTTCTTCAATTC
GBAA_1242 P2	GAATTGAAGAAATTTCAATTTTATAGGAAAGCTTCTCTCATATGCTATC
GBAA_1242 P3	GAACAAAAGCTGGAGCTCCACCGCGGTGGCGAAACGGTCAATTGGTTGTTTCGTAATAG
GBAA_1242 P4	GATATCAGATCTGACGTCTCTAGAGCGGCCGTTGAAGCGCTAAAATAATTGTCC
GBAA_1242 P5	GTTCCCTTTCCAAGG



GBAA\_1242 P6 CAATACACACTACACCTAATATCG

GBAA\_1392 P1 GTGGAAGAGTTTAATTGCGGCGATAAGATTACTAAAATCATAGAGAAATATAAAAAAAG

GBAA\_1392 P2 GATTTTAGTAATCTTATCGCCGCAATTAAGCTCTCCACACTCTATTC

GBAA\_1392 P3 GAACAAAAGCTGGAGCTCCACCGCGGTGGCCATAACGTTCCCACCCTAAAATTTCG

GBAA\_1392 P4 GATATCAGATCTGACGTCTCTAGAGCGGCCCTTCAATTTTCATTTTCTGTTTCACGAATC

GBAA\_1392 P5 CATAACGTTCCCACCC

GBAA\_1392 P6 CTTCAATTTTCATTTTCTGTTTC

GBAA\_2694 P1 CTTCTAAAGCTTTATGTAGGATTATTGTAGTCACCTCTCTCCTCCTT

GBAA\_2694 P2 GAGAGGTGACTACAATAATCCTACATAAAGCTTTAGAAGAAAAGAAATACCC

GBAA\_2694 P3 GAACAAAAGCTGGAGCTCCACCGCGGTGGCCACCCTCGTTTTTTTTCGCGCAC

GBAA\_2694 P4 GATATCAGATCTGACGTCTCTAGAGCGGCCCATTTCTTAATGGTATTATCAAATATCAAGAAAAC

GBAA\_2694 P5 CGGAATTTGAAGTTGATAC

GBAA\_2694 P6 GAAGTACATATAGAATATGTGTGAGG

GBAA\_3863 P1 CTATTGAAAAACAGCAGGGATTAAGATTCATTAGTCACGTATCCATC

GBAA\_3863 P2 AATGAATCTTAATCCCTGCTGTTTTTCAATAGTAGTGTTTCATTTTATA

GBAA\_3863 P3 GAACAAAAGCTGGAGCTCCACCGCGGTGGCGGGCATTAGATATAACGAAAACCTTCTGA

GBAA\_3863 P4 GATATCAGATCTGACGTCTCTAGAGCGGCCGTAATAACATTATCTTGCCGATCAATAATATG

GBAA\_3863 P5 CAAAAGATAAAGAGATGATTGAC

GBAA\_3863 P6 GAAAACAATCATTTACTCGAAC

**Table A.3 Candidate petrobactin iron-removal enzyme phenotypes at six hours post-inoculation in IDM**

Enzyme	Deletion strain type	Growth (OD <sub>600</sub> )		Catechols (% WT) <sup>a</sup>	
		Avg	SD	Avg	SD
Reductase	$\Delta 0352$ <sup>b</sup>	0.60	0.01		
	$\Delta 0766$	0.55	0.01	93.31	6.38
	$\Delta 1859$	0.53	0.01	108.88	14.39
	$\Delta 1187$	0.57		90.65	
	$\Delta 3181$	0.64		103.15	
	$\Delta 3863$	0.56		100.01	
	$\Delta 4110$	0.59		92.66	
	$\Delta 0766 \Delta 1859$	0.48	0.01	95.57	19.53
Hydrolase	$\Delta 1242$	0.60	0.02	99.28	16.41
	$\Delta 1392$	0.51	0.06	107.48	11.36
	$\Delta 2694$ <sup>b</sup>	0.50	0.03	100.48	11.19
	$\Delta 1392 \Delta 1242$	0.47	0.03	97.09	19.04
	$\Delta 1392 \Delta 2694$	0.46	0.03	105.89	3.78
	$\Delta 1242 \Delta 1392 \Delta 2694$	0.53		94.49	

<sup>a</sup>Normalized to cell density (OD600) and presented as relative to the wild-type set as 100%

<sup>b</sup>Data compiled from two biological replicates

## References

1. Wandersman C, Delepelaire P. 2004. Bacterial iron sources: From siderophores to hemophores. *Annu Rev Microbiol* 58:611–47.
2. Miethke M, Marahiel MA. 2007. Siderophore-based iron acquisition and pathogen control. *Microbiol Mol Biol Rev* 71:413–451.
3. Ganz T. 2013. Systemic iron homeostasis. *Physiol Rev* 93:1721–41.
4. Finkelstein R, Sciortino C, McIntosh M. 1983. Role of iron in microbe-host interactions. *Rev Infect Dis* 5 Suppl 4:S759–S777.
5. Braun V, Hantke K. 2011. Recent insights into iron import by bacteria. *Curr Opin Chem Biol* 15:328–34.
6. Dixon TC, Meselson M, Guillemin J, Hanna PC. 1999. Anthrax. *N Engl J Med* 341:815–826.
7. Cote CK, Welkos SL, Bozue J. 2011. Key aspects of the molecular and cellular basis of inhalational anthrax. *Microbes Infect* 13:1146–1155.
8. Palmateer NE, Hope VD, Roy K, Marongiu A, White JM, Grant K a, Ramsay CN, Goldberg DJ, Ncube F. 2013. Infections with spore-forming bacteria in persons who inject drugs, 2000–2009. *Emerg Infect Dis* 19:29–34.
9. Ross JM. 1957. The pathogenesis of anthrax following the administration of spores by the respiratory route. *J Pathol Bacteriol* 73:485–494.
10. Brittingham KC, Ruthel G, Panchal RG, Fuller CL, Ribot WJ, Hoover TA, Young HA, Anderson AO, Bavari S. 2005. Dendritic cells endocytose *Bacillus anthracis* spores: Implications for anthrax pathogenesis. *J Immunol* 174:5545–5552.
11. Banks DJ, Barnajian M, Maldonado-Arocho FJ, Sanchez AM, Bradley KA. 2005. Anthrax toxin receptor 2 mediates *Bacillus anthracis* killing of macrophages following spore challenge. *Cell Microbiol* 7:1173–1185.
12. Friedlander A, Welkos S, Pitt M, Ezzell J, Worsham P, Rose K, Ivins B, Lowe J, Howe G, Mikesell P, Lawrence W. 1993. Postexposure prophylaxis against experimental inhalation anthrax. *J Infect Dis* 167:1239–1242.
13. Lincoln R, Walker J, Klein F, Rosenwald A, Jones WJ. 1967. Technical manuscript 349: Value of field data for extrapolation in anthrax.
14. Carlson PE, Dixon SD, Hanna PC. 2013. Anthrax and iron, p. 307–314. *In* Vasil, ML, Darwin, AJ (eds.), *Regulation of Bacterial Virulence*. ASM Press, Washington, DC.
15. Miethke M. 2013. Molecular strategies of microbial iron assimilation: from high-affinity complexes to cofactor assembly systems. *Met Integr biometal Sci* 5:15–28.
16. Cendrowski S, MacArthur W, Hanna P. 2004. *Bacillus anthracis* requires siderophore biosynthesis for growth in macrophages and mouse virulence. *Mol Microbiol* 51:407–17.
17. Carlson PE, Carr KA, Janes BK, Anderson EC, Hanna PC. 2009. Transcriptional profiling of *Bacillus anthracis* Sterne (34F2) during iron starvation. *PLoS One* 4:e6988.
18. Barbeau K, Zhang G, Live DH, Butler A. 2002. Petrobactin, a photoreactive siderophore

- produced by the oil-degrading marine bacterium *Marinobacter hydrocarbonoclasticus*. J Am Chem Soc 124:378–9.
19. Homann V V, Edwards KJ, Webb EA, Butler A. 2009. Siderophores of *Marinobacter aquaeolei*: Petrobactin and its sulfonated derivatives. Biometals 22:565–71.
  20. Koppisch AT, Dhungana S, Hill KK, Boukhalfa H, Heine HS, Colip L a, Romero RB, Shou Y, Ticknor LO, Marrone BL, Hersman LE, Iyer S, Ruggiero CE. 2008. Petrobactin is produced by both pathogenic and non-pathogenic isolates of the *Bacillus cereus* group of bacteria. Biometals 21:581–9.
  21. Zhang G, Amin SA, Küpper FC, Holt PD, Carrano CJ, Butler A. 2009. Ferric stability constants of representative marine siderophores: Marinobactins, aquachelins, and petrobactin. Inorg Chem 48:11466–73.
  22. Gardner RA, Kinkade R, Wang C, Phanstiel O. 2004. Total synthesis of petrobactin and its homologues as potential growth stimuli for *Marinobacter hydrocarbonoclasticus*, an oil-degrading bacteria. J Org Chem 69:3530–7.
  23. Hider RC, Kong X. 2010. Chemistry and biology of siderophores. Nat Prod Rep 27:637–57.
  24. Abergel RJ, Zawadzka AM, Raymond KN. 2008. Petrobactin-mediated iron transport in pathogenic bacteria: Coordination chemistry of an unusual 3,4-catecholate/citrate siderophore. J Am Chem Soc 130:2124–2125.
  25. Saha R, Saha N, Donofrio RS, Bestervelt LL. 2013. Microbial siderophores: A mini review. J Basic Microbiol 53:303–17.
  26. Finking R, Marahiel M. 2004. Biosynthesis of nonribosomal peptides. Annu Rev Microbiol 58:453–488.
  27. Conti E, Stachelhaus T, Marahiel M, Brick P. 1997. Structural basis for the activation of phenylalanine in the non-ribosomal biosynthesis of gramicidin S. EMBO J 16:4174–4183.
  28. Keating T, Marshall C, Walsh C. 2000. Reconstitution and characterization of the *Vibrio cholerae* vibriobactin synthetase from VibB, VibE, VibF, and VibH. Biochemistry 39:15522–15530.
  29. Keating T, Marshall C, Walsh C, Keating A. 2002. The structure of VibH represents nonribosomal peptide synthetase condensation, cyclization and epimerization domains. Nat Struct Biol 9:522–526.
  30. May JJ, Kessler N, Marahiel M a, Stubbs MT. 2002. Crystal structure of DhbE, an archetype for aryl acid activating domains of modular nonribosomal peptide synthetases. Proc Natl Acad Sci U S A 99:12120–5.
  31. Stachelhaus T, Mootz H, Marahiel M. 1999. The specificity-conferring code of adenylation domains in nonribosomal peptide synthetases. Chem Biol 6:493–505.
  32. Weber T, Baumgartner R, Renner C, Marahiel M, Holak T. 2000. Solution structure of PCP, a prototype for the peptidyl carrier domains of modular peptide synthetases. Structure 8:407–418.
  33. Schneider A, Marahiel M. 1998. Genetic evidence for a role of thioesterase domains, integrated in or associated with peptide synthetases, in non-ribosomal peptide biosynthesis in *Bacillus subtilis*. Arch Microbiol 169:404–410.
  34. Sieber S, Marahiel M. 2008. Learning from nature's drug factories: Nonribosomal synthesis of macrocyclic peptides. J Bacteriol 185:7036–7043.
  35. Challis GL. 2005. A widely distributed bacterial pathway for siderophore biosynthesis independent of nonribosomal peptide synthetases. ChemBioChem 6:601–611.

36. Oves-Costales D, Kadi N, Challis GL. 2009. The long-overlooked enzymology of a nonribosomal peptide synthetase-independent pathway for virulence-conferring siderophore biosynthesis. *Chem Commun* 6530–41.
37. Kadi N, Oves-Costales D, Barona-Gomez F, Challis GL. 2007. A new family of ATP-dependent oligomerization-macrocyclization biocatalysts. *Nat Chem Biol* 3:652–656.
38. Schmelz S, Kadi N, McMahon SA, Song L, Oves-Costales D, Oke M, Liu H, Johnson KA, Carter LG, Botting CH, White MF, Challis GL, Naismith JH. 2009. AcsD catalyzes enantioselective citrate desymmetrization in siderophore biosynthesis. *Nat Chem Biol* 5:174–82.
39. Oves-Costales D, Kadi N, Fogg MJ, Song L, Wilson KS, Challis GL. 2007. Enzymatic logic of anthrax stealth siderophore biosynthesis: AsbA catalyzes ATP-dependent condensation of citric acid and spermidine. *J Am Chem Soc* 129:8416–8417.
40. Lee JY, Janes BK, Passalacqua KD, Pflieger BF, Bergman NH, Liu H, Håkansson K, Somu R V, Aldrich CC, Cendrowski S, Hanna PC, Sherman DH. 2007. Biosynthetic analysis of the petrobactin siderophore pathway from *Bacillus anthracis*. *J Bacteriol* 189:1698–710.
41. Pflieger BF, Kim Y, Nusca TD, Maltseva N, Lee JY, Rath CM, Scaglione JB, Janes BK, Anderson EC, Bergman NH, Hanna PC, Joachimiak A, Sherman DH. 2008. Structural and functional analysis of AsbF: Origin of the stealth 3,4-dihydroxybenzoic acid subunit for petrobactin biosynthesis. *Proc Natl Acad Sci U S A* 105:17133–8.
42. Fox DT, Hotta K, Kim CY, Koppisch AT. 2008. The missing link in petrobactin biosynthesis: *asbF* encodes a (-)-3-dehydroshikimate dehydratase. *Biochemistry* 47:12251–12253.
43. Nusca TD, Kim Y, Maltseva N, Lee JY, Eschenfeldt W, Stols L, Schofield MM, Scaglione JB, Dixon SD, Oves-Costales D, Challis GL, Hanna PC, Pflieger BF, Joachimiak A, Sherman DH. 2012. Functional and structural analysis of the siderophore synthetase AsbB through reconstitution of the petrobactin biosynthetic pathway from *Bacillus anthracis*. *J Biol Chem* 287:16058–72.
44. Guex N, Peitsch MC. 1997. SWISS-MODEL and the Swiss-PdbViewer: An environment for comparative protein modeling. *Electrophoresis* 18:2714–2723.
45. Pflieger BF, Lee JY, Somu R V, Aldrich CC, Hanna PC, Sherman DH. 2007. Characterization and analysis of early enzymes for petrobactin biosynthesis in *Bacillus anthracis*. *Biochemistry* 46:4147–57.
46. Oves-Costales D, Kadi N, Fogg MJ, Song L, Wilson KS, Challis GL. 2008. Petrobactin biosynthesis: AsbB catalyzes condensation of spermidine with N8-citryl-spermidine and its N1-(3,4-dihydroxybenzoyl) derivative. *Chem Commun* 4034–6.
47. Oves-Costales D, Song L, Challis GL. 2009. Enantioselective desymmetrisation of citric acid catalysed by the substrate-tolerant petrobactin biosynthetic enzyme AsbA. *Chem Commun* 1389–91.
48. Ernst J, Bennett R, Rothfield L. 1978. Constitutive expression of the iron-enterochelin and ferrichrome uptake systems in a mutant strain of *Salmonella typhimurium*. *J Bacteriol* 135:928–934.
49. Hantke K. 1981. Regulation of ferric iron transport in *Escherichia coli* K12: Isolation of a constitutive mutant. *Mol Gen Genet* 182:288–292.
50. Bagg A, Neilands J. 1987. Ferric uptake regulation protein acts as a repressor, employing iron (II) as a cofactor to bind the operator of an iron transport operon in *Escherichia coli*.

- Biochemistry 26:5471–5477.
51. Stojiljkovic I, Baumler A, Hantke K. 1994. Identification and characterization of new iron-regulated *Escherichia coli* genes by a Fur titration assay. *J Mol Biol* 236:531–545.
  52. Lavrrar J, Mcintosh M. 2003. Architecture of a Fur binding site: A comparative analysis. *J Bacteriol* 185:2194–2202.
  53. Hotta K, Kim C-Y, Fox DT, Koppisch AT. 2010. Siderophore-mediated iron acquisition in *Bacillus anthracis* and related strains. *Microbiology* 156:1918–25.
  54. Sierra N, Makita Y, de Hoon M, Nakai K. 2008. DBTBS: A database of transcriptional regulation in *Bacillus subtilis* containing upstream intergenic conservation information. *Nucleic Acids Res* 36:D93–6.
  55. Carlson PE, Bourgis AET, Hagan AK, Hanna PC. 2015. Global gene expression by *Bacillus anthracis* during growth in mammalian blood. *Pathog Dis* 73:ftv061.
  56. Lee JY, Passalacqua KD, Hanna PC, Sherman DH. 2011. Regulation of petrobactin and bacillibactin biosynthesis in *Bacillus anthracis* under iron and oxygen variation. *PLoS One* 6:e20777.
  57. Pohl S, Tu WY, Aldridge PD, Gillespie C, Hahne H, Mäder U, Read TD, Harwood CR. 2011. Combined proteomic and transcriptomic analysis of the response of *Bacillus anthracis* to oxidative stress. *Proteomics* 11:3036–55.
  58. Tu WY, Pohl S, Gray J, Robinson NJ, Harwood CR, Waldron KJ. 2012. Cellular iron distribution in *Bacillus anthracis*. *J Bacteriol* 194:932–40.
  59. Passalacqua KD, Bergman NH, Lee JY, Sherman DH, Hanna PC. 2007. The global transcriptional responses of *Bacillus anthracis* Sterne (34F2) and a Delta *sodA1* mutant to paraquat reveal metal ion homeostasis imbalances during endogenous superoxide stress. *J Bacteriol* 189:3996–4013.
  60. Koppisch AT, Browder CC, Moe AL, Shelley JT, Kinkel BA, Hersman LE, Iyer S, Ruggiero CE. 2005. Petrobactin is the primary siderophore synthesized by *Bacillus anthracis* str. Sterne under conditions of iron starvation. *Biometals* 18:577–85.
  61. Garner BL, Arceneaux JEL, Byers BR. 2004. Temperature control of a 3,4-dihydroxybenzoate (protocatechuate)-based siderophore in *Bacillus anthracis*. *Curr Microbiol* 49:89–94.
  62. Wilson MK, Abergel RJ, Arceneaux JEL, Raymond KN, Byers BR. 2010. Temporal production of the two *Bacillus anthracis* siderophores, petrobactin and bacillibactin. *Biometals* 23:129–34.
  63. Carlson PE, Dixon SD, Janes BK, Carr KA, Nusca TD, Anderson EC, Keene SE, Sherman DH, Hanna PC. 2010. Genetic analysis of petrobactin transport in *Bacillus anthracis*. *Mol Microbiol* 75:900–9.
  64. Dixon SD, Janes BK, Bourgis A, Carlson PE, Hanna PC. 2012. Multiple ABC transporters are involved in the acquisition of petrobactin in *Bacillus anthracis*. *Mol Microbiol* 84:370–82.
  65. Yeterian E, Martin LW, Guillon L, Journet L, Lamont IL, Schalk IJ. 2010. Synthesis of the siderophore pyoverdine in *Pseudomonas aeruginosa* involves a periplasmic maturation. *Amino Acids* 38:1447–59.
  66. Langman L, Young IG, Frost GE, Rosenberg H, Gibson F. 1972. Enterochelin system of iron transport in *Escherichia coli*: Mutations affecting ferric-enterochelin esterase. *J Bacteriol* 112:1142–1149.
  67. Müller K, Matzanke BF, Schünemann V, Trautwein a X, Hantke K. 1998. FhuF, an iron-

- regulated protein of *Escherichia coli* with a new type of [2Fe-2S] center. Eur J Biochem 258:1001–8.
68. Yeterian E, Martin LW, Lamont IL, Schalk IJ. 2010. An efflux pump is required for siderophore recycling by *Pseudomonas aeruginosa*. Environ Microbiol Rep 2:412–8.
  69. Gat O, Zaide G, Inbar I, Grosfeld H, Chitlaru T, Levy H, Shafferman A. 2008. Characterization of *Bacillus anthracis* iron-regulated surface determinant (Isd) proteins containing NEAT domains. Mol Microbiol 70:983–99.
  70. Abergel RJ, Clifton MC, Pizarro JC, Warner J a, Shuh DK, Strong RK, Raymond KN. 2008. The siderocalin/enterobactin interaction: A link between mammalian immunity and bacterial iron transport. J Am Chem Soc 130:11524–34.
  71. Abergel RJ, Wilson MK, Arceneaux JEL, Hoette TM, Strong RK, Byers BR, Raymond KN. 2006. Anthrax pathogen evades the mammalian immune system through stealth siderophore production. Proc Natl Acad Sci U S A 103:18499–18503.
  72. Ferreras JA, Ryu JS, Di Lello F, Tan DS, Quadri LEN. 2005. Small-molecule inhibition of siderophore biosynthesis in *Mycobacterium tuberculosis* and *Yersinia pestis*. Nat Chem Biol 1:29–32.
  73. Tripathi A, Schofield MM, Chlipala GE, Schultz PJ, Yim I, Newmister SA, Nusca TD, Scaglione JB, Hanna PC, Tamayo-Castillo G, Sherman DH. 2014. Baulamycins A and B, broad-spectrum antibiotics identified as inhibitors of siderophore biosynthesis in *Staphylococcus aureus* and *Bacillus anthracis*. J Am Chem Soc 136:1579–1586.
  74. Jomova K, Valko M. 2011. Importance of iron chelation in free radical-induced oxidative stress and human disease. Curr Pharm Des 17:3460–73.
  75. Skaar EP, Gaspar AH, Schneewind O. 2006. *Bacillus anthracis* IsdG, a heme-degrading monooxygenase. J Bacteriol 188:1071–1080.
  76. Ringertz SH, Hoiby EA, Jensenius M, Maehlen J, Caugant DA, Myklebust A, Fossum K. 2000. Injectional anthrax in a heroin skin-popper. Lancet 356:1574–1575.
  77. Hagan AK, Carlson Jr PE, Hanna PC. 2016. Flying under the radar: The non-canonical biochemistry and molecular biology of petrobactin from *Bacillus anthracis*. Mol Microbiol 102:196–206.
  78. Davidson AL, Dassa E, Orelle C, Chen J. 2008. Structure, function, and evolution of bacterial ATP-binding cassette systems. Microbiol Mol Biol Rev 72:317–364.
  79. Crouch M-L V, Castor M, Karlinsey JE, Kalthorn T, Fang FC. 2008. Biosynthesis and IroC-dependent export of the siderophore salmochelin are essential for virulence of *Salmonella enterica* serovar Typhimurium. Mol Microbiol 67:971–83.
  80. Zhu W, Arceneaux JEL, Beggs ML, Byers BR, Eisenach KD, Lundrigan MD. 1998. Exochelin genes in *Mycobacterium smegmatis*: Identification of an ABC transporter and two non-ribosomal peptide synthetase genes. Mol Microbiol 29:629–639.
  81. Yan N. 2013. Structural advances for the major facilitator superfamily (MFS) transporters. Trends Biochem Sci 38:151–159.
  82. Deng X, Sun F, Ji Q, Liang H, Missiakas D, Lan L, He C. 2012. Expression of multidrug resistance efflux pump gene *norA* is iron responsive in *Staphylococcus aureus*. J Bacteriol 194:1753–62.
  83. Furrer JL, Sanders DN, Hook-Barnard IG, McIntosh MA. 2002. Export of the siderophore enterobactin in *Escherichia coli*: involvement of a 43 kDa membrane exporter. Mol Microbiol 44:1225–34.
  84. Page WJ, Kwon E, Cornish AS, Tindale AE. 2003. The *csbX* gene of *Azotobacter*

- vinelandii* encodes an MFS efflux pump required for catechololate siderophore export. FEMS Microbiol Lett 228:211–216.
85. Blair JM, Piddock LJ. 2009. Structure, function and inhibition of RND efflux pumps in Gram-negative bacteria: An update. Curr Opin Microbiol 12:512–9.
  86. Horiyama T, Nishino K. 2014. AcrB, AcrD, and MdtABC multidrug efflux systems are involved in enterobactin export in *Escherichia coli*. PLoS One 9.
  87. Wells RM, Jones CM, Xi Z, Speer A, Danilchanka O, Doornbos KS, Sun P, Wu F, Tian C, Niederweis M. 2013. Discovery of a siderophore export system essential for virulence of *Mycobacterium tuberculosis*. PLoS Pathog 9:e1003120.
  88. Jones C, Wells R, Madduri A, Renfrow M, Ratledge C, Moody D, Niederweis M. 2014. Self-poisoning of *Mycobacterium tuberculosis* by interrupting siderophore recycling. Proc Natl Acad Sci 111:1945–1950.
  89. Wilson MK, Abergel RJ, Raymond KN, Arceneaux JEL, Byers BR. 2006. Siderophores of *Bacillus anthracis*, *Bacillus cereus*, and *Bacillus thuringiensis*. Biochem Biophys Res Commun 348:320–5.
  90. Nemes P, Vértés Á. 2007. Laser ablation electrospray ionization for atmospheric pressure, in vivo, and imaging mass spectrometry. Anal Chem 79:8098–8106.
  91. Nemes P, Barton AA, Li Y, Vertes A. 2008. Ambient molecular imaging and depth profiling of live tissue by infrared laser ablation electrospray ionization mass spectrometry. Anal Chem 80:4575–4582.
  92. Nemes P, Barton AA, Vertes A. 2009. Three-dimensional imaging of metabolites in tissues under ambient conditions by laser ablation electrospray ionization mass spectrometry. Anal Biochem 81:6668–6675.
  93. Shrestha B, Javonillo R, Burns JR, Pirger Z, Vertes A. 2013. Comparative local analysis of metabolites, lipids and proteins in intact fish tissues by LAESI mass spectrometry. Analyst 138:3444–3449.
  94. Shrestha B, Sripadi P, Reschke BR, Henderson HD, Powell MJ, Moody SA, Vertes A. 2014. Subcellular metabolite and lipid analysis of *Xenopus laevis* eggs by LAESI mass spectrometry. PLoS One 9:1–22.
  95. Stopka SA, Agtuca BJ, Koppenaar DW, Pasa-Tolic L, Stacey G, Vertes A, Anderton CR. 2017. Laser-ablation electrospray ionization mass spectrometry with ion mobility separation reveals metabolites in the symbiotic interactions of soybean roots and rhizobia. Plant J 91:340–354.
  96. Motley JL, Stamps BW, Mitchell CA, Thompson AT, Cross J, You J, Powell DR, Stevenson BS, Cichewicz RH. 2017. Opportunistic sampling of roadkill as an entry point to accessing natural products assembled by bacteria associated with non-anthropoidal mammalian microbiomes. J Nat Prod 80:598–608.
  97. Janes BK, Stibitz S. 2006. Routine markerless gene replacement in *Bacillus anthracis*. Infect Immun 74:1949–1953.
  98. Wilson MJ, Carlson PE, Janes BK, Hanna PC. 2012. Membrane topology of the *Bacillus anthracis* GerH germinant receptor proteins. J Bacteriol 194:1369–77.
  99. Passalacqua KD, Bergman NH. 2006. *Bacillus anthracis*: Interactions with the host and establishment of inhalational anthrax. Future Microbiol 1:397–415.
  100. Arnow LE. 1937. Colorimetric determination of the components of 3,4-dihydroxyphenylalaninetyrosine mixtures. J Biol Chem 118:531–537.
  101. Elvebak II LE. 2002. GMSU/QC - Gubbs Mass Spec Utilities. Gubbs, Inc.

102. Heffernan BJ, Thomason B, Herring-Palmer A, Hanna P. 2007. *Bacillus anthracis* anthrolysin O and three phospholipases C are functionally redundant in a murine model of inhalation anthrax. *FEMS Microbiol Lett* 271:98–105.
103. Bergman NH, Anderson EC, Swenson EE, Janes BK, Fisher N, Niemeyer MM, Miyoshi AD, Hanna PC. 2007. Transcriptional profiling of *Bacillus anthracis* during infection of host macrophages. *Infect Immun* 75:3434–3444.
104. Altschul SF, Madden TL, Schäffer AA, Zhang J, Zhang Z, Miller W, Lipman DJ. 1997. Gapped BLAST and PSI-BLAST: A new generation of protein database search programs. *Nucleic Acids Res* 25:3389–3402.
105. Huang M-Z, Cheng S-C, Cho Y-T, Shiea J. 2011. Ambient ionization mass spectrometry: A tutorial. *Anal Chim Acta* 702:1–15.
106. Kaneko Y, Thoendel M, Olakanmi O, Britigan BE, Singh PK. 2007. The transition metal gallium disrupts *Pseudomonas aeruginosa* iron metabolism and has antimicrobial and antibiofilm activity. *J Clin Invest* 117:877–888.
107. Kelley LA, Sternberg MJE. 2009. Protein structure prediction on the Web: a case study using the Phyre server. *Nat Protoc* 4:363–371.
108. Kelly L, Mezulis S, Yates C, Wass M, Sternberg M. 2015. The Phyre2 web portal for protein modelling, prediction, and analysis. *Nat Protoc* 10:845–858.
109. Frost GE, Rosenberg H. 1973. The inducible citrate-dependent iron transport system in *Escherichia coli* K12. *Biochim Biophys Acta* 330:90–101.
110. Hantke K. 1990. Dihydroxybenzoylserine - A siderophore for *E. coli*. *FEMS Microbiol Lett* 67:5–8.
111. Grootveld M, Bell JD, Halliwell B, Aruoma OI, Bomford A, Sadler PJ. 1989. Non-transferrin-bound iron in plasma or serum from patients with idiopathic hemochromatosis. Characterization by high performance liquid chromatography and nuclear magnetic resonance spectroscopy. *J Biol Chem* 264:4417–4422.
112. Okujo N, Saito M, Yamamoto S, Yoshida T, Miyoshi S, Shinoda S. 1994. Structure of vulnibactin, a new polyamine-containing siderophore from *Vibrio vulnificus*. *Biometals* 109–116.
113. Caza M, Lépine F, Dozois CM. 2011. Secretion, but not overall synthesis, of catecholate siderophores contributes to virulence of extraintestinal pathogenic *Escherichia coli*. *Mol Microbiol* 80:266–282.
114. Cote C, Rossi C, Kang A, Morrow P, Lee J, Welkos S. 2005. The detection of protective antigen (PA) associated with spores of *Bacillus anthracis* and the effects of anti-PA antibodies on spore germination and macrophage interactions. *Microb Pathog* 38:209–225.
115. Setlow P. 2006. Spores of *Bacillus subtilis*: Their resistance to and killing by radiation, heat and chemicals. *J Appl Microbiol* 101:514–525.
116. Paidhungat M, Setlow B, Driks A, Setlow P. 2000. Characterization of spores of *Bacillus subtilis* which lack dipicolinic acid. *J Bacteriol* 182:5505–5512.
117. Moeller R, Setlow P, Horneck G, Berger T, Reitz G, Rettberg P, Doherty AJ, Okayasu R, Nicholson WL. 2008. Roles of the major, small, acid-soluble spore proteins and spore-specific and universal DNA repair mechanisms in resistance of *Bacillus subtilis* spores to ionizing radiation from X rays and high-energy charged-particle bombardment. *J Bacteriol* 190:1134–40.
118. Turnbull PCB. 1998. Guidelines for the surveillance and control of anthrax in human and



- animals. Salisbury, Wiltshire, UK.
119. Errington J. 2003. Regulation of endospore formation in *Bacillus subtilis*. *Nat Rev Microbiol* 1:117–126.
  120. Kroos L, Yu YT. 2000. Regulation of sigma factor activity during *Bacillus subtilis* development. *Curr Opin Microbiol* 3:553–560.
  121. Takamatsu H, Watabe K. 2002. Assembly and genetics of spore protective structures. *Cell Mol Life Sci* 59:434–444.
  122. Britton RA, Eichenberger P, Gonzalez-Pastor JE, Fawcett P, Monson R, Losick R, Grossman AD. 2002. Genome-wide analysis of the stationary-phase sigma factor (sigma-H) regulon of *Bacillus subtilis*. *J Bacteriol* 184:4881–4890.
  123. Fujita M, Losick R. 2003. The master regulator for entry into sporulation in *Bacillus subtilis* becomes a cell-specific transcription factor after asymmetric division. *Genes Dev* 17:1166–1174.
  124. Eichenberger P, Fawcett P, Losick R. 2001. A three-protein inhibitor of polar septation during sporulation in *Bacillus subtilis*. *Mol Microbiol* 42:1147–1162.
  125. Rudner DZ, Losick R. 2002. A sporulation membrane protein tethers the pro- $\sigma$ K processing enzyme to its inhibitor and dictates its subcellular localization. *Genes Dev* 16:1007–1018.
  126. Sun D, Stragier P, Setlow P. 1989. Identification of a new  $\sigma$ -factor involved in compartmentalized gene expression during sporulation of *Bacillus subtilis*. *Genes Dev* 3:141–149.
  127. Liu H, Bergman NH, Thomason B, Shallom S, Hazen A, Crossno J, Rasko DA, Ravel J, Read TD, Peterson SN, Yates III J, Hanna PC. 2004. Formation and composition of the *Bacillus anthracis* endospore. *J Bacteriol* 186:164–178.
  128. Kolodziej BJ, Slepecky RA. 1964. Trace metal requirements for sporulation of *Bacillus megaterium*. *J Bacteriol* 88:821–830.
  129. Purohit M, Sassi-Gaha S, Rest RF. 2010. Rapid sporulation of *Bacillus anthracis* in a high iron, glucose-free medium. *J Microbiol Methods* 82:282–287.
  130. Haley KP, Skaar EP. 2012. A battle for iron: Host sequestration and *Staphylococcus aureus* acquisition. *Microbes Infect* 14:217–227.
  131. Bergman NH, Anderson EC, Swenson EE, Niemeyer MM, Miyoshi AD, Hanna PC. 2006. Transcriptional profiling of the *Bacillus anthracis* life cycle in vitro and an implied model for regulation of spore formation. *J Bacteriol* 188:6092–6100.
  132. Hagan AK, Tripathi A, Berger D, Sherman DH, Hanna PC. 2017. Petrobactin is exported from *Bacillus anthracis* by the RND-type exporter ApeX. *MBio* 8:1–18.
  133. Maresso AW, Chapa TJ, Schneewind O. 2006. Surface protein IsdC and Sortase B are required for heme-iron scavenging of *Bacillus anthracis*. *J Bacteriol* 188:8145–52.
  134. Cormack B, Valdivia R, Falkow S. 1998. FACS-optimized mutants of the green fluorescent protein (GFP). *Gene* 173:33–38.
  135. Cendrowski S. 2004. Role of the *asb* operon in *Bacillus anthracis* pathogenesis.
  136. Hugh-Jones M, Blackburn J. 2009. The ecology of *Bacillus anthracis*. *Mol Aspects Med* 30:356–367.
  137. Minett F. 1950. Sporulation and viability of *B. anthracis* in relation to environmental temperature and humidity. *J Comp Path* 60:161–176.
  138. Schaer DJ, Buehler PW, Alayash AI, Belcher JD, Vercellotti GM. 2013. Hemolysis and free hemoglobin revisited: Exploring hemoglobin and hemin scavengers as a novel class

- of therapeutic proteins. *Blood* 121:1276–1284.
139. Maresso AW, Garufi G, Schneewind O. 2008. *Bacillus anthracis* secretes proteins that mediate heme acquisition from hemoglobin. *PLoS Pathog* 4:e1000132.
  140. Grandchamp GM, Caro L, Shank EA. 2017. Pirated siderophores promote sporulation in *Bacillus subtilis*. *Appl Environ Microbiol* AEM.03293-16.
  141. Achard MES, Chen KW, Sweet MJ, Watts RE, Schroder K, Schembri M a, McEwan AG. 2013. An antioxidant role for catecholate siderophores in *Salmonella*. *Biochem J* 454:543–9.
  142. Nobre LS, Saraiva LM. 2014. Role of the siderophore transporter SirABC in the *Staphylococcus aureus* resistance to oxidative stress. *Curr Microbiol* 69:164–168.
  143. Mols M, Abee T. 2011. Primary and secondary oxidative stress in *Bacillus*. *Environ Microbiol* 13:1387–1394.
  144. Liu H, Bergman NH, Thomason B, Shallom S, Hazen A, Crossno J, Rasko DA, Ravel J, Read TD, Peterson SN, Yates J, Hanna PC. 2004. Formation and Composition of the *Bacillus anthracis* Endospore. *J Bacteriol* 186:164–178.
  145. Ollinger J, Song K-B, Antelmann H, Hecker M, Helmann JD. 2006. Role of the Fur regulon in iron transport in *Bacillus subtilis*. *J Bacteriol* 188:3664–3673.
  146. Serio AW, Pechter KB, Sonenshein AL. 2006. *Bacillus subtilis* aconitase is required for efficient late-sporulation gene expression. *J Bacteriol* 188:6396–6405.
  147. Tindale AE, Mehrotra M, Ottem D, Page WJ. 2000. Dual regulation of catecholate siderophore biosynthesis in *Azotobacter vinelandii* by iron and oxidative stress. *Microbiology* 146:1617–26.
  148. Fouet A, Namy O, Lambert G. 2000. Characterization of the operon encoding the alternative *sigB* factor from *Bacillus anthracis* and its role in virulence. *J Bacteriol* 182:5036–5045.
  149. Canale-Parola E. 1963. A red pigment produced by aerobic sporeforming bacteria. *Arch Mikrobiol* 46:414–427.
  150. Zawadzka AM, Kim Y, Maltseva N, Nichiporuk R, Fan Y, Joachimiak A, Raymond KN. 2009. Characterization of a *Bacillus subtilis* transporter for petrobactin, an anthrax stealth siderophore. *Proc Natl Acad Sci U S A* 106:21854–9.
  151. Harvie DR, Ellar DJ. 2005. A ferric dicitrate uptake system is required for the full virulence of *Bacillus cereus*. *Curr Microbiol* 50:246–250.
  152. Ollinger J, Song K, Antelmann H, Hecker M, Helmann JD. 2006. Role of the Fur regulon in iron transport in *Bacillus subtilis*. *J Bacteriol* 188:3664–3673.
  153. Butterson JR, Calderwood SB. 1994. Identification, cloning, and sequencing of a gene required for ferric vibriobactin utilization by *Vibrio cholerae*. *J Bacteriol* 176:5631–5638.
  154. Miethke M, Hou J, Marahiel M a. 2011. The siderophore-interacting protein YqjH acts as a ferric reductase in different iron assimilation pathways of *Escherichia coli*. *Biochemistry* 50:10951–64.
  155. Zhu M, Valdebenito M, Winkelmann G, Hantke K. 2005. Functions of the siderophore esterases IroD and IroE in iron-salmochelin utilization. *Microbiology* 151:2363–2372.
  156. Miethke M, Klotz O, Linne U, May JJ, Beckering CL, Marahiel M a. 2006. Ferri-bacillibactin uptake and hydrolysis in *Bacillus subtilis*. *Mol Microbiol* 61:1413–27.
  157. Johnstone TC, Nolan EM. 2015. Beyond iron: Non-classical biological functions of bacterial siderophores. *R Soc Chem* 44:6320–39.
  158. Passalacqua KD. 2007. Characterization of the superoxide dismutases of *Bacillus*

- anthracis*: Global and local approaches to the study of bacterial oxidative stress and metal ion homeostasis.
159. Peralta DR, Adler C, Corbalán NS, Paz García EC, Pomares MF, Vincent PA. 2016. Enterobactin as part of the oxidative stress response repertoire. *PLoS One* 11:1–15.
  160. Adler C, Corbalan NS, Peralta DR, Pomares MF, De Cristóbal RE, Vincent PA. 2014. The alternative role of enterobactin as an oxidative stress protector allows *Escherichia coli* colony development. *PLoS One* 9:1–10.
  161. Chaturvedi KS, Hung CS, Crowley JR, Stapleton AE, Henderson JP. 2012. The siderophore yersiniabactin binds copper to protect pathogens during infection. *Nat Chem Biol* 8:731–6.
  162. Holden VI, Breen P, Houle S, Dozois CM, Bachman MA. 2016. *Klebsiella pneumoniae* siderophores induce inflammation, bacterial dissemination, and HIF-1 $\alpha$  stabilization during pneumonia. *MBio* 7:e01397-16.
  163. Etalo DW, De Vos RCH, Joosten MHAJ, Hall RD. 2015. Spatially resolved plant metabolomics: Some potentials and limitations of laser-ablation electrospray ionization mass spectrometry metabolite imaging. *Plant Physiol* 169:1424–1435.